# RETHINKING PROGRESS IN ATTRIBUTE-MISSING GRAPH CLUSTERING: A BENCHMARK AND A SIMPLE SCALABLE FRAMEWORK

**Anonymous authors**
Paper under double-blind review

## ABSTRACT

Graph clustering aims to uncover latent communities by jointly exploiting graph structure and node attributes in an unsupervised manner. In real-world applications, however, some nodes may have completely missing attributes due to privacy constraints, data acquisition failures, and cold-start nodes. Missing semantic information makes learning discriminative representations for clustering more challenging. Despite substantial recent efforts on attribute-missing graph clustering, it remains unclear how much genuine progress has been made and how much model complexity is actually needed. Current evaluations are often too narrow to establish generality, while increasingly elaborate pipelines obscure which mechanisms are actually necessary for effective clustering. To systematically revisit these questions, we establish a comprehensive and reproducible benchmark covering 22 graph datasets and 32 baselines from four method families across diverse graph scales. The benchmark reveals that specialized attribute-missing methods can even underperform conventional graph clustering methods. Moreover, we propose VISTA, a lightweight and scalable framework. By performing bounded sparse topology propagation, VISTA recovers missing semantics from locally observed attributes without a learnable imputer. By adopting topology-conditioned cross-view prototype learning, it learns clustering-oriented representations without graph reconstruction or dense node-pair modeling. Extensive experiments demonstrate that VISTA achieves competitive clustering performance, remains robust under high attribute-missing rates, and scales efficiently to large graphs.

## 1 INTRODUCTION

Graph clustering jointly exploits node attributes and graph structure to discover latent groups of nodes without label supervision (Liu et al., 2022b; Wang et al., 2019; Tsitsulin et al., 2023). In real-world graphs, however, node attributes are not always fully observed. Privacy concerns may make some nodes' attributes inaccessible (Guo et al., 2023); data acquisition failures may leave nodes with observed connections but missing attributes (Zhao et al., 2025a); and newly introduced nodes may not yet have accumulated sufficient attribute information (Taguchi et al., 2021). Unlike missing only some feature dimensions, *node-wise attribute missingness* makes the entire feature vector unavailable for a node (Tu et al., 2024; Zhao et al., 2025a). This creates an asymmetry in the information available for clustering. Nodes with observed attributes can draw on both their own semantic information and structural relationships. In contrast, attribute-missing nodes must rely primarily on graph topology and information from other nodes to infer their cluster assignments (Chen et al., 2022; Rossi et al., 2022). Without label supervision, the model cannot use ground-truth assignments to guide how this limited and unevenly distributed information should be combined into a coherent clustering partition. The central challenge is therefore to learn discriminative representations from the remaining attributes and graph structure.

Existing research addresses this challenge by exploiting the relationship between graph topology and node attributes to recover missing semantic information and support representation learning (Chen et al., 2022; Yoo et al., 2022; Peng et al., 2024). Recovering plausible attributes, however, does not necessarily yield representations that distinguish different clusters. Clustering-specific methods therefore bring attribute recovery and clustering learning together, using the evolving clustering in-



Reviewers: please read the Reviewer Guidelines (iclr.cc/Conferences/2027/ReviewerGuidelines) and the AI Policy for Reviewers (iclr.cc/Conferences/2027/AIPolicyForReviewers). If you used AI to expand, edit, or polish your review, please provide the input text to the LLM. Better still, consider skipping the LLM and submitting your original text: we, and the authors, are much more interested in your unedited thoughts than in what an LLM has to say. AI-assisted or not, you are putting your name and reputation behind your review: LLM-generated falsehoods, hallucinations or misrepresentations are subject to disciplinary action, which may include desk-rejecting all papers you have authored.

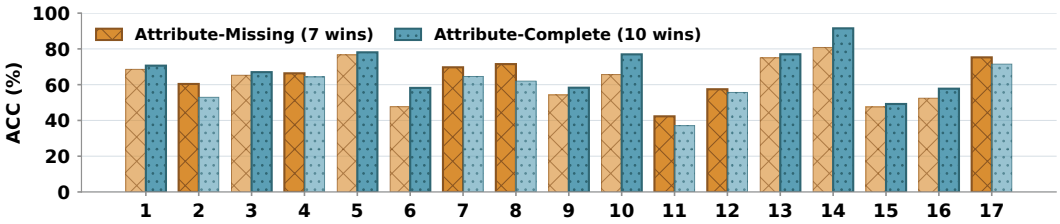


Figure 1: Motivation 1 — Are specialized methods making real progress? Across 17 comparable datasets, specialized attribute-missing methods outperform conventional graph clustering methods on only 7 datasets, while the latter lead on 10..

formation to guide recovery and the recovered information to refine node representations (Tu et al., 2024; Guan et al., 2025). This coupling is implemented through recovery modules, complementary representation views, and joint learning objectives that encourage consistent cluster assignments (Zhao et al., 2025a; Li et al., 2025b). Alongside these learned approaches, propagation-based methods directly transfer observed attributes through graph connections, providing recovered features or views for subsequent learning without a separately trained imputer (Rossi et al., 2022; Um et al., 2023; Hu et al., 2025a).

Despite these advances, improvements within a limited set of methods and datasets do not establish how broadly the benefits of specialization hold. Graph clustering encompasses diverse representation objectives and structural inductive biases (Liu et al., 2022b; Tsitsulin et al., 2023). Conventional methods already combine node attributes with graph aggregation, which provides a basis for using the information that survives attribute missingness (Bo et al., 2020; Tu et al., 2021). Assessing progress therefore calls for comparisons across method families under the same missing inputs. This motivates examining whether specialized methods consistently improve over conventional graph clustering methods when both have access to the same observed information (Figure 1). This further raises the question of whether effectively handling missing attributes requires the elaborate modeling and optimization procedures adopted by existing methods. Coupling recovery with clustering can improve task alignment (Tu et al., 2024; Zhao et al., 2025a), yet effective feature propagation and scalable neighborhood-based recovery show that useful missing-attribute processing is also possible without a separately learned imputer (Rossi et al., 2022; Hu et al., 2025a). These findings lead us to ask whether a compact framework can retain the benefits of recovery and clustering-oriented learning without elaborate reconstruction or repeated imputation–clustering feedback (Figure 2).

To address these questions, we combine systematic benchmarking with the design of **VISTA**, a streamlined framework that separates topology-based recovery from clustering-oriented learning. Our main contributions are summarized as follows:

- We establish a comprehensive and reproducible benchmark for attribute-missing graph clustering, revealing scalability limitations of specialized methods and showing that conventional attribute-complete methods often outperform them under the same missing inputs.
- We find that effective attribute-missing graph clustering hinges more on how information is organized for clustering than on elaborate pipelines. Building on this insight, we propose VISTA, a lightweight and scalable framework that decouples topology-based recovery from clustering-oriented representation learning.
- We evaluate VISTA on 22 graph datasets against 32 baselines from four method families, covering diverse missingness mechanisms and rates, and graph scales from small benchmarks to million-node networks. Results demonstrate VISTA's effectiveness, robustness, and scalability, with ablations validating its components.

## 2 Related Work

### 2.1 Graph Clustering with Complete Attributes

Research on attributed graph clustering has expanded from reconstructing graph structure to learning representations and assignments tailored to clustering. VGAE learns latent representations through

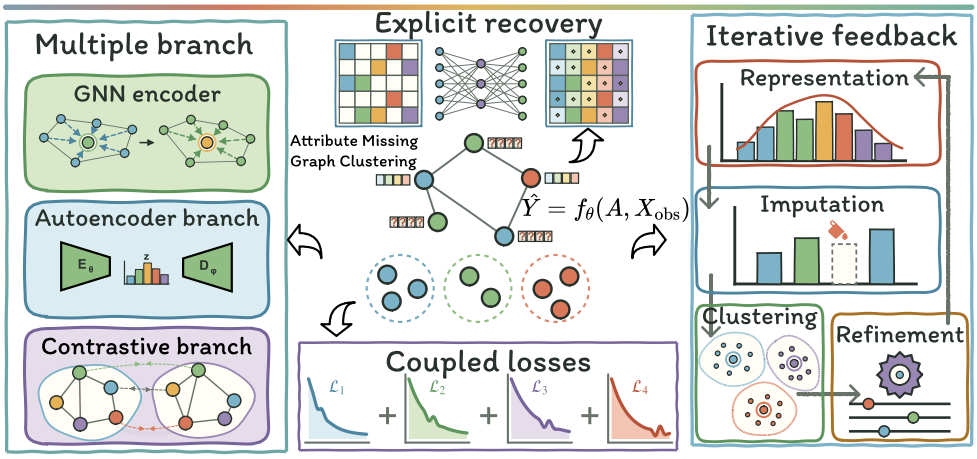


Figure 2: Motivation 2 — Is all this complexity necessary? Existing methods often rely on multiple branches, explicit recovery, coupled losses, and iterative feedback, resulting in increasingly complex pipelines whose essential components remain unclear.

graph reconstruction, while DAEGC combines attention-based reconstruction with a clustering objective (Kipf and Welling, 2016; Wang et al., 2019). SDCN and DFCN strengthen attribute–structure integration through representation transfer and fusion (Bo et al., 2020; Tu et al., 2021). Beyond reconstruction, DGI and MVGRL learn representations through local–global agreement and contrasting graph views (Veličković et al., 2019; Hassani and Khasahmadi, 2020). DCRN, HSAN, THESAURUS, and CoCo further improve discriminability through correlation reduction, hard-sample weighting, transport-based alignment, and compactness-consistency learning, respectively (Liu et al., 2022a; 2023b; Deng et al., 2025; Ju et al., 2026). At the assignment level, MinCutPool and DMoN incorporate normalized-cut and modularity objectives (Bianchi et al., 2020; Tsitsulin et al., 2023). Unlike these methods designed for complete-attribute settings, VISTA is specifically designed for attribute-missing graph clustering.

### 2.2 Attribute-Missing Graph Clustering

Work relevant to attribute-missing graph clustering follows two main directions. The first recovers usable attributes or representations for downstream tasks. GCNMF, T2-GNN, SAT, SVGA, and MATE use probabilistic modeling, distillation, or reconstruction-based learning (Taguchi et al., 2021; Huo et al., 2023; Chen et al., 2022; Yoo et al., 2022; Peng et al., 2024); FP, PCFI, and Propagate and Inject instead exploit graph propagation, confidence estimates, and feature injection (Rossi et al., 2022; Um et al., 2023; 2025). The second incorporates clustering guidance into recovery: AMGC couples imputation and clustering, while PMAGC and AMMGC exploit prototypes and cross-view consistency (Tu et al., 2024; Guan et al., 2025; Zhao et al., 2025a). MVCG and CGIR combine cluster refinement with generative imputation (Li et al., 2025b; Chen et al., 2025), whereas HCN-PAI and DTRGC use hypergraph-based partial imputation and cluster-driven hierarchical interpolation (Wang et al., 2025; Hu et al., 2025b). In contrast, VISTA revisits the necessity of complex recovery–clustering coupling through lightweight topology-based recovery and clustering-oriented representation learning.

### 2.3 Scalable Graph Clustering

Scalable graph clustering builds on advances in efficient graph learning. GraphSAGE, FastGCN, Cluster-GCN, and GraphSAINT reduce neighborhood expansion and full-graph training costs through sampling (Hamilton et al., 2017; Chen et al., 2018; Chiang et al., 2019; Zeng et al., 2020). SIGN and SSGC reduce repeated propagation through precomputation, while GGD simplifies self-supervised training through group discrimination (Frasca et al., 2020; Zhu and Koniusz, 2021; Zheng et al., 2022). Beyond efficient encoding, S3GC, Dink-Net, and MAGI adapt self-supervision and clustering objectives to large graphs (Devvrit et al., 2022; Liu et al., 2023a; 2024), while SAGSC, M-S2CAG, and ANCKA develop efficient subspace and neighbor-augmentation for-

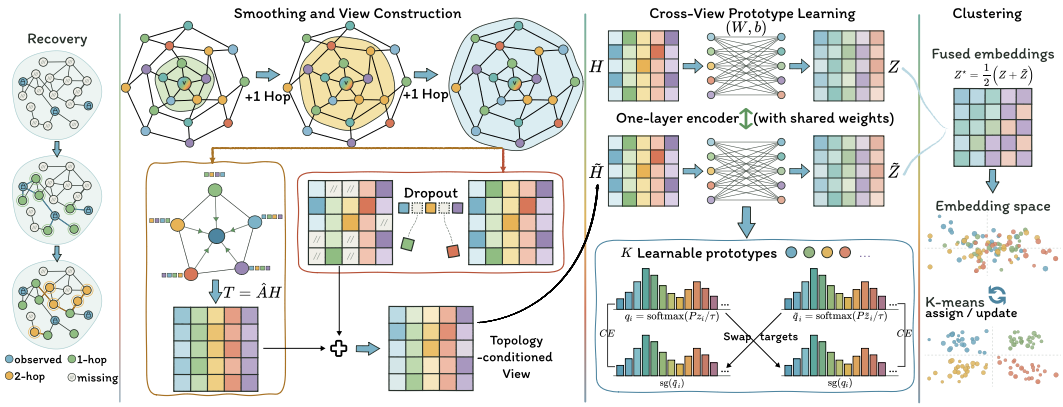


Figure 3: Overview of VISTA. VISTA recovers missing attributes via sparse topology propagation, learns clustering-oriented representations through cross-view prototype learning, and performs the final clustering with KMeans.

mulations (Fettal et al., 2023; Lin et al., 2025; Li et al., 2024). Extending scalability to incomplete inputs, CMV-ND constructs complementary neighborhood views for attribute-missing graph clustering (Hu et al., 2025a). Building on scalable graph clustering and scalable missing-attribute processing, VISTA combines efficient missing-attribute handling with clustering-oriented learning in an integrated framework.

## 3 Preliminary

Let $\mathcal{G} = (\mathcal{V}, \mathcal{E}, \mathbf{X})$ be an attributed graph with $N = |\mathcal{V}|$ nodes, adjacency matrix $\mathbf{A} \in \{0,1\}^{N \times N}$, and attributes $\mathbf{X} \in \mathbb{R}^{N \times d}$. Let $\mathcal{O}$ and $\mathcal{M}$ partition $\mathcal{V}$ into observed and missing nodes. We obtain $\mathbf{X}^{\text{obs}}$ by setting the rows indexed by $\mathcal{M}$ to zero. The self-loop normalized adjacency is $\hat{\mathbf{A}} = \mathbf{D}^{-1/2}(\mathbf{A} + \mathbf{I})\mathbf{D}^{-1/2}$, where $\mathbf{D}$ is the degree matrix of $\mathbf{A} + \mathbf{I}$. Given only $(\mathbf{A}, \mathbf{X}^{\text{obs}})$, our goal is to infer cluster assignments $\hat{y}_i \in \{1, \ldots, K\}$ without label supervision, where $K$ is predefined. Table 1 contrasts its key design choices with representative methods, while Figure 3 shows the framework.

## 4 Methodology

### 4.1 Recovery and Smoothing

Starting from $\mathbf{X}^{(0)} = \mathbf{X}^{\text{obs}}$, VISTA performs bounded attribute recovery for at most $S$ steps. Let $\mathbf{M}^{(s)} = \text{Diag}(\mathbf{m}^{(s)})$, where $m_i^{(s)} = \mathbb{I}[d_{\mathcal{G}}(i, \mathcal{O}) = s]$ indicates whether node $i$ is first reached at step $s$. Here, $d_{\mathcal{G}}(i, \mathcal{O}) = \min_{j \in \mathcal{O}} \text{dist}_{\mathcal{G}}(i, j)$ denotes the shortest distance from node $i$ to the observed node set $\mathcal{O}$. The recovery is updated as:

$$\mathbf{X}^{(s)} = \big(\mathbf{I} - \mathbf{M}^{(s)}\big)\mathbf{X}^{(s-1)} + \mathbf{M}^{(s)}\hat{\mathbf{A}}\mathbf{X}^{(s-1)}, \qquad s = 1, \ldots, S. \tag{1}$$

The first term preserves all existing rows, while the second writes propagated information only to newly reached nodes. Hence, each missing row is recovered once at its first reachable hop and remains fixed thereafter. After $S$ steps, $\bar{\mathbf{X}} = \mathbf{X}^{(S)}$, with unreached rows remaining zero.

Recovery provides missing nodes with semantic evidence but leaves observed nodes with raw attributes and recovered nodes with first-reach aggregates. To incorporate neighborhood context into both observed and recovered features before clustering-oriented learning, VISTA applies $L$ steps of fixed Laplacian smoothing:

$$\mathbf{H}^{(\ell+1)} = \hat{\mathbf{A}}\mathbf{H}^{(\ell)}, \qquad \mathbf{H}^{(0)} = \bar{\mathbf{X}}, \quad \ell = 0, \ldots, L-1. \tag{2}$$

We use $\mathbf{H} := \mathbf{H}^{(L)}$ as the smoothed base representation and compute its one-hop topology-enriched counterpart as $\mathbf{T} := \hat{\mathbf{A}}\mathbf{H}$. The extra propagation thus provides a structured source of view varia-

| Method | Venue | No learnable imputer† | Integrated clustering framework‡ | Large-scale validated§ | Broadly validated (≥10 datasets) |
|---|---|---|---|---|---|
| AMGC | AAAI 2024 | ✗ | ✓ | ✗ | ✗ |
| MVCG | ICASSP 2025 | ✗ | ✓ | ✗ | ✗ |
| AMMGC | CVPR 2025 | ✗ | ✓ | ✗ | ✗ |
| PMAGC | TMM 2025 | ✗ | ✓ | ✗ | ✗ |
| CGIR | ACM MM 2025 | ✗ | ✓ | ✗ | ✗ |
| CSAGC | Neurocomputing 2026 | ✗ | ✓ | ✗ | ✗ |
| HyperAE | ICASSP 2026 | ✗ | ✓ | ✗ | ✗ |
| HCN-PAI | ICCV 2025 | ✓ | ✓ | ✗ | ✗ |
| CMV-ND | ICML 2025 | ✓ | ✗ | ✓ | ✗ |
| DTRGC | ACM MM 2025 | ✓ | ✗ | ✗ | ✗ |
| AMGC2 | TPAMI 2026 | ✗ | ✓ | ✗ | ✗ |
| **VISTA** | Ours | ✓ | ✓ | ✓ | ✓ |

Table 1: Design coverage of attribute-missing graph clustering methods. ✓ and ✗ indicate whether a capability is demonstrated. † No learnable imputer: deterministic recovery is allowed without trained or generative imputers. ‡ Integrated clustering framework: includes representation learning and clustering objectives. § Large-scale validation: experiments on graphs with ≥100K nodes.

tion, allowing subsequent cross-view learning to encourage consistent prototype predictions under changes in neighborhood aggregation.

### 4.2 Topology-Conditioned Cross-View Learning

For cross-view learning under attribute missingness, we seek informative view variation that does not rely solely on discarding available semantic evidence. We therefore retain $\mathbf{H}$ as the base view and construct a second view by combining feature perturbation with additional neighborhood context:

$$\widetilde{\mathbf{H}} = (1-\beta)\,\mathcal{D}_\rho(\mathbf{H}) + \beta\,\mathbf{T}, \tag{3}$$

where $D_\rho$ denotes feature dropout with rate $\rho$, and $\beta \in [0,1]$ controls topology injection. We compute $T$ before dropout so that stable neighborhood information is preserved without propagating the sampled feature perturbation through the graph. As a result, the augmented view not only removes part of the available feature evidence but also increases the influence of neighborhood structure. The resulting variation therefore captures both reduced semantic evidence and stronger structural dependence, rather than merely producing a perturbed copy of $H$. This design allows topology to actively shape the view variation instead of serving only as a smoothing operator, yielding a more structurally meaningful augmentation under attribute missingness.

Fixed graph propagation aggregates neighborhood evidence but does not learn which feature combinations are useful for clustering. We therefore apply a shared one-layer encoder to the base and augmented views, learning a common feature transformation without further graph propagation:

$$\mathbf{z}_i = \mathbf{W}\mathbf{h}_i + \mathbf{b}, \qquad \widetilde{\mathbf{z}}_i = \mathbf{W}\widetilde{\mathbf{h}}_i + \mathbf{b}. \tag{4}$$

The two views encode different feature and neighborhood evidence. To provide a common reference for cross-view comparison, we introduce $K$ learnable prototypes $\mathbf{P} = [\mathbf{p}_1, \ldots, \mathbf{p}_K]^\top$ as latent anchors and express each node's relative affinities to them through the prototype distributions:

$$\mathbf{q}_i = \mathrm{softmax}(\mathbf{P}\mathbf{z}_i/\tau), \qquad \widetilde{\mathbf{q}}_i = \mathrm{softmax}(\mathbf{P}\widetilde{\mathbf{z}}_i/\tau), \tag{5}$$

where $\tau > 0$ controls distribution sharpness. Each prototype distribution captures node affinity to shared prototypes, enabling comparison in a common clustering-oriented space.

Each node and its augmented view form a natural positive pair, enabling self-supervision without complete attributes. We encourage the two views to preserve consistent nodeprototype relationships by predicting each others prototype distributions with a symmetric cross-entropy objective:

$$\mathcal{L}_{\mathrm{VISTA}} = -\frac{1}{2N}\sum_{i=1}^{N}\left[\mathrm{sg}(\widetilde{\mathbf{q}}_i)^\top \log \mathbf{q}_i + \mathrm{sg}(\mathbf{q}_i)^\top \log \widetilde{\mathbf{q}}_i\right]. \tag{6}$$

where $sg(\cdot)$ denotes the stop-gradient operator. Each view predicts the other views prototype distribution as a detached target, while both prediction terms update the shared encoder. This reciprocal constraint preserves nodeprototype consistency under feature and neighborhood perturbations, enabling robust clustering representation learning.

After training, we fuse the embeddings of the base and augmented views to integrate their complementary information and perform KMeans clustering:

$$\mathbf{Z}^{\star} = \tfrac{1}{2}\left(\mathbf{Z} + \widetilde{\mathbf{Z}}\right). \tag{7}$$

# 5 Experiments

## 5.1 Experimental Setup

**Datasets.** We evaluate on 22 graph datasets spanning diverse graph types and scales; detailed statistics are provided in Appendix A.1.

**Baselines.** We compare VISTA with 32 baselines from four categories: attribute-missing graph clustering methods (AMGC (Tu et al., 2024), MVCG (Li et al., 2025b), AMMGC (Zhao et al., 2025a), PMAGC (Guan et al., 2025), CGIR (Chen et al., 2025), CSAGC (Yu et al., 2026), HyperAE (Yang et al., 2026), and HCN-PAI (Wang et al., 2025)), conventional graph clustering methods (SDCN (Bo et al., 2020), DFCN (Tu et al., 2021), DCRN (Liu et al., 2022a), HSAN (Liu et al., 2023b), THESAURUS (Deng et al., 2025), DGAC (Xie et al., 2025), RAGC (Zhao et al., 2025b), and CoCo (Ju et al., 2026)), scalable graph clustering methods (MAGI (Liu et al., 2024), Dink-Net (Liu et al., 2023a), S3GC (Devvrit et al., 2022), GGD (Zheng et al., 2022), SSGC (Zhu and Koniusz, 2021), SAGSC (Fettal et al., 2023), M-S2CAG (Lin et al., 2025), and ANCKA (Li et al., 2024)), and attribute completion methods (SVGA (Yoo et al., 2022), TDAR (Li et al., 2025a), MIGDiff (Liu et al., 2026), MATE (Peng et al., 2024), AMER (Jin et al., 2023), SAT (Chen et al., 2022), ITR (Tu et al., 2022), and PCFI (Um et al., 2023)).

**Implementation Details.** Experiments are conducted under 60% node-wise attribute missingness. We prioritize official implementations and use dataset-specific configurations provided by the original papers or released code when available; otherwise, default settings are adopted. Results are reported over five random seeds (41–45) using ACC, Macro-F1, NMI, and ARI. Runs that exceed the available memory or fail to produce valid results are reported as OOM or FAIL, respectively.

## 5.2 Main Results

Table 2 compares VISTA with four families of methods on 22 datasets under a 60% attribute-missing rate. For each dataset, we select the baseline with the highest mean ACC within each family and report both its ACC and NMI. Full results are provided in Appendix A.2. Among the 17 datasets with complete results, conventional graph clustering methods achieve higher ACC than specialized attribute-missing methods on 10 datasets, while the latter lead on 7. Thus, tailoring a method to attribute-missing graphs does not inherently yield stronger clustering performance. The remaining five datasets—Flickr, TwitchGamers, Arxiv, Reddit, and Products—lack complete family-level comparisons because existing specialized methods have limited scalability on larger graphs. Overall, VISTA achieves the highest ACC on 16 of 22 datasets and the highest NMI on 17 of 22, demonstrating consistently competitive performance across diverse graph scales and datasets.

## 5.3 Mechanism Analysis

To examine sensitivity to the extent of missingness, we increase the node-wise attribute-missing rate from 40% to 95%, evaluating at intervals of five percentage points. As shown in Figure 4, VISTA maintains a consistent advantage on most datasets as the missing rate increases, with only a few exceptions concentrated primarily on Computers. This suggests that the observed performance fluctuations are not widespread. Overall, VISTA retains a stable relative advantage even at higher missing rates, demonstrating robustness to changes in the extent of missingness. The corresponding NMI, Macro-F1, and ARI results in Appendix A.3 show the same overall trend.

| Dataset | AM | CG | SC | AC | VISTA |
|---|---|---|---|---|---|
| | HyperAE | DGAC | S3GC | MIGDiff | |
| Cora | 68.57 | 70.63 | 70.10 | 69.33 | **72.70** |
| | 48.58 | 50.72 | 53.56 | 50.61 | **54.97** |
| | HyperAE | DCRN | ANCKA | MATE | |
| CiteSeer | 60.39 | 52.94 | 60.21 | 56.21 | **65.37** |
| | 32.30 | 28.38 | 33.14 | 28.03 | **37.67** |
| | PMAGC | THESAURUS | MAGI | MATE | |
| DBLP | 65.28 | 67.00 | 67.95 | 66.44 | **78.26** |
| | 32.67 | 31.97 | 28.39 | 33.28 | **47.03** |
| | AMMGC | DCRN | M-S2CAG | TDAR | |
| PubMed | 66.35 | 64.32 | 70.33 | 68.12 | **70.70** |
| | 25.86 | 26.91 | 28.41 | 28.24 | **32.29** |
| | AMMGC | THESAURUS | ANCKA | AMER | |
| Photo | 76.65 | 78.09 | 76.42 | 74.67 | **78.61** |
| | 67.60 | 68.42 | 66.86 | 63.25 | **71.40** |
| | | | Dink-Net | | |
| Flickr | — | — | **39.09** | — | 33.12 |
| | | | 5.18 | | **7.83** |
| | AMGC | DGAC | ANCKA | SVGA | |
| BlogCatalog | 47.65 | 58.19 | **65.64** | 45.68 | 62.49 |
| | 30.34 | 36.55 | **40.11** | 27.27 | 38.02 |
| | HCN-PAI | RAGC | M-S2CAG | MATE | |
| USPS | 69.71 | 64.58 | 73.59 | 73.67 | **91.81** |
| | 67.01 | 57.03 | 73.64 | 72.24 | **83.68** |
| | AMMGC | DGAC | M-S2CAG | TDAR | |
| HHAR | 71.50 | 62.02 | 78.93 | 71.51 | **79.70** |
| | 67.17 | 62.95 | **75.86** | 72.66 | 74.91 |
| | AMMGC | RAGC | SAGSC | SAT | |
| EAT | 54.24 | **58.30** | 45.26 | 49.32 | 58.25 |
| | 30.77 | 34.21 | 24.66 | 28.02 | **34.38** |
| | AMMGC | HSAN | SAGSC | SAT | |
| BAT | 65.65 | 76.95 | 50.84 | 59.85 | **80.61** |
| | 46.93 | 52.53 | 24.95 | 41.08 | **56.77** |

| Dataset | AM | CG | SC | AC | VISTA |
|---|---|---|---|---|---|
| | AMMGC | DGAC | SAGSC | MATE | |
| CoraFull | 42.29 | 37.07 | 38.36 | 40.12 | **42.42** |
| | 54.30 | 48.30 | 52.74 | 53.81 | **54.48** |
| | PMAGC | DGAC | M-S2CAG | MATE | |
| Computers | 57.44 | 55.65 | 60.33 | 63.94 | **64.02** |
| | 51.95 | **54.20** | 52.99 | 50.91 | 54.07 |
| | AMMGC | CoCo | ANCKA | MATE | |
| CS | 74.98 | 77.00 | 70.74 | 70.22 | **81.54** |
| | 71.51 | 71.90 | 72.77 | 72.36 | **75.34** |
| | HCN-PAI | CoCo | SSGC | SVGA | |
| Physics | 80.80 | 91.50 | 88.78 | 86.23 | **92.31** |
| | 60.28 | 75.05 | 71.81 | 68.75 | **76.06** |
| | AMMGC | DGAC | ANCKA | TDAR | |
| Wiki | 47.52 | 49.19 | 45.44 | 45.82 | **52.68** |
| | 40.64 | 46.11 | 41.67 | 44.92 | **47.22** |
| | AMMGC | RAGC | SAGSC | MATE | |
| UAT | 52.45 | **57.75** | 46.59 | 48.97 | 54.69 |
| | 23.87 | **27.05** | 17.75 | 19.28 | 25.92 |
| | CSAGC | THESAURUS | M-S2CAG | MIGDiff | |
| ACM | 75.27 | 71.51 | 80.26 | 77.98 | **82.84** |
| | 42.12 | 34.67 | 48.17 | 39.74 | **50.84** |
| | | | SSGC | | |
| Twitch Gamers | — | — | 54.90 | — | **58.89** |
| | | | 0.59 | | **2.15** |
| | | | SAGSC | | |
| Arxiv | — | — | 48.02 | — | **48.21** |
| | | | **45.72** | | 45.04 |
| | | | MAGI | | |
| Reddit | — | — | **88.90** | — | 87.18 |
| | | | 85.50 | | **85.97** |
| | | | ANCKA | | |
| Products | — | — | **50.06** | — | 45.45 |
| | | | 50.96 | | **54.20** |

Table 2: Best-per-family ACC and NMI compared with VISTA. AM: attribute-missing graph clustering; CG: conventional graph clustering; SC: scalable graph clustering; AC: attribute completion.

**Robustness to Non-Random Missingness.** Existing attribute-missing graph clustering methods are primarily evaluated under random missingness, while their robustness to non-random missingness mechanisms remains insufficiently explored. To address this gap, we further consider high-degree and high-norm missingness at a fixed 60% node-wise attribute-missing rate, making missingness dependent on graph structure and node attributes, respectively. Full results are provided in Appendix C. Table 3 presents representative datasets covering diverse graph structures, scales, and clustering characteristics. VISTA maintains a consistent advantage under both non-random missingness mechanisms. This indicates that VISTA's performance does not rely on the assumption of uniformly random missingness.

**Ablation Analysis.**

We analyze the contribution of each VISTA component, including bounded attribute recovery (BAR), Laplacian smoothing (LS), and topology-conditioned view construction (TV). The complete model consists of BAR+LS+TV. The w/o variants remove one component from the complete model, whereas the component-only variants retain only the corresponding input construction with

| Metric | VISTA | w/o TV | w/o BAR | w/o LS | LS-only | BAR-only | Raw-only | LS+KMeans |
|---|---|---|---|---|---|---|---|---|
| ACC | **71.12** | 70.61 | 70.58 | 52.97 | 69.58 | 51.08 | 33.40 | 57.93 |
| F1 | **67.42** | 66.86 | 66.75 | 48.88 | 65.93 | 46.78 | 26.66 | 51.61 |
| NMI | **53.83** | 53.22 | 53.11 | 34.17 | 52.27 | 31.72 | 14.54 | 43.69 |
| ARI | **50.10** | 49.54 | 49.71 | 26.70 | 48.45 | 24.31 | 2.73 | 36.60 |

Table 4: Macro-average results for the VISTA ablation study.

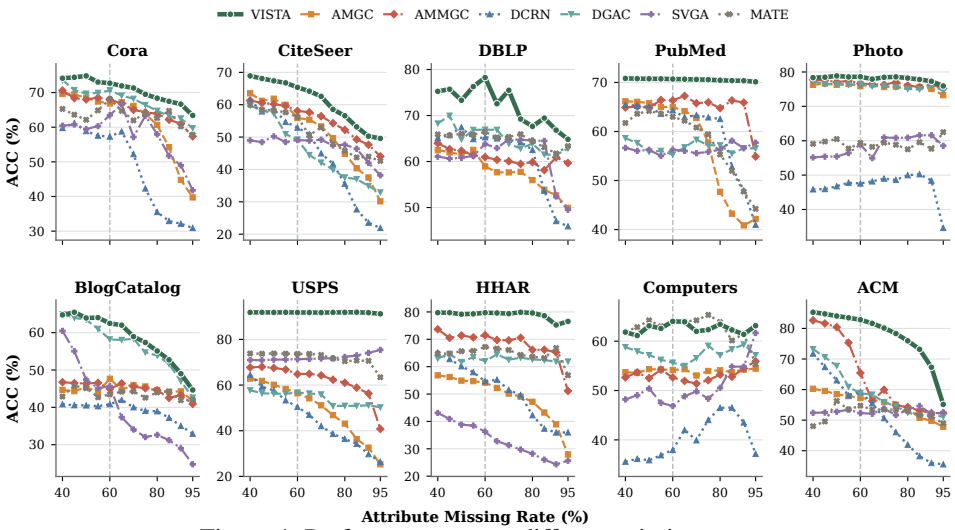


Figure 4: Performance across different missing rates.

| Missingness | Dataset | Metric | SDCN | DGAC | THESAURUS | AMGC | AMMGC | HCN-PAI | SVGA | VISTA |
|---|---|---|---|---|---|---|---|---|---|---|
| High-degree | ACM | ACC | 46.70 ± 1.40 | 52.75 ± 1.90 | 53.17 ± 1.66 | 43.54 ± 8.30 | 68.40 ± 10.28 | 57.26 ± 4.89 | 53.32 ± 0.97 | **85.45 ± 0.49** |
| | | F1 | 46.73 ± 1.17 | 52.96 ± 1.67 | 54.18 ± 1.74 | 38.57 ± 7.17 | 68.38 ± 10.40 | 56.27 ± 4.48 | 54.60 ± 0.96 | **85.44 ± 0.48** |
| | | NMI | 11.11 ± 0.81 | 16.99 ± 2.04 | 20.08 ± 2.20 | 9.74 ± 15.69 | 37.62 ± 6.96 | 29.24 ± 3.23 | 26.49 ± 0.94 | **55.06 ± 1.35** |
| | | ARI | 6.42 ± 1.38 | 14.70 ± 3.15 | 15.33 ± 1.60 | 9.62 ± 15.02 | 38.22 ± 10.45 | 24.34 ± 6.20 | 18.43 ± 1.95 | **61.25 ± 1.24** |
| | USPS | ACC | 36.42 ± 2.59 | 55.91 ± 2.12 | 56.59 ± 1.77 | 61.17 ± 2.58 | 61.41 ± 1.61 | 69.36 ± 0.37 | 70.56 ± 0.60 | **91.96 ± 0.14** |
| | | F1 | 39.22 ± 1.27 | 53.45 ± 2.32 | 54.77 ± 1.61 | 59.99 ± 3.10 | 60.64 ± 1.78 | 67.50 ± 0.43 | 68.74 ± 0.59 | **91.28 ± 0.15** |
| | | NMI | 35.26 ± 0.99 | 58.79 ± 2.45 | 48.89 ± 1.19 | 51.52 ± 1.06 | 56.32 ± 1.39 | 66.24 ± 0.56 | 69.91 ± 0.48 | **83.98 ± 0.20** |
| | | ARI | 6.59 ± 1.17 | 42.88 ± 2.94 | 40.27 ± 1.60 | 43.16 ± 1.39 | 46.32 ± 1.04 | 58.63 ± 0.74 | 60.59 ± 0.77 | **84.75 ± 0.27** |
| | CS | ACC | 42.35 ± 3.20 | 68.55 ± 1.56 | 68.16 ± 0.78 | 75.42 ± 0.73 | 76.27 ± 1.34 | 61.58 ± 1.07 | 67.03 ± 1.74 | **81.10 ± 1.27** |
| | | F1 | 20.19 ± 3.08 | 63.31 ± 1.85 | 59.54 ± 1.66 | 71.73 ± 1.24 | 70.14 ± 1.53 | 50.93 ± 2.15 | 66.71 ± 1.82 | **76.30 ± 3.50** |
| | | NMI | 37.21 ± 4.82 | 72.41 ± 0.45 | 72.70 ± 1.00 | 76.40 ± 0.47 | 73.95 ± 0.88 | 61.08 ± 1.56 | 75.02 ± 1.00 | **77.06 ± 0.57** |
| | | ARI | 26.62 ± 3.69 | 60.74 ± 2.12 | 62.15 ± 1.27 | 67.47 ± 0.46 | 68.01 ± 1.09 | 51.91 ± 2.14 | 59.99 ± 3.08 | **75.90 ± 3.59** |
| High-norm | ACM | ACC | 48.20 ± 2.29 | 57.85 ± 1.55 | 77.57 ± 1.52 | 58.21 ± 1.32 | 63.21 ± 8.51 | 59.03 ± 6.33 | 53.30 ± 0.76 | **82.86 ± 0.26** |
| | | F1 | 42.83 ± 2.07 | 57.91 ± 2.52 | 77.71 ± 1.45 | 55.72 ± 1.45 | 62.19 ± 9.10 | 58.08 ± 6.47 | 54.68 ± 0.74 | **82.97 ± 0.37** |
| | | NMI | 9.81 ± 4.58 | 19.52 ± 2.34 | 42.94 ± 2.77 | 35.35 ± 1.03 | 36.01 ± 5.28 | 21.83 ± 3.66 | 28.07 ± 1.08 | **50.96 ± 0.70** |
| | | ARI | 8.39 ± 6.22 | 17.18 ± 4.04 | 43.11 ± 2.84 | 34.85 ± 0.85 | 35.17 ± 6.60 | 21.56 ± 3.87 | 20.33 ± 1.35 | **54.75 ± 0.33** |
| | USPS | ACC | 45.62 ± 1.97 | 54.01 ± 1.62 | 41.80 ± 3.37 | 51.14 ± 0.73 | 64.88 ± 1.94 | 63.96 ± 3.41 | 72.96 ± 0.90 | **90.61 ± 0.21** |
| | | F1 | 44.85 ± 2.89 | 49.68 ± 2.28 | 41.87 ± 3.57 | 53.42 ± 0.86 | 63.24 ± 2.57 | 62.22 ± 3.88 | 71.10 ± 0.74 | **89.70 ± 0.23** |
| | | NMI | 44.24 ± 1.06 | 59.18 ± 1.09 | 36.77 ± 2.31 | 44.84 ± 0.53 | 59.69 ± 2.53 | 58.92 ± 1.88 | 73.23 ± 0.60 | **81.91 ± 0.26** |
| | | ARI | 15.00 ± 0.83 | 42.39 ± 1.86 | 19.92 ± 2.19 | 26.13 ± 0.36 | 50.01 ± 2.47 | 49.93 ± 2.65 | 64.39 ± 0.92 | **82.52 ± 0.34** |
| | CS | ACC | 41.22 ± 5.33 | 67.47 ± 1.79 | 66.69 ± 1.43 | 72.22 ± 0.89 | 72.41 ± 1.76 | 62.24 ± 0.76 | 69.27 ± 4.86 | **80.23 ± 2.06** |
| | | F1 | 17.39 ± 2.97 | 61.62 ± 2.69 | 56.20 ± 3.35 | 66.21 ± 1.56 | 65.41 ± 4.47 | 50.52 ± 1.63 | 67.61 ± 5.36 | **73.51 ± 2.43** |
| | | NMI | 37.58 ± 7.50 | 71.20 ± 0.94 | 68.89 ± 1.05 | 73.48 ± 0.19 | 71.85 ± 1.35 | 60.36 ± 2.05 | 74.10 ± 1.04 | **74.97 ± 0.50** |
| | | ARI | 28.10 ± 9.32 | 60.08 ± 1.24 | 59.02 ± 1.30 | 64.80 ± 0.50 | 65.42 ± 0.98 | 52.19 ± 1.37 | 61.78 ± 4.61 | **75.92 ± 0.72** |

Table 3: Clustering results under high-degree and high-norm missingness.

the shared learner; LS+KMeans directly clusters the smoothed representation without the learner. As shown in Table 4, the complete VISTA achieves the best overall performance. Within this ablation study, LS provides the largest performance contribution, while BAR and TV introduce complementary improvements. In addition, the gap between LS-only and LS+KMeans demonstrates the effectiveness of the VISTA learner beyond topology smoothing. Complete dataset-level results are deferred to Appendix B.

**Comparison of Attribute Recovery Strategies.** To examine attribute recovery strategies and how their outputs are used, we compare three representative approaches: FP recovers missing attributes through feature propagation, DTRGC uses clustering-driven hierarchical interpolation, and BAR is VISTA's bounded attribute recovery. We also use CMV-ND to construct multi-hop neighborhood representations and examine how recovered information is organized. Table 5 reports the macro-average results, with full dataset-level results provided in Appendix D. When the recovery outputs are held fixed, the shared learner generally outperforms direct clustering. Under the same FP recovery and encoder capacity, FP-VISTA performs better overall than FP-CMV-VISTA. When the CMV representations and learner are kept unchanged, replacing FP with BAR does not yield an overall improvement. These results suggest that recovering usable attributes alone is not sufficient for effec-

| Metric | Fixed representations + KMeans | | | Shared VISTA learner | | | | Reference |
|---|---|---|---|---|---|---|---|---|
| | FP-KMeans | FP-CMV-KMeans | DTRGC-KMeans | FP-VISTA | FP-CMV-VISTA | DTRGC-VISTA | BAR-CMV-VISTA | VISTA (Ours) |
| ACC | 41.81 | 45.36 | 32.04 | 58.84 | 50.74 | 40.94 | 49.57 | **71.12** |
| F1 | 34.29 | 37.01 | 17.80 | 53.88 | 46.11 | 31.88 | 45.29 | **67.42** |
| NMI | 27.40 | 32.42 | 8.47 | 46.00 | 35.63 | 20.08 | 33.90 | **53.83** |
| ARI | 15.33 | 22.39 | 5.12 | 37.49 | 26.86 | 13.47 | 25.48 | **50.10** |

Table 5: Macro-average results for attribute recovery strategies.

tive clustering. More complex recovery or additional views do not necessarily improve performance; what matters is how the recovered information is organized and incorporated into clustering-oriented representation learning.

**Transferability of the Recovery Module.**

To examine whether bounded attribute recovery provides transferable benefits beyond VISTA, we prepend one BAR step and one smoothing step (BAR+LS) to five existing clustering learners: CoCo, Dink-Net, SDCN, SAGSC, and GGD. Figure 5 summarizes the mean gains over their original results, with full dataset-level results provided in Appendix D.1. BAR+LS consistently improves all evaluated learners across all metrics, with the largest gains observed for SDCN and GGD. These results suggest that topology-guided recovery can provide useful semantic evidence independently of VISTAs representation learning framework.

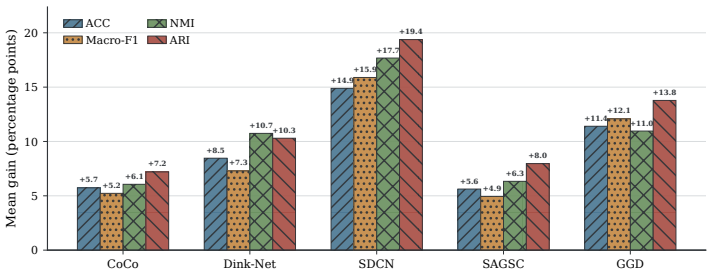


Figure 5: Mean gains from BAR+LS over the corresponding raw results.

**Computational Efficiency.** Table 6 summarizes the average runtime and peak GPU memory of existing specialized attribute-missing graph clustering methods and VISTA across benchmark datasets. VISTA maintains consistently low computational costs in both runtime and memory usage, while several existing specialized methods incur substantially higher overhead due to more complex recovery or clustering procedures. These results demonstrate that VISTA achieves competitive clustering performance without introducing additional computational complexity. Detailed dataset-level efficiency comparisons and scaling analysis are provided in Appendices J and K.

| Metric | VISTA | AMGC | MVCG | AMMGC | PMAGC | CGIR | CSAGC | HyperAE | HCN-PAI |
|---|---|---|---|---|---|---|---|---|---|
| Time (s) | **16.97** | 3748.51 | 701.28 | 273.54 | 165.49 | 1314.99 | 330.30 | 404.56 | 142.13 |
| GPU (GiB) | **2.12** | 3.13 | 13.21 | 6.29 | 3.93 | 7.81 | 10.94 | 10.48 | 6.40 |

Table 6: Average runtime and peak GPU memory across benchmark datasets.

## 6 Conclusion

This work revisits progress in attribute-missing graph clustering and establishes a comprehensive, reproducible benchmark. Our results show that methods specifically designed for attribute-missing graphs do not necessarily outperform conventional graph clustering methods, and that greater model complexity is not a prerequisite for strong performance. Motivated by these findings, we introduce VISTA and demonstrate its competitive clustering performance, robustness, and scalability across varying missing rates, missingness mechanisms, and graph scales.

## AI USE STATEMENT

Generative AI tools were used for language editing and assistance with code implementation and debugging. All AI-assisted text and code were reviewed and verified by the authors. The authors take full responsibility for the final content of this work.

## REFERENCES


Filippo Maria Bianchi, Daniele Grattarola, and Cesare Alippi. Spectral clustering with graph neural networks for graph pooling. In *Proceedings of ICML*, pages 874–883, 2020. https://proceedings.mlr.press/v119/bianchi20a.html.

Deyu Bo, Xiao Wang, Chuan Shi, Meiqi Zhu, Emiao Lu, and Peng Cui. Structural deep clustering network. In *Proceedings of the Web Conference*, pages 1400–1410, 2020.

Jie Chen, Tengfei Ma, and Cao Xiao. FastGCN: Fast learning with graph convolutional networks via importance sampling. In *Proceedings of ICLR*, 2018. https://openreview.net/forum?id=rytstxWAW.

Xu Chen, Siheng Chen, Jiangchao Yao, Huangjie Zheng, Ya Zhang, and Ivor W. Tsang. Learning on attribute-missing graphs. *IEEE Transactions on Pattern Analysis and Machine Intelligence*, 44(2):740–757, 2022.

Mulin Chen, Bocheng Wang, Jiaxin Zhong, Zongcheng Miao, and Xuelong Li. Clustering-oriented generative attribute graph imputation. In *Proceedings of ACM Multimedia*, 2025.

Wei-Lin Chiang, Xuanqing Liu, Si Si, Yang Li, Samy Bengio, and Cho-Jui Hsieh. Cluster-GCN: An efficient algorithm for training deep and large graph convolutional networks. In *Proceedings of KDD*, pages 257–266, 2019.

Bowen Deng, Tong Wang, Lele Fu, Sheng Huang, Chuan Chen, and Tao Zhang. THESAURUS: Contrastive graph clustering by swapping fused Gromov-Wasserstein couplings. In *Proceedings of the AAAI Conference on Artificial Intelligence*, 39(15):16199–16207, 2025.

Fnu Devvrit, Aditya Sinha, Inderjit Dhillon, and Prateek Jain. S3GC: Scalable self-supervised graph clustering. In *Advances in Neural Information Processing Systems*, 35:3248–3261, 2022.

Chakib Fettal, Lazhar Labiod, and Mohamed Nadif. Scalable attributed-graph subspace clustering. In *Proceedings of the AAAI Conference on Artificial Intelligence*, 2023.

Fabrizio Frasca, Emanuele Rossi, Davide Eynard, Ben Chamberlain, Michael Bronstein, and Federico Monti. SIGN: Scalable inception graph neural networks. arXiv preprint arXiv:2004.11198, 2020.

Renxiang Guan, Wenxuan Tu, Dayu Hu, Weixuan Liang, Ke Liang, Yaowen Hu, Yue Liu, and Xinwang Liu. Prototype-driven multi-view attribute-missing graph clustering. *IEEE Transactions on Multimedia*, 27, 2025.

Dongliang Guo, Zhixuan Chu, and Sheng Li. Fair attribute completion on graph with missing attributes. In *Proceedings of ICLR*, 2023. https://openreview.net/forum?id=9vcXCMp9VEp.

William Hamilton, Zhitao Ying, and Jure Leskovec. Inductive representation learning on large graphs. In *Advances in Neural Information Processing Systems*, 30, 2017.

Kaveh Hassani and Amir Hosein Khasahmadi. Contrastive multi-view representation learning on graphs. In *Proceedings of ICML*, pages 4116–4126, 2020.

Yaowen Hu, Wenxuan Tu, Yue Liu, Xinhang Wan, Junyi Yan, Taichun Zhou, and Xinwang Liu. Scalable attribute-missing graph clustering via neighborhood differentiation. In *Proceedings of ICML*, pages 71865–71883, 2025.

Yaowen Hu, Wenxuan Tu, Yue Liu, Miaomiao Li, Wenpeng Lu, and others. Divide-Then-Rule: A cluster-driven hierarchical interpolator for attribute-missing graphs. In *Proceedings of ACM Multimedia*, 2025.

Cuiying Huo, Di Jin, Yawen Li, Dongxiao He, Yu-Bin Yang, and Lingfei Wu. T2-GNN: Graph neural networks for graphs with incomplete features and structure via teacher-student distillation. In *Proceedings of the AAAI Conference on Artificial Intelligence*, 37(4):4339–4346, 2023.

Di Jin, Rui Wang, Tao Wang, Dongxiao He, Weiping Ding, Yuxiao Huang, Longbiao Wang, and Witold Pedrycz. AMER: A new attribute-missing network embedding approach. *IEEE Transactions on Cybernetics*, 53(7):4306–4319, 2023.

Wei Ju, Siyu Yi, Kangjie Zheng, Yifan Wang, Ziyue Qiao, Li Shen, Yongdao Zhou, Xiaochun Cao, and Jiancheng Lv. Compactness and consistency: A conjoint framework for deep graph clustering. In *Proceedings of ICLR*, 2026. https://openreview.net/forum?id=9jdQLmPUHW.

Thomas N. Kipf and Max Welling. Variational graph auto-encoders. arXiv preprint arXiv:1611.07308, 2016.

Mengran Li, Junzhou Chen, Chenyun Yu, Guanying Jiang, Ronghui Zhang, Yanming Shen, and Houbing Herbert Song. Topology-driven attribute recovery for attribute missing graph learning in social Internet of Things. *IEEE Internet of Things Journal*, 12(11), 2025.

Shijun Li, Changjian Wang, Kele Xu, Xiaojin Li, Gaojin He, and Xu Liu. Mutual-view contrastive generative framework for attribute-missing graph clustering. In *Proceedings of ICASSP*, pages 1–5, 2025.

Yiran Li, Gongyao Guo, Jieming Shi, Renchi Yang, Shiqi Shen, Qing Li, and Jun Luo. A versatile framework for attributed network clustering via K-nearest neighbor augmentation. *The VLDB Journal*, 33(6):1913–1943, 2024.

Xiaoyang Lin, Renchi Yang, Haoran Zheng, and Xiangyu Ke. Spectral subspace clustering for attributed graphs. In *Proceedings of KDD*, pages 789–799, 2025.

Ye Liu, Yang Chen, and Hongmin Cai. MIGDiff: Multi-attributes imputations for attribute-missing graphs via graph denoising diffusion model. In *Proceedings of the AAAI Conference on Artificial Intelligence*, 40(18):15369–15376, 2026.

Yue Liu, Wenxuan Tu, Sihang Zhou, Xinwang Liu, Linxuan Song, Xihong Yang, and En Zhu. Deep graph clustering via dual correlation reduction. In *Proceedings of the AAAI Conference on Artificial Intelligence*, 36(7):7603–7611, 2022.

Yue Liu, Jun Xia, Sihang Zhou, Xihong Yang, Ke Liang, Chenchen Fan, Yan Zhuang, Stan Z. Li, Xinwang Liu, and Kunlun He. A survey of deep graph clustering: Taxonomy, challenge, application, and open resource. arXiv preprint arXiv:2211.12875, 2022.

Yue Liu, Ke Liang, Jun Xia, Sihang Zhou, Xihong Yang, Xinwang Liu, and Z. Stan Li. Dink-Net: Neural clustering on large graphs. In *Proceedings of ICML*, pages 21794–21812, 2023.

Yue Liu, Xihong Yang, Sihang Zhou, Xinwang Liu, Zhen Wang, Ke Liang, Wenxuan Tu, Liang Li, Jingcan Duan, and Cancan Chen. Hard sample aware network for contrastive deep graph clustering. In *Proceedings of the AAAI Conference on Artificial Intelligence*, 37:8914–8922, 2023.

Yunfei Liu, Jintang Li, Yuehe Chen, Ruofan Wu, Baokun Wang, Jing Zhou, Sheng Tian, Shuheng Shen, Xing Fu, Changhua Meng, Weiqiang Wang, and Liang Chen. Revisiting modularity maximization for graph clustering: A contrastive learning perspective. In *Proceedings of KDD*, 2024.

Shengsheng Pan, Ruiqi Hu, Shixian Fung, Guodong Long, Jing Jiang, and Chengqi Zhang. Learning graph embedding with adversarial training methods. *IEEE Transactions on Cybernetics*, 50(6):2475–2487, 2019.

Xin Peng, Jieren Cheng, Xiangyan Tang, Bin Zhang, and Wenxuan Tu. Multi-view graph imputation network. *Information Fusion*, 102:102024, 2024.

Emanuele Rossi, Henry Kenlay, Maria I. Gorinova, Benjamin P. Chamberlain, Xiaowen Dong, and Michael M. Bronstein. On the unreasonable effectiveness of feature propagation in learning on graphs with missing node features. In *Learning on Graphs Conference*, pages 11–1, 2022.

Hibiki Taguchi, Xin Liu, and Tsuyoshi Murata. Graph convolutional networks for graphs containing missing features. *Future Generation Computer Systems*, 117:155–168, 2021.

Anton Tsitsulin, John Palowitch, Bryan Perozzi, and Emmanuel Müller. Graph clustering with graph neural networks. *Journal of Machine Learning Research*, 24(127):1–21, 2023.

Wenxuan Tu, Sihang Zhou, Xinwang Liu, Xifeng Guo, Zhiping Cai, En Zhu, and Jieren Cheng. Deep fusion clustering network. In *Proceedings of the AAAI Conference on Artificial Intelligence*, 35:9978–9987, 2021.

Wenxuan Tu, Sihang Zhou, Xinwang Liu, Yue Liu, Zhiping Cai, En Zhu, Changwang Zhang, and Jieren Cheng. Initializing then refining: A simple graph attribute imputation network. In *Proceedings of IJCAI*, pages 3494–3500, 2022.

Wenxuan Tu, Renxiang Guan, Sihang Zhou, Chuan Ma, Xin Peng, Zhiping Cai, Zhe Liu, Jieren Cheng, and Xinwang Liu. Attribute-missing graph clustering network. In *Proceedings of the AAAI Conference on Artificial Intelligence*, 38:15392–15401, 2024.

Daeho Um, Jiwoong Park, Seulki Park, and Jin Young Choi. Confidence-based feature imputation for graphs with partially known features. In *Proceedings of ICLR*, 2023.

Daeho Um, Sunoh Kim, Jiwoong Park, Jongin Lim, Seong Jin Ahn, and Seulki Park. Propagate and inject: Revisiting propagation-based feature imputation for graphs with partially observed features. In *Proceedings of ICML*, pages 60530–60560, 2025. https://proceedings.mlr.press/v267/um25a.html.

Petar Veličković, William Fedus, William L. Hamilton, Pietro Liò, Yoshua Bengio, and R Devon Hjelm. Deep graph infomax. In *Proceedings of ICLR*, 2019. https://openreview.net/forum?id=rklz9iAcKQ.

Chun Wang, Shirui Pan, Ruiqi Hu, Guodong Long, Jing Jiang, and Chengqi Zhang. Attributed graph clustering: A deep attentional embedding approach. arXiv preprint arXiv:1906.06532, 2019.

Qianqian Wang, Bowen Zhao, Zhengming Ding, Wei Feng, and Quanxue Gao. Hypergraph clustering network with partial attribute imputation. In *Proceedings of ICCV*, pages 2697–2706, 2025.

Kun Xie, Renchi Yang, and Sibo Wang. Diffusion-based graph-agnostic clustering. In *Proceedings of the ACM Web Conference*, pages 1353–1364, 2025.

Ze Yang, Changjian Wang, Yuanpu Cai, Tiange Jiao, Weiguo Chen, Shijun Li, Tianpeng Yang, and Zhengsheng Peng. Hypergraph-based asymmetric embedding framework for attribute-missing graph clustering. In *Proceedings of ICASSP*, 2026.

Jaemin Yoo, Hyunsik Jeon, Jinhong Jung, and U Kang. Accurate node feature estimation with structured variational graph autoencoder. In *Proceedings of KDD*, pages 2336–2346, 2022.

Yingxing Yu, Jingjing Song, Xibei Yang, Keyu Liu, Ming Zhang, and Eric C. C. Tsang. Cross-view structure awareness network for attribute-missing graph clustering. *Neurocomputing*, 696:134067, 2026.

Hanqing Zeng, Hongkuan Zhou, Ajitesh Srivastava, Rajgopal Kannan, and Viktor Prasanna. Graph-SAINT: Graph sampling based inductive learning method. In *Proceedings of ICLR*, 2020. https://openreview.net/forum?id=BJe8pkHFwS.

Bowen Zhao, Qianqian Wang, Zhengming Ding, and Quanxue Gao. Attribute-missing multi-view graph clustering. In *Proceedings of CVPR*, 2025.

Tianxiang Zhao, Youqing Wang, Jinlu Wang, Jiapu Wang, Mingliang Cui, Junbin Gao, and Jipeng Guo. Hybrid-collaborative augmentation and contrastive sample adaptive-differential awareness for robust attributed graph clustering. In *Advances in Neural Information Processing Systems*, 2025.

Yizhen Zheng, Shirui Pan, Vincent C. S. Lee, Yu Zheng, and Philip S. Yu. Rethinking and scaling up graph contrastive learning: An extremely efficient approach with group discrimination. In *Advances in Neural Information Processing Systems*, 2022.

Hao Zhu and Piotr Koniusz. Simple spectral graph convolution. In *Proceedings of ICLR*, 2021. https://openreview.net/forum?id=CYO5T-YjWZV.

# A Full Benchmark Results

## A.1 Dataset Statistics

We use 22 datasets spanning diverse sources, graph structures, and scales, including academic networks, social and content networks, product co-purchase graphs, transportation networks, and graphs constructed from non-graph data. The benchmark ranges from BAT with 131 nodes to Products with 2,449,029 nodes, and covers between 2 and 70 classes. This range combines classic small benchmarks with medium- and large-scale graphs, allowing us to evaluate both clustering quality and scalability. Table 7 reports the number of nodes, edges, attribute dimensions, and classes for all datasets. Edge counts follow the stored graph representation; undirected edges are counted in both directions when represented by bidirectional edge indices.

**Academic and bibliographic networks.** Cora, CiteSeer, and PubMed are citation networks in which nodes represent papers, edges represent citations, and attributes are derived primarily from paper text. DBLP and CoraFull provide larger or more fine-grained bibliographic settings, with CoraFull covering 70 classes. ACM is another paper network with three research classes, while CS and Physics are co-authorship networks whose attributes describe research topics. Arxiv further extends this group to a large paper network with 40 research areas and text-derived attributes.

**Social and content networks.** BlogCatalog represents a social network of blog users with keyword-based attributes. Flickr, TwitchGamers, and Reddit provide larger online-network settings, while Wiki represents a network of Wikipedia pages and their links. These datasets introduce social, interaction, and text-content relations that differ from citation and co-authorship graphs.

**Product co-purchase networks.** Photo and Computers are Amazon product co-purchase graphs in which nodes represent products and edges connect frequently co-purchased items; their attributes are derived from product review text. Products extends this setting to more than 2.4 million nodes and 47 product classes, providing the largest scalability test in the benchmark.

**Non-graph data and transportation networks.** USPS contains handwritten-digit samples represented by 256-dimensional pixel features, and HHAR contains sensor records from human-activity recognition with 561 attributes. Their graph versions are constructed from sample relationships, allowing evaluation beyond naturally occurring networks. EAT, BAT, and UAT are transportation graphs from different regions, adding graph structures that are distinct from academic, social, and product networks.

## A.2 Benchmark Results by Method Family

Tables 8–11 report ACC, Macro-F1, NMI, and ARI for attribute-missing, conventional, scalable, and attribute-completion methods, respectively. Each table includes VISTA as a common reference under the shared benchmark protocol. Reporting the metrics together reveals both differences within each family and cases where label-matching accuracy, class-balanced performance, and partition agreement favor different methods.

Among the attribute-missing methods in Table 8, the strongest baseline changes across datasets and sometimes across metrics on the same dataset. Their strengths are therefore complementary rather than concentrated in one consistently dominant approach. VISTA's improvements over this family generally extend beyond ACC to the other clustering measures, while some baselines remain competitive on individual metrics. This broader pattern distinguishes improvements in overall clustering quality from advantages confined to a particular score.

Table 9 shows substantial variation within the conventional family. Strong results are distributed across multiple methods, with relative performance changing across datasets. Therefore, the best-of-family comparison does not imply that any single conventional method is consistently effective under missing attributes. VISTA remains competitive against this diverse set of alternatives.

For the scalable methods in Table 10, execution coverage and clustering quality provide distinct information. Several methods produce results on large graphs, but their relative rankings still vary across datasets and metrics. In particular, a leading ACC result does not always coincide with the strongest Macro-F1 or NMI, making the joint assessment of these measures important. VISTA combines broad execution coverage with competitive scores, while other scalable methods remain

| Dataset | Nodes | Edges | Dim. | Classes |
|---|---|---|---|---|
| Cora | 2,708 | 10,556 | 1,433 | 7 |
| CiteSeer | 3,327 | 9,104 | 3,703 | 6 |
| DBLP | 17,716 | 105,734 | 1,639 | 4 |
| PubMed | 19,717 | 88,648 | 500 | 3 |
| Photo | 7,650 | 238,162 | 745 | 8 |
| Flickr | 89,250 | 899,756 | 500 | 7 |
| BlogCatalog | 5,196 | 343,486 | 8,189 | 6 |
| USPS | 9,298 | 27,894 | 256 | 10 |
| HHAR | 10,299 | 30,897 | 561 | 6 |
| EAT | 399 | 11,988 | 203 | 4 |
| BAT | 131 | 2,077 | 81 | 4 |
| CoraFull | 19,793 | 126,842 | 8,710 | 70 |
| Computers | 13,752 | 491,722 | 767 | 10 |
| CS | 18,333 | 163,788 | 6,805 | 15 |
| Physics | 34,493 | 495,924 | 8,415 | 5 |
| Wiki | 2,405 | 17,981 | 4,973 | 17 |
| UAT | 1,190 | 27,198 | 239 | 4 |
| ACM | 3,025 | 26,256 | 1,870 | 3 |
| TwitchGamers | 168,114 | 13,595,114 | 7 | 2 |
| Arxiv | 169,343 | 2,315,598 | 128 | 40 |
| Reddit | 232,965 | 114,615,892 | 602 | 41 |
| Products | 2,449,029 | 123,718,152 | 100 | 47 |

Table 7: Dataset statistics.

strong competitors. Resource and execution failures are recorded separately from numerical scores rather than treated as poor clustering results.

The attribute-completion methods in Table 11 also exhibit dataset-dependent strengths: different completion pipelines provide the closest comparisons to VISTA in different settings. Their clustering results reflect the complete pipeline, including both attribute completion and subsequent representation learning, rather than reconstruction quality in isolation. The variation therefore motivates examining how completed attributes are used downstream, not merely whether a completion stage is present. The controlled comparisons in Appendix D examine these choices more directly.

### A.3 Robustness to Different Missing Rates

Figures 6–8 report NMI, Macro-F1, and ARI across different missing rates, complementing the ACC results in Figure 4. As the missing rate increases from 40% to 95% in five-percentage-point increments, different methods exhibit varying degrees of performance degradation. Nevertheless, VISTA maintains a relative advantage on most datasets across the evaluated range, indicating robustness to different degrees of attribute information loss.

The curves show pronounced degradation for some baselines as the missing rate increases, whereas VISTA retains competitive performance in many of these settings. This pattern is consistent with VISTA's use of the remaining semantic evidence and graph structure. Specifically, VISTA recovers missing semantic information through local topology and subsequently combines structural propagation with clustering-oriented representation learning. This design allows the limited observed information to be exploited more fully, helping the resulting representations retain discriminative power even at high missing rates.

Importantly, this robustness does not mean that VISTA is entirely insensitive to the missing rate. As missingness increases, the initial attribute evidence available for semantic recovery diminishes, and VISTA's performance also declines on some datasets. However, it retains a relative advantage in most settings. Robustness here therefore refers primarily to maintaining relative competitiveness

| Dataset | Metric | AMGC | MVCG | AMMGC | PMAGC | CGIR | CSAGC | HyperAE | HCN-PAI | VISTA |
|---|---|---|---|---|---|---|---|---|---|---|
| Cora | ACC | 66.84 ± 1.88 | 64.76 ± 1.13 | 67.95 ± 1.89 | 65.81 ± 0.76 | 60.27 ± 2.14 | 57.05 ± 3.54 | 68.57 ± 0.63 | 60.13 ± 2.19 | **72.70 ± 1.65** |
| | F1 | 61.13 ± 1.92 | 59.78 ± 1.96 | 66.04 ± 2.50 | 63.74 ± 1.23 | 59.41 ± 1.42 | 55.63 ± 3.05 | 63.96 ± 1.38 | 58.45 ± 2.62 | **70.23 ± 1.70** |
| | NMI | 48.32 ± 1.36 | 43.45 ± 1.63 | 50.88 ± 1.32 | 47.66 ± 1.22 | 40.77 ± 1.28 | 38.19 ± 2.54 | 48.58 ± 0.62 | 42.58 ± 2.06 | **54.97 ± 1.96** |
| | ARI | 43.23 ± 1.72 | 39.39 ± 1.91 | 44.28 ± 1.76 | 41.74 ± 0.58 | 32.14 ± 1.99 | 31.03 ± 3.77 | 44.70 ± 1.22 | 34.86 ± 2.41 | **50.98 ± 4.13** |
| CiteSeer | ACC | 55.87 ± 2.57 | 51.58 ± 2.49 | 58.10 ± 1.52 | 53.08 ± 1.10 | 48.76 ± 1.72 | 54.60 ± 4.31 | 60.39 ± 1.21 | 46.79 ± 2.20 | **65.37 ± 0.75** |
| | F1 | 51.89 ± 2.66 | 48.68 ± 2.57 | 54.41 ± 1.40 | 51.50 ± 1.93 | 48.72 ± 2.09 | 52.37 ± 4.20 | 56.49 ± 1.31 | 44.39 ± 2.25 | **60.22 ± 0.96** |
| | NMI | 30.21 ± 1.21 | 25.41 ± 1.82 | 30.18 ± 1.13 | 28.24 ± 1.06 | 24.06 ± 1.73 | 28.89 ± 2.63 | 32.30 ± 1.10 | 20.93 ± 2.14 | **37.67 ± 0.71** |
| | ARI | 29.59 ± 1.58 | 23.08 ± 2.38 | 29.59 ± 1.61 | 25.55 ± 0.79 | 18.72 ± 2.15 | 24.40 ± 5.43 | 32.89 ± 1.30 | 19.57 ± 1.87 | **39.69 ± 0.67** |
| DBLP | ACC | 58.93 ± 1.27 | 62.73 ± 2.85 | 60.95 ± 1.45 | 65.28 ± 0.40 | 56.55 ± 2.05 | 59.35 ± 1.18 | 63.13 ± 0.85 | 57.14 ± 0.24 | **78.26 ± 0.24** |
| | F1 | 53.78 ± 1.25 | 51.17 ± 5.50 | 54.23 ± 2.27 | 53.96 ± 3.43 | 38.46 ± 0.43 | 50.32 ± 1.04 | 49.65 ± 1.14 | 51.08 ± 0.33 | **73.95 ± 0.32** |
| | NMI | 30.16 ± 0.72 | 29.32 ± 2.92 | 31.84 ± 1.08 | 32.67 ± 0.93 | 21.48 ± 2.66 | 25.89 ± 0.48 | 31.79 ± 2.85 | 30.61 ± 0.65 | **47.03 ± 0.50** |
| | ARI | 31.07 ± 1.56 | 32.42 ± 3.71 | 34.60 ± 1.45 | 40.84 ± 0.29 | 25.91 ± 2.07 | 27.02 ± 1.31 | 33.34 ± 2.98 | 32.95 ± 0.52 | **52.06 ± 0.44** |
| PubMed | ACC | 65.02 ± 1.01 | 60.76 ± 2.43 | 66.35 ± 2.55 | 45.76 ± 0.48 | 49.46 ± 3.50 | 42.15 ± 1.59 | 60.23 ± 2.53 | 61.47 ± 0.84 | **70.70 ± 0.25** |
| | F1 | 64.75 ± 0.70 | 60.56 ± 2.53 | 66.07 ± 2.09 | 36.54 ± 0.81 | 42.99 ± 6.44 | 41.20 ± 1.87 | 58.99 ± 2.53 | 61.47 ± 0.89 | **69.86 ± 0.22** |
| | NMI | 25.59 ± 2.27 | 21.71 ± 3.44 | 25.86 ± 4.02 | 12.72 ± 0.90 | 9.79 ± 2.96 | 4.17 ± 1.76 | 22.71 ± 4.39 | 18.12 ± 1.35 | **32.29 ± 0.24** |
| | ARI | 25.22 ± 1.84 | 20.00 ± 3.47 | 26.31 ± 4.38 | 10.34 ± 0.80 | 6.91 ± 3.32 | 3.16 ± 1.09 | 21.05 ± 4.37 | 18.05 ± 1.20 | **33.10 ± 0.47** |
| Photo | ACC | 75.89 ± 0.92 | 73.32 ± 2.78 | 76.65 ± 1.26 | 76.54 ± 1.74 | 62.09 ± 4.83 | 62.78 ± 0.89 | 76.13 ± 0.86 | 54.39 ± 2.53 | **78.61 ± 0.95** |
| | F1 | 70.44 ± 1.13 | 66.35 ± 3.70 | 72.22 ± 0.46 | 71.81 ± 1.90 | 57.57 ± 4.37 | 61.14 ± 1.04 | 71.46 ± 1.43 | 42.95 ± 3.27 | **73.56 ± 1.19** |
| | NMI | 66.33 ± 0.73 | 62.73 ± 2.59 | 67.60 ± 2.21 | 67.64 ± 1.34 | 50.38 ± 3.89 | 49.88 ± 1.34 | 64.73 ± 1.29 | 42.25 ± 3.21 | **71.40 ± 0.98** |
| | ARI | 56.76 ± 0.56 | 53.36 ± 2.67 | 58.34 ± 1.94 | 58.27 ± 1.50 | 35.55 ± 5.20 | 38.64 ± 1.55 | 57.54 ± 1.24 | 32.90 ± 2.20 | **61.47 ± 1.68** |
| BlogCatalog | ACC | 47.65 ± 1.71 | 38.72 ± 2.54 | 44.94 ± 1.17 | 39.53 ± 1.48 | 40.27 ± 1.50 | 46.77 ± 2.59 | 42.04 ± 1.66 | 39.94 ± 1.92 | **62.49 ± 1.08** |
| | F1 | 45.24 ± 2.02 | 36.99 ± 3.07 | 44.92 ± 1.17 | 38.41 ± 1.46 | 35.25 ± 0.76 | 45.83 ± 3.11 | 37.58 ± 1.11 | 35.37 ± 1.42 | **60.10 ± 1.86** |
| | NMI | 30.34 ± 1.07 | 18.48 ± 2.55 | 23.96 ± 0.43 | 20.05 ± 3.74 | 22.89 ± 0.64 | 24.30 ± 2.32 | 23.92 ± 3.07 | 22.12 ± 1.67 | **38.02 ± 0.78** |
| | ARI | 23.32 ± 1.94 | 10.96 ± 2.62 | 17.25 ± 0.63 | 11.94 ± 2.39 | 11.02 ± 2.04 | 20.23 ± 1.88 | 13.10 ± 1.30 | 13.06 ± 1.55 | **33.19 ± 0.83** |
| USPS | ACC | 56.39 ± 1.76 | 55.93 ± 2.48 | 64.81 ± 3.00 | 60.08 ± 1.31 | 51.33 ± 2.42 | 62.60 ± 2.50 | 56.50 ± 3.10 | 69.71 ± 0.92 | **91.81 ± 0.06** |
| | F1 | 58.12 ± 1.89 | 57.31 ± 2.95 | 62.66 ± 3.94 | 58.83 ± 1.22 | 53.83 ± 2.33 | 61.43 ± 2.68 | 58.04 ± 3.62 | 68.06 ± 1.02 | **91.13 ± 0.09** |
| | NMI | 46.95 ± 1.50 | 48.16 ± 1.23 | 61.04 ± 2.25 | 54.33 ± 0.70 | 43.95 ± 2.31 | 58.22 ± 2.04 | 51.23 ± 1.50 | 67.01 ± 1.15 | **83.68 ± 0.11** |
| | ARI | 32.68 ± 1.60 | 33.51 ± 1.27 | 51.12 ± 2.38 | 43.28 ± 1.53 | 25.00 ± 5.06 | 48.61 ± 2.36 | 35.37 ± 1.72 | 59.18 ± 1.59 | **84.42 ± 0.10** |
| HHAR | ACC | 54.16 ± 1.53 | 51.88 ± 1.62 | 71.50 ± 3.24 | 68.90 ± 4.94 | 52.96 ± 1.69 | 57.22 ± 0.60 | 56.57 ± 1.28 | 52.44 ± 3.11 | **79.70 ± 1.61** |
| | F1 | 52.83 ± 1.09 | 50.23 ± 1.44 | 69.46 ± 4.43 | 69.10 ± 5.40 | 53.40 ± 1.72 | 56.28 ± 0.80 | 53.65 ± 2.85 | 50.33 ± 3.61 | **78.91 ± 3.11** |
| | NMI | 50.08 ± 1.63 | 49.63 ± 1.72 | 67.17 ± 3.82 | 59.53 ± 2.95 | 49.21 ± 1.83 | 50.39 ± 1.29 | 54.23 ± 1.20 | 48.24 ± 2.34 | **74.91 ± 1.68** |
| | ARI | 38.22 ± 2.63 | 37.50 ± 2.55 | 60.55 ± 4.12 | 51.03 ± 4.64 | 33.15 ± 2.02 | 38.89 ± 1.86 | 44.17 ± 1.47 | 33.94 ± 3.32 | **66.32 ± 1.37** |
| EAT | ACC | 34.54 ± 0.78 | 34.54 ± 0.25 | 54.24 ± 1.82 | 49.02 ± 0.56 | 44.51 ± 0.85 | 48.77 ± 1.35 | 45.36 ± 2.40 | 40.30 ± 1.46 | **58.25 ± 0.23** |
| | F1 | 28.67 ± 1.53 | 28.72 ± 1.42 | 51.22 ± 1.25 | 44.40 ± 0.60 | 38.35 ± 3.51 | 47.52 ± 1.58 | 42.45 ± 2.93 | 36.75 ± 1.31 | **58.42 ± 0.21** |
| | NMI | 7.60 ± 1.07 | 6.96 ± 0.85 | 30.77 ± 2.17 | 26.60 ± 0.18 | 22.53 ± 2.26 | 22.61 ± 1.29 | 14.86 ± 1.44 | 12.55 ± 5.61 | **34.38 ± 0.18** |
| | ARI | 3.78 ± 0.76 | 3.10 ± 0.43 | **27.88 ± 2.29** | 24.10 ± 0.15 | 19.26 ± 1.97 | 19.32 ± 1.29 | 13.57 ± 1.89 | 9.93 ± 4.52 | 27.83 ± 0.29 |
| BAT | ACC | 47.02 ± 5.89 | 38.32 ± 1.48 | 65.65 ± 0.68 | 51.60 ± 4.44 | 55.57 ± 4.98 | 33.13 ± 1.14 | 51.45 ± 3.66 | 50.23 ± 1.89 | **80.61 ± 1.02** |
| | F1 | 44.07 ± 6.81 | 34.61 ± 3.37 | 61.94 ± 0.64 | 46.91 ± 4.22 | 51.62 ± 6.45 | 25.01 ± 1.83 | 50.13 ± 4.03 | 46.90 ± 3.95 | **80.65 ± 0.97** |
| | NMI | 25.48 ± 4.75 | 13.24 ± 2.31 | 46.93 ± 0.78 | 37.36 ± 3.48 | 38.45 ± 3.84 | 12.83 ± 2.26 | 24.77 ± 3.24 | 26.20 ± 8.01 | **56.77 ± 1.52** |
| | ARI | 17.54 ± 6.30 | 5.83 ± 2.64 | 41.61 ± 0.88 | 28.54 ± 5.28 | 29.44 ± 4.14 | 1.32 ± 0.51 | 18.36 ± 4.20 | 19.54 ± 7.74 | **55.76 ± 2.13** |
| CoraFull | ACC | 39.13 ± 0.52 | 31.19 ± 0.77 | 42.29 ± 1.05 | 32.33 ± 0.45 | 27.14 ± 0.92 | 24.64 ± 0.89 | 32.96 ± 1.03 | 23.51 ± 0.60 | **42.42 ± 0.43** |
| | F1 | 32.86 ± 0.44 | 26.12 ± 1.06 | **34.42 ± 0.73** | 26.53 ± 0.54 | 22.15 ± 0.76 | 18.86 ± 0.71 | 25.48 ± 1.45 | 16.01 ± 0.78 | 33.62 ± 0.68 |
| | NMI | 53.62 ± 0.11 | 45.27 ± 0.56 | 54.30 ± 0.31 | 48.61 ± 0.38 | 43.29 ± 0.85 | 39.61 ± 0.86 | 46.86 ± 0.85 | 36.36 ± 1.17 | **54.48 ± 0.28** |
| | ARI | 27.03 ± 0.32 | 18.20 ± 1.30 | **30.29 ± 1.13** | 21.32 ± 0.34 | 16.75 ± 0.69 | 15.35 ± 0.49 | 21.98 ± 0.48 | 15.55 ± 0.58 | 29.47 ± 0.77 |
| Computers | ACC | 54.16 ± 0.94 | 57.02 ± 1.21 | 52.65 ± 2.89 | 57.44 ± 1.30 | 47.85 ± 2.46 | 40.49 ± 1.06 | 57.22 ± 1.94 | 48.51 ± 0.95 | **64.02 ± 3.93** |
| | F1 | 40.07 ± 0.86 | 41.26 ± 1.37 | 47.28 ± 1.80 | 49.16 ± 1.86 | 36.92 ± 3.66 | 27.90 ± 1.99 | 42.43 ± 0.59 | 20.13 ± 2.19 | **53.62 ± 2.75** |
| | NMI | 50.23 ± 1.45 | 49.59 ± 1.16 | 50.21 ± 2.44 | 51.95 ± 1.78 | 41.08 ± 2.32 | 30.75 ± 3.27 | 50.46 ± 0.59 | 24.92 ± 1.22 | **54.07 ± 1.80** |
| | ARI | 38.17 ± 1.41 | 39.50 ± 1.80 | 33.62 ± 3.47 | 39.99 ± 1.56 | 25.48 ± 3.10 | 24.04 ± 1.18 | 39.51 ± 1.87 | 26.65 ± 2.64 | **45.07 ± 6.16** |
| CS | ACC | 73.73 ± 0.59 | 62.50 ± 2.90 | 74.98 ± 1.31 | 70.19 ± 1.13 | 69.54 ± 1.10 | 73.04 ± 2.05 | 69.27 ± 1.55 | 61.82 ± 1.32 | **81.54 ± 3.27** |
| | F1 | 68.87 ± 1.49 | 54.56 ± 3.89 | 67.64 ± 3.23 | 62.98 ± 2.88 | 60.01 ± 2.03 | 60.61 ± 2.11 | 61.02 ± 1.68 | 50.07 ± 1.84 | **74.36 ± 4.26** |
| | NMI | 74.21 ± 0.27 | 63.50 ± 1.94 | 71.51 ± 0.81 | 70.51 ± 0.66 | 67.30 ± 0.71 | 66.94 ± 1.55 | 68.06 ± 1.20 | 60.10 ± 0.60 | **75.34 ± 0.72** |
| | ARI | 65.81 ± 0.42 | 54.47 ± 2.26 | 66.40 ± 1.66 | 60.87 ± 0.82 | 59.89 ± 0.69 | 64.64 ± 2.35 | 62.54 ± 1.42 | 51.52 ± 1.53 | **76.52 ± 1.78** |
| Physics | ACC | 56.68 ± 2.81 | 75.05 ± 11.76 | 76.78 ± 7.54 | 72.91 ± 4.41 | 73.36 ± 1.46 | OOM | 76.24 ± 4.27 | 80.80 ± 0.27 | **92.31 ± 0.26** |
| | F1 | 55.70 ± 3.14 | 69.59 ± 10.14 | 68.17 ± 12.68 | 63.92 ± 6.93 | 62.95 ± 8.25 | | 66.69 ± 6.00 | 66.71 ± 0.73 | **89.37 ± 0.39** |
| | NMI | 58.21 ± 2.33 | 61.09 ± 5.56 | 59.39 ± 8.98 | 55.52 ± 3.73 | 57.64 ± 1.49 | | 57.91 ± 3.28 | 60.28 ± 0.74 | **76.06 ± 0.39** |
| | ARI | 45.16 ± 3.12 | 63.75 ± 14.33 | 63.14 ± 10.87 | 59.84 ± 6.24 | 62.02 ± 6.53 | | 60.68 ± 5.98 | 72.11 ± 0.76 | **85.32 ± 0.33** |
| Wiki | ACC | 40.69 ± 2.75 | 30.06 ± 1.15 | 47.52 ± 1.38 | 35.48 ± 1.74 | 32.87 ± 0.73 | 46.43 ± 1.06 | 32.17 ± 1.01 | 36.23 ± 2.11 | **52.68 ± 1.22** |
| | F1 | 36.47 ± 2.14 | 26.52 ± 1.60 | 40.40 ± 0.71 | 32.93 ± 1.42 | 29.29 ± 1.64 | 40.40 ± 1.48 | 28.80 ± 1.60 | 31.39 ± 2.50 | **42.97 ± 1.12** |
| | NMI | 39.78 ± 1.46 | 24.66 ± 1.59 | 40.64 ± 0.59 | 32.00 ± 2.28 | 28.91 ± 1.80 | 42.31 ± 1.13 | 27.86 ± 2.33 | 31.19 ± 3.27 | **47.22 ± 1.06** |
| | ARI | 19.32 ± 2.62 | 7.63 ± 1.02 | 27.09 ± 1.10 | 14.36 ± 2.04 | 8.36 ± 1.50 | 25.58 ± 1.47 | 10.87 ± 0.90 | 13.43 ± 2.03 | **31.11 ± 0.65** |
| UAT | ACC | 45.46 ± 2.09 | 47.48 ± 0.82 | 52.45 ± 1.44 | 50.89 ± 1.41 | 43.55 ± 3.73 | 49.68 ± 0.36 | 47.06 ± 1.87 | 50.59 ± 0.46 | **54.69 ± 1.99** |
| | F1 | 42.27 ± 2.69 | 44.59 ± 1.69 | 50.04 ± 1.63 | 48.63 ± 1.86 | 41.09 ± 5.02 | 48.83 ± 0.96 | 42.65 ± 2.26 | 47.80 ± 0.46 | **52.56 ± 5.60** |
| | NMI | 15.11 ± 2.48 | 17.60 ± 0.86 | 23.87 ± 1.36 | 21.45 ± 0.83 | 16.79 ± 4.84 | 18.94 ± 1.06 | 18.29 ± 2.29 | 17.38 ± 0.69 | **25.92 ± 2.40** |
| | ARI | 12.35 ± 2.34 | 16.79 ± 0.83 | 21.49 ± 0.86 | 20.85 ± 1.05 | 12.16 ± 4.28 | 17.18 ± 0.77 | 16.37 ± 2.77 | 14.92 ± 0.83 | **24.03 ± 1.69** |
| ACM | ACC | 57.24 ± 0.52 | 54.63 ± 4.34 | 65.43 ± 10.80 | 73.25 ± 2.90 | 65.97 ± 2.75 | 75.27 ± 1.34 | 58.83 ± 0.81 | 52.46 ± 1.51 | **82.84 ± 0.78** |
| | F1 | 54.04 ± 0.75 | 53.45 ± 4.67 | 64.12 ± 12.13 | 73.40 ± 2.77 | 65.73 ± 2.58 | 75.88 ± 1.31 | 54.76 ± 0.98 | 53.06 ± 1.17 | **82.69 ± 0.78** |
| | NMI | 36.59 ± 0.78 | 14.64 ± 5.40 | 38.35 ± 5.41 | 36.66 ± 2.77 | 32.26 ± 3.93 | 42.12 ± 1.87 | 33.56 ± 2.27 | 17.94 ± 2.85 | **50.84 ± 1.64** |
| | ARI | 34.96 ± 0.76 | 15.01 ± 5.02 | 37.91 ± 6.88 | 35.13 ± 5.57 | 24.04 ± 2.75 | 39.76 ± 2.41 | 33.17 ± 1.73 | 15.05 ± 2.41 | **55.32 ± 1.74** |

Table 8: Comparison with attribute-missing graph clustering methods.

as information becomes scarcer, rather than keeping absolute performance unchanged. These results support the effectiveness of combining lightweight attribute recovery with clustering-oriented learning across different degrees of missingness.

Taken together, Figure 4 and Figures 6–8 show that VISTA's strength lies not in eliminating the performance loss caused by missing attributes, but in retaining useful clustering information as the available evidence decreases. By combining local attribute recovery, graph propagation, and

| Dataset | Metric | SDCN | DFCN | DCRN | HSAN | THESAURUS | DGAC | RAGC | CoCo | VISTA |
|---|---|---|---|---|---|---|---|---|---|---|
| Cora | ACC | 36.41 ± 3.65 | 47.17 ± 1.69 | 57.30 ± 1.75 | 59.22 ± 1.18 | 68.38 ± 1.67 | 70.63 ± 1.55 | 63.01 ± 1.42 | 62.32 ± 3.59 | **72.70 ± 1.65** |
| | F1 | 21.50 ± 4.30 | 43.47 ± 3.38 | 45.12 ± 0.52 | 59.67 ± 1.39 | 65.90 ± 2.91 | 68.11 ± 2.15 | 62.10 ± 1.62 | 56.46 ± 2.56 | **70.23 ± 1.70** |
| | NMI | 13.46 ± 6.24 | 32.59 ± 2.12 | 39.69 ± 2.07 | 42.76 ± 1.66 | 49.16 ± 0.94 | 50.72 ± 0.85 | 45.45 ± 1.92 | 39.53 ± 2.77 | **54.97 ± 1.96** |
| | ARI | 8.19 ± 5.63 | 20.52 ± 2.46 | 30.65 ± 2.48 | 33.71 ± 0.98 | 44.62 ± 2.59 | 47.87 ± 2.46 | 38.55 ± 1.81 | 31.02 ± 4.71 | **50.98 ± 4.13** |
| CiteSeer | ACC | 31.36 ± 1.28 | 46.16 ± 3.01 | 52.94 ± 2.16 | 45.43 ± 1.04 | 50.97 ± 2.50 | 49.24 ± 2.24 | 45.40 ± 1.81 | 44.85 ± 1.98 | **65.37 ± 0.75** |
| | F1 | 23.93 ± 1.77 | 43.76 ± 4.24 | 48.38 ± 2.48 | 45.40 ± 3.56 | 48.11 ± 2.20 | 43.18 ± 2.53 | 46.96 ± 2.24 | 40.64 ± 1.55 | **60.22 ± 0.96** |
| | NMI | 10.51 ± 2.39 | 23.71 ± 3.86 | 28.38 ± 1.01 | 24.09 ± 1.54 | 26.05 ± 1.65 | 22.02 ± 1.79 | 23.99 ± 2.10 | 23.06 ± 3.39 | **37.67 ± 0.71** |
| | ARI | 4.00 ± 1.92 | 15.93 ± 4.33 | 20.19 ± 0.91 | 14.71 ± 1.28 | 23.87 ± 2.63 | 16.19 ± 2.37 | 15.33 ± 1.46 | 12.66 ± 1.40 | **39.69 ± 0.67** |
| DBLP | ACC | 49.35 ± 2.53 | 62.35 ± 4.13 | 65.28 ± 2.14 | OOM | 67.00 ± 3.73 | 66.92 ± 3.53 | OOM | 56.72 ± 2.90 | **78.26 ± 0.24** |
| | F1 | 30.85 ± 5.99 | 45.81 ± 4.55 | 43.59 ± 6.75 | | 60.64 ± 3.92 | 55.15 ± 6.75 | | 48.90 ± 3.88 | **73.95 ± 0.32** |
| | NMI | 6.50 ± 3.79 | 29.23 ± 2.22 | 32.35 ± 1.60 | | 31.97 ± 3.88 | 31.59 ± 3.39 | | 21.70 ± 2.62 | **47.03 ± 0.50** |
| | ARI | 7.24 ± 3.92 | 34.27 ± 4.22 | 36.85 ± 1.45 | | 38.38 ± 4.09 | 35.41 ± 4.57 | | 22.42 ± 0.99 | **52.06 ± 0.44** |
| PubMed | ACC | 46.79 ± 2.35 | 60.91 ± 3.97 | 64.32 ± 3.44 | OOM | 40.80 ± 0.81 | 55.28 ± 3.49 | OOM | 54.77 ± 3.49 | **70.70 ± 0.25** |
| | F1 | 36.96 ± 3.00 | 56.74 ± 9.05 | 60.67 ± 8.82 | | 33.99 ± 2.34 | 43.11 ± 1.92 | | 52.64 ± 4.11 | **69.86 ± 0.22** |
| | NMI | 3.81 ± 2.33 | 24.07 ± 5.36 | 26.91 ± 4.59 | | 0.92 ± 0.86 | 9.58 ± 2.58 | | 11.56 ± 5.77 | **32.29 ± 0.24** |
| | ARI | 3.54 ± 2.60 | 21.52 ± 6.97 | 24.20 ± 6.46 | | 1.31 ± 1.17 | 11.30 ± 3.69 | | 12.11 ± 3.56 | **33.10 ± 0.47** |
| Photo | ACC | 36.40 ± 4.92 | 60.44 ± 5.35 | 47.58 ± 2.97 | 68.37 ± 0.69 | 78.09 ± 1.77 | 76.49 ± 1.41 | 69.96 ± 1.33 | 53.40 ± 2.22 | **78.61 ± 0.95** |
| | F1 | 20.64 ± 4.65 | 51.80 ± 6.14 | 42.15 ± 3.73 | 65.76 ± 0.94 | 73.48 ± 1.82 | 73.04 ± 1.80 | 67.76 ± 1.80 | 50.85 ± 3.08 | **73.56 ± 1.19** |
| | NMI | 19.99 ± 7.66 | 49.65 ± 4.64 | 35.65 ± 5.29 | 53.88 ± 1.34 | 68.42 ± 2.69 | 66.55 ± 1.29 | 57.75 ± 2.28 | 40.38 ± 3.03 | **71.40 ± 0.98** |
| | ARI | 12.15 ± 8.01 | 39.16 ± 5.63 | 21.90 ± 4.29 | 45.55 ± 1.02 | 60.56 ± 3.07 | 58.53 ± 1.54 | 48.20 ± 2.22 | 28.39 ± 3.17 | **61.47 ± 1.68** |
| BlogCatalog | ACC | 25.43 ± 2.58 | 37.49 ± 1.71 | 40.86 ± 1.62 | 44.65 ± 2.39 | 36.10 ± 3.27 | 58.19 ± 3.05 | 44.52 ± 2.00 | 44.43 ± 2.61 | **62.49 ± 1.08** |
| | F1 | 14.44 ± 2.08 | 32.35 ± 2.97 | 35.35 ± 2.74 | 41.83 ± 2.75 | 35.36 ± 3.22 | 57.41 ± 2.35 | 41.72 ± 2.61 | 40.33 ± 3.44 | **60.10 ± 1.86** |
| | NMI | 6.34 ± 3.27 | 22.49 ± 1.03 | 23.97 ± 1.29 | 27.10 ± 2.00 | 15.10 ± 1.37 | 36.55 ± 1.26 | 27.02 ± 1.86 | 27.46 ± 1.85 | **38.02 ± 0.78** |
| | ARI | 3.58 ± 2.39 | 12.03 ± 0.88 | 12.99 ± 2.34 | 16.61 ± 3.84 | 10.30 ± 1.43 | 28.81 ± 2.38 | 16.68 ± 3.71 | 16.87 ± 3.75 | **33.19 ± 0.83** |
| USPS | ACC | 34.63 ± 1.48 | 41.43 ± 5.45 | 50.41 ± 1.68 | 62.67 ± 1.11 | 47.75 ± 3.84 | 56.72 ± 1.76 | 64.58 ± 0.65 | 64.23 ± 1.52 | **91.81 ± 0.06** |
| | F1 | 37.19 ± 3.28 | 38.93 ± 4.48 | 48.45 ± 1.75 | 63.67 ± 0.95 | 48.25 ± 4.45 | 54.28 ± 1.69 | 65.53 ± 1.04 | 65.13 ± 1.39 | **91.13 ± 0.09** |
| | NMI | 34.43 ± 3.30 | 43.47 ± 7.90 | 50.30 ± 2.73 | 54.75 ± 0.84 | 41.00 ± 4.45 | 61.02 ± 2.23 | 57.03 ± 1.16 | 57.18 ± 1.52 | **83.68 ± 0.11** |
| | ARI | 5.41 ± 1.17 | 24.74 ± 10.04 | 30.93 ± 2.48 | 41.94 ± 1.65 | 27.21 ± 3.66 | 44.60 ± 1.62 | 45.96 ± 1.05 | 45.68 ± 2.23 | **84.42 ± 0.10** |
| HHAR | ACC | 36.51 ± 0.85 | 45.08 ± 6.74 | 54.67 ± 5.55 | 48.96 ± 0.92 | 43.85 ± 0.97 | 62.02 ± 3.16 | 55.93 ± 3.17 | 47.51 ± 0.63 | **79.70 ± 1.61** |
| | F1 | 36.34 ± 4.23 | 40.97 ± 4.80 | 53.56 ± 6.46 | 47.99 ± 1.07 | 43.50 ± 1.10 | 58.25 ± 2.67 | 58.49 ± 4.61 | 48.22 ± 0.74 | **78.91 ± 3.11** |
| | NMI | 30.34 ± 1.84 | 49.91 ± 9.45 | 56.94 ± 2.99 | 47.58 ± 1.09 | 37.13 ± 1.80 | 62.95 ± 4.64 | 47.59 ± 2.02 | 43.85 ± 0.27 | **74.91 ± 1.68** |
| | ARI | 8.28 ± 2.11 | 35.20 ± 13.39 | 39.88 ± 4.25 | 34.17 ± 0.83 | 23.01 ± 2.56 | 49.07 ± 5.55 | 33.07 ± 1.52 | 27.30 ± 0.69 | **66.32 ± 1.37** |
| EAT | ACC | 31.43 ± 0.70 | 32.28 ± 1.95 | 47.82 ± 1.39 | 58.20 ± 0.49 | 56.64 ± 0.61 | 51.58 ± 1.33 | **58.30 ± 0.38** | 55.99 ± 0.41 | 58.25 ± 0.23 |
| | F1 | 21.68 ± 1.20 | 24.58 ± 3.07 | 43.56 ± 4.39 | 58.19 ± 0.49 | 56.99 ± 0.55 | 48.58 ± 2.45 | 58.37 ± 0.30 | 55.34 ± 0.99 | **58.42 ± 0.21** |
| | NMI | 6.63 ± 2.02 | 6.04 ± 1.99 | 29.36 ± 2.65 | **34.61 ± 0.28** | 32.70 ± 0.99 | 25.63 ± 1.93 | 34.21 ± 0.38 | 31.90 ± 1.99 | 34.38 ± 0.18 |
| | ARI | 1.37 ± 0.45 | 1.85 ± 1.38 | 22.39 ± 1.07 | **28.36 ± 0.44** | 27.07 ± 1.24 | 22.57 ± 0.71 | 27.77 ± 0.57 | 25.40 ± 0.76 | 27.83 ± 0.29 |
| BAT | ACC | 33.89 ± 0.78 | 40.00 ± 4.50 | 52.67 ± 4.71 | 76.95 ± 3.22 | 75.42 ± 2.43 | 59.08 ± 1.33 | 75.73 ± 2.43 | 74.05 ± 2.10 | **80.61 ± 1.02** |
| | F1 | 25.37 ± 1.45 | 34.79 ± 4.58 | 48.82 ± 5.59 | 76.70 ± 3.17 | 75.22 ± 2.49 | 54.56 ± 2.17 | 75.34 ± 2.70 | 73.18 ± 2.22 | **80.65 ± 0.97** |
| | NMI | 10.09 ± 4.43 | 14.41 ± 2.57 | 33.57 ± 3.36 | 52.53 ± 3.91 | 50.57 ± 3.08 | 40.39 ± 2.53 | 50.85 ± 2.40 | 50.49 ± 2.17 | **56.77 ± 1.52** |
| | ARI | 1.60 ± 0.76 | 6.62 ± 4.84 | 25.63 ± 3.44 | 50.45 ± 5.21 | 47.68 ± 4.15 | 33.36 ± 2.89 | 48.51 ± 3.32 | 47.13 ± 2.73 | **55.76 ± 2.13** |
| CoraFull | ACC | 12.13 ± 0.93 | 27.19 ± 0.45 | 30.28 ± 0.86 | OOM | 32.68 ± 0.63 | 37.07 ± 0.59 | OOM | 36.85 ± 0.58 | **42.42 ± 0.43** |
| | F1 | 5.34 ± 0.55 | 20.64 ± 0.52 | 21.13 ± 0.43 | | 28.95 ± 0.86 | 30.28 ± 0.73 | | 28.86 ± 0.84 | **33.62 ± 0.68** |
| | NMI | 18.07 ± 0.77 | 41.58 ± 0.28 | 44.75 ± 0.32 | | 47.46 ± 0.35 | 48.30 ± 0.46 | | 47.28 ± 0.32 | **54.48 ± 0.28** |
| | ARI | 3.13 ± 0.97 | 15.59 ± 0.21 | 17.90 ± 0.65 | | 17.03 ± 0.86 | 24.71 ± 0.56 | | 19.67 ± 1.21 | **29.47 ± 0.77** |
| Computers | ACC | 40.40 ± 3.05 | 49.66 ± 2.24 | 37.97 ± 2.81 | 47.33 ± 1.26 | 48.91 ± 5.49 | 55.65 ± 1.27 | 49.00 ± 0.75 | 40.15 ± 0.75 | **64.02 ± 3.93** |
| | F1 | 12.61 ± 3.32 | 35.38 ± 3.36 | 27.13 ± 2.75 | 44.39 ± 3.55 | 38.38 ± 7.00 | 47.12 ± 2.31 | 47.62 ± 2.19 | 43.79 ± 4.66 | **53.62 ± 2.75** |
| | NMI | 12.02 ± 7.36 | 38.03 ± 1.91 | 26.28 ± 1.52 | 43.65 ± 0.54 | 44.47 ± 5.38 | **54.20 ± 1.14** | 45.27 ± 1.85 | 32.34 ± 1.71 | 54.07 ± 1.80 |
| | ARI | 10.08 ± 7.57 | 32.48 ± 3.26 | 18.71 ± 3.15 | 29.29 ± 0.41 | 30.86 ± 5.99 | 36.57 ± 2.16 | 30.56 ± 1.87 | 16.63 ± 1.15 | **45.07 ± 6.16** |
| CS | ACC | 49.97 ± 3.59 | 51.24 ± 2.51 | 58.54 ± 1.37 | OOM | 68.38 ± 1.49 | 67.97 ± 1.11 | OOM | 77.00 ± 1.38 | **81.54 ± 3.27** |
| | F1 | 23.32 ± 1.98 | 39.63 ± 3.46 | 44.34 ± 1.87 | | 59.19 ± 1.66 | 62.88 ± 1.75 | | 69.66 ± 1.86 | **74.36 ± 4.26** |
| | NMI | 45.23 ± 3.45 | 53.88 ± 1.41 | 62.91 ± 0.68 | | 69.74 ± 1.49 | 68.37 ± 3.43 | | 71.90 ± 0.80 | **75.34 ± 0.72** |
| | ARI | 37.77 ± 6.19 | 32.92 ± 1.84 | 46.23 ± 1.94 | | 60.00 ± 2.35 | 55.76 ± 5.81 | | 69.04 ± 2.87 | **76.52 ± 1.78** |
| Physics | ACC | 63.41 ± 4.11 | 72.22 ± 2.40 | OOM | OOM | 90.26 ± 1.80 | 82.26 ± 4.27 | OOM | 91.50 ± 0.21 | **92.31 ± 0.26** |
| | F1 | 35.54 ± 5.52 | 68.89 ± 3.19 | | | 87.02 ± 2.10 | 75.81 ± 7.31 | | 89.19 ± 0.32 | **89.37 ± 0.39** |
| | NMI | 39.83 ± 10.93 | 55.31 ± 1.77 | | | 72.63 ± 4.42 | 60.56 ± 1.55 | | 75.05 ± 0.28 | **76.06 ± 0.39** |
| | ARI | 44.21 ± 10.92 | 52.16 ± 3.67 | | | 80.63 ± 5.26 | 67.78 ± 3.71 | | 82.20 ± 0.74 | **85.32 ± 0.33** |
| Wiki | ACC | 34.13 ± 4.08 | 33.02 ± 2.23 | 34.56 ± 0.86 | 47.73 ± 0.74 | 45.63 ± 0.71 | 49.19 ± 1.76 | 47.93 ± 1.16 | 47.01 ± 0.72 | **52.68 ± 1.22** |
| | F1 | 21.52 ± 4.15 | 22.15 ± 3.01 | 21.90 ± 1.80 | 40.08 ± 1.11 | 38.55 ± 0.83 | 42.26 ± 1.28 | 40.66 ± 0.67 | 39.93 ± 1.81 | **42.97 ± 1.12** |
| | NMI | 26.07 ± 1.59 | 25.94 ± 3.19 | 28.77 ± 1.98 | 42.24 ± 1.05 | 39.74 ± 0.18 | 46.11 ± 0.93 | 42.79 ± 1.09 | 41.39 ± 1.15 | **47.22 ± 1.06** |
| | ARI | 11.02 ± 3.67 | 6.64 ± 1.56 | 8.16 ± 0.55 | 27.67 ± 1.46 | 23.25 ± 1.68 | 29.44 ± 1.26 | 27.41 ± 1.47 | 23.05 ± 1.79 | **31.11 ± 0.65** |
| UAT | ACC | 34.91 ± 1.60 | 43.21 ± 2.14 | 36.45 ± 1.95 | 55.11 ± 1.05 | 56.42 ± 2.39 | 42.32 ± 1.17 | **57.75 ± 1.29** | 53.06 ± 1.58 | 54.69 ± 1.99 |
| | F1 | 26.40 ± 0.82 | 39.36 ± 2.69 | 27.78 ± 3.54 | 52.65 ± 1.95 | 53.75 ± 3.01 | 37.94 ± 2.95 | **56.54 ± 1.91** | 47.62 ± 1.46 | 52.56 ± 5.60 |
| | NMI | 6.70 ± 1.03 | 10.97 ± 0.92 | 8.64 ± 1.13 | 24.11 ± 2.26 | 26.72 ± 0.81 | 19.12 ± 1.35 | **27.05 ± 1.10** | 23.00 ± 1.18 | 25.92 ± 2.40 |
| | ARI | 3.17 ± 2.09 | 7.95 ± 2.13 | 4.51 ± 0.27 | 23.85 ± 2.59 | **25.59 ± 1.41** | 12.93 ± 1.53 | 25.30 ± 1.72 | 21.59 ± 1.69 | 24.03 ± 1.69 |
| ACM | ACC | 50.47 ± 2.34 | 50.86 ± 6.88 | 59.27 ± 7.80 | 52.13 ± 1.22 | 71.51 ± 7.45 | 58.78 ± 2.23 | 54.12 ± 0.89 | 41.77 ± 4.43 | **82.84 ± 0.78** |
| | F1 | 48.61 ± 4.86 | 46.59 ± 9.51 | 56.99 ± 10.24 | 51.38 ± 1.21 | 71.29 ± 7.79 | 59.49 ± 1.96 | 53.15 ± 1.20 | 38.75 ± 6.74 | **82.69 ± 0.78** |
| | NMI | 15.34 ± 4.42 | 15.09 ± 10.85 | 25.63 ± 6.85 | 16.02 ± 1.60 | 34.67 ± 7.38 | 18.89 ± 0.49 | 17.26 ± 0.95 | 4.78 ± 6.47 | **50.84 ± 1.64** |
| | ARI | 12.48 ± 2.60 | 13.09 ± 7.62 | 20.88 ± 6.47 | 14.71 ± 2.35 | 35.59 ± 7.67 | 17.35 ± 1.73 | 16.92 ± 0.63 | 4.23 ± 5.41 | **55.32 ± 1.74** |

Table 9: Comparison with conventional graph clustering methods.

clustering-oriented representation learning, VISTA maintains effective clustering performance over a broad range of missing rates.

| Dataset | Metric | MAGI | Dink-Net | S3GC | GGD | SSGC | SAGSC | M-S2CAG | ANCKA | VISTA |
|---|---|---|---|---|---|---|---|---|---|---|
| Cora | ACC | 66.04 ± 1.05 | 44.08 ± 9.63 | 70.10 ± 1.45 | 46.80 ± 3.29 | 61.05 ± 4.02 | 54.70 ± 1.78 | 68.05 ± 1.78 | 61.49 ± 6.16 | **72.70 ± 1.65** |
| | F1 | 63.80 ± 0.88 | 43.90 ± 9.09 | 68.72 ± 1.51 | 44.09 ± 5.13 | 59.19 ± 5.86 | 53.82 ± 3.21 | 66.56 ± 1.49 | 54.56 ± 7.94 | **70.23 ± 1.70** |
| | NMI | 45.63 ± 0.81 | 25.64 ± 7.16 | 53.56 ± 1.85 | 33.09 ± 2.66 | 48.66 ± 2.13 | 38.09 ± 2.25 | 50.04 ± 1.18 | 48.00 ± 2.02 | **54.97 ± 1.96** |
| | ARI | 37.08 ± 1.54 | 17.99 ± 8.35 | 46.72 ± 1.99 | 16.19 ± 2.84 | 37.84 ± 3.82 | 30.66 ± 1.78 | 44.09 ± 1.75 | 38.35 ± 3.98 | **50.98 ± 4.13** |
| CiteSeer | ACC | 41.17 ± 1.34 | 28.85 ± 2.29 | 50.54 ± 1.51 | 34.61 ± 3.69 | 50.72 ± 2.86 | 49.83 ± 4.60 | 55.28 ± 1.17 | 60.21 ± 1.35 | **65.37 ± 0.75** |
| | F1 | 40.95 ± 1.25 | 25.70 ± 1.96 | 49.88 ± 3.33 | 33.63 ± 4.03 | 51.19 ± 2.54 | 49.28 ± 4.15 | 53.81 ± 1.08 | 56.34 ± 0.98 | **60.22 ± 0.96** |
| | NMI | 26.15 ± 0.88 | 5.83 ± 1.55 | 30.27 ± 0.86 | 13.55 ± 2.80 | 30.90 ± 0.80 | 25.26 ± 2.91 | 31.18 ± 0.56 | 33.14 ± 0.94 | **37.67 ± 0.71** |
| | ARI | 8.07 ± 0.75 | 3.01 ± 1.05 | 18.95 ± 2.13 | 7.32 ± 2.05 | 20.31 ± 2.07 | 21.71 ± 3.87 | 28.16 ± 0.66 | 32.96 ± 1.55 | **39.69 ± 0.67** |
| DBLP | ACC | 67.95 ± 0.53 | 56.33 ± 5.00 | 57.72 ± 1.88 | 45.35 ± 2.45 | 58.72 ± 0.54 | 46.01 ± 5.98 | 48.92 ± 2.43 | 64.81 ± 2.39 | **78.26 ± 0.24** |
| | F1 | 63.02 ± 1.26 | 48.68 ± 4.28 | 51.83 ± 2.13 | 40.82 ± 3.80 | 54.96 ± 0.47 | 43.53 ± 5.14 | 46.43 ± 3.04 | 55.98 ± 6.05 | **73.95 ± 0.32** |
| | NMI | 28.39 ± 2.01 | 25.26 ± 3.05 | 34.55 ± 1.05 | 22.32 ± 2.00 | 30.92 ± 0.62 | 15.67 ± 4.21 | 21.16 ± 1.80 | 35.66 ± 0.73 | **47.03 ± 0.50** |
| | ARI | 30.80 ± 0.95 | 25.34 ± 3.27 | 35.31 ± 2.39 | 15.08 ± 0.59 | 30.10 ± 1.11 | 13.50 ± 5.25 | 18.87 ± 1.67 | 41.91 ± 0.49 | **52.06 ± 0.44** |
| PubMed | ACC | 60.27 ± 0.59 | 49.34 ± 6.23 | 63.69 ± 0.27 | 60.14 ± 0.65 | 68.66 ± 0.34 | 68.45 ± 4.53 | 70.33 ± 0.04 | 62.43 ± 1.63 | **70.70 ± 0.25** |
| | F1 | 58.46 ± 0.66 | 49.25 ± 5.86 | 63.90 ± 0.27 | 58.52 ± 0.77 | 68.18 ± 0.35 | 67.31 ± 4.46 | 69.24 ± 0.07 | 62.71 ± 1.71 | **69.86 ± 0.22** |
| | NMI | 18.14 ± 0.73 | 11.57 ± 2.81 | 22.63 ± 0.34 | 21.39 ± 0.57 | 32.19 ± 0.38 | 27.83 ± 4.97 | 28.41 ± 0.17 | 19.78 ± 1.73 | **32.29 ± 0.24** |
| | ARI | 17.55 ± 0.71 | 9.07 ± 3.49 | 22.03 ± 0.39 | 18.64 ± 0.56 | 31.10 ± 0.49 | 29.95 ± 6.15 | 32.14 ± 0.08 | 19.64 ± 2.30 | **33.10 ± 0.47** |
| Photo | ACC | 76.10 ± 0.48 | 59.32 ± 1.29 | 73.93 ± 0.25 | 36.49 ± 4.05 | 66.08 ± 2.22 | 68.23 ± 1.38 | 71.89 ± 3.80 | 76.42 ± 1.68 | **78.61 ± 0.95** |
| | F1 | 70.71 ± 0.42 | 53.51 ± 1.35 | 69.59 ± 0.28 | 28.29 ± 4.14 | 58.02 ± 3.69 | 69.17 ± 1.38 | 68.56 ± 4.92 | 69.83 ± 2.08 | **73.56 ± 1.19** |
| | NMI | 66.97 ± 0.50 | 50.88 ± 0.85 | 65.59 ± 0.46 | 29.76 ± 3.76 | 62.01 ± 0.29 | 58.08 ± 0.71 | 66.26 ± 0.67 | 66.86 ± 0.68 | **71.40 ± 0.98** |
| | ARI | 55.58 ± 0.90 | 40.69 ± 0.90 | 57.83 ± 0.27 | 15.18 ± 2.24 | 47.54 ± 0.73 | 44.40 ± 1.69 | 55.76 ± 3.71 | 58.44 ± 1.14 | **61.47 ± 1.68** |
| Flickr | ACC | 23.48 ± 0.47 | **39.09 ± 2.51** | 19.89 ± 0.62 | 30.39 ± 2.78 | 32.59 ± 0.28 | 26.67 ± 1.41 | 26.19 ± 0.97 | 21.31 ± 0.69 | 33.12 ± 1.16 |
| | F1 | 15.64 ± 0.60 | 17.23 ± 0.71 | 16.01 ± 0.23 | 14.87 ± 1.26 | 17.75 ± 0.21 | 20.89 ± 0.72 | 20.46 ± 0.52 | 16.58 ± 0.40 | **21.71 ± 0.51** |
| | NMI | 1.51 ± 0.13 | 5.18 ± 0.49 | 1.46 ± 0.04 | 1.01 ± 0.36 | 3.00 ± 0.06 | 6.62 ± 0.38 | 6.24 ± 0.44 | 1.82 ± 0.49 | **7.83 ± 0.32** |
| | ARI | 0.38 ± 0.13 | **3.97 ± 1.16** | 0.90 ± 0.06 | 1.47 ± 0.79 | 3.09 ± 0.11 | 3.22 ± 0.53 | 3.20 ± 0.29 | 1.07 ± 0.10 | 3.77 ± 0.52 |
| BlogCatalog | ACC | 40.96 ± 0.43 | 32.36 ± 4.11 | 43.58 ± 0.45 | 36.80 ± 2.30 | 29.50 ± 2.35 | 35.75 ± 0.60 | 55.22 ± 3.25 | **65.64 ± 3.26** | 62.49 ± 1.08 |
| | F1 | 39.40 ± 0.41 | 27.61 ± 5.75 | 43.45 ± 0.37 | 36.06 ± 2.22 | 23.77 ± 4.00 | 35.92 ± 0.99 | 54.02 ± 2.51 | **64.59 ± 3.86** | 60.10 ± 1.86 |
| | NMI | 22.07 ± 0.79 | 12.44 ± 5.76 | 24.42 ± 0.18 | 17.90 ± 2.46 | 15.02 ± 3.69 | 15.95 ± 0.37 | 34.68 ± 3.00 | **40.11 ± 2.10** | 38.02 ± 0.78 |
| | ARI | 13.63 ± 0.85 | 9.04 ± 4.91 | 17.16 ± 0.65 | 8.19 ± 1.73 | 3.15 ± 0.65 | 8.77 ± 0.21 | 28.57 ± 3.45 | **36.31 ± 3.27** | 33.19 ± 0.83 |
| USPS | ACC | 55.92 ± 0.60 | 41.82 ± 3.15 | 68.84 ± 0.63 | 43.15 ± 0.41 | 56.26 ± 3.50 | 45.08 ± 3.02 | 73.59 ± 0.28 | 61.99 ± 3.55 | **91.81 ± 0.06** |
| | F1 | 56.22 ± 0.57 | 43.13 ± 3.75 | 67.00 ± 0.62 | 45.24 ± 0.75 | 57.13 ± 3.82 | 48.03 ± 3.49 | 72.01 ± 0.29 | 59.25 ± 5.60 | **91.13 ± 0.09** |
| | NMI | 52.28 ± 0.81 | 36.97 ± 2.31 | 65.92 ± 0.69 | 43.07 ± 0.98 | 48.14 ± 1.70 | 37.89 ± 2.29 | 73.64 ± 0.27 | 71.09 ± 1.89 | **83.68 ± 0.11** |
| | ARI | 31.33 ± 1.18 | 18.76 ± 2.61 | 57.19 ± 0.68 | 17.48 ± 0.92 | 34.58 ± 2.22 | 18.21 ± 1.61 | 65.73 ± 0.36 | 55.44 ± 2.31 | **84.42 ± 0.10** |
| HHAR | ACC | 63.63 ± 0.14 | 38.71 ± 5.41 | 55.66 ± 0.36 | 39.10 ± 0.80 | 56.94 ± 0.22 | 55.87 ± 4.59 | 78.93 ± 0.22 | 57.21 ± 4.32 | **79.70 ± 1.61** |
| | F1 | 62.51 ± 0.18 | 33.80 ± 7.63 | 52.82 ± 0.24 | 38.88 ± 0.83 | 50.94 ± 0.33 | 57.45 ± 5.49 | **79.37 ± 0.23** | 52.92 ± 6.21 | 78.91 ± 3.11 |
| | NMI | 60.96 ± 0.95 | 35.94 ± 5.39 | 61.31 ± 0.28 | 40.09 ± 0.38 | 59.01 ± 0.31 | 45.32 ± 2.80 | **75.86 ± 0.25** | 61.74 ± 2.34 | 74.91 ± 1.68 |
| | ARI | 49.83 ± 0.70 | 23.37 ± 4.27 | 45.42 ± 0.40 | 22.18 ± 0.41 | 49.97 ± 0.17 | 33.23 ± 3.26 | **67.63 ± 0.21** | 45.23 ± 1.18 | 66.32 ± 1.37 |
| EAT | ACC | 34.39 ± 1.85 | 42.71 ± 2.87 | 33.88 ± 0.96 | 43.66 ± 1.08 | 33.28 ± 1.50 | 45.26 ± 0.63 | 32.53 ± 0.93 | 33.13 ± 1.14 | **58.25 ± 0.23** |
| | F1 | 28.24 ± 2.42 | 40.07 ± 3.97 | 29.40 ± 1.29 | 35.63 ± 1.50 | 25.14 ± 2.35 | 40.24 ± 1.79 | 27.01 ± 1.19 | 27.91 ± 1.83 | **58.42 ± 0.21** |
| | NMI | 6.14 ± 1.88 | 15.26 ± 1.85 | 5.31 ± 0.38 | 22.23 ± 2.06 | 7.97 ± 1.51 | 24.66 ± 0.74 | 5.26 ± 1.52 | 5.51 ± 1.06 | **34.38 ± 0.18** |
| | ARI | 2.22 ± 0.66 | 12.79 ± 1.88 | 3.97 ± 0.48 | 17.58 ± 1.53 | 2.36 ± 0.53 | 22.11 ± 0.17 | 2.24 ± 0.71 | 2.64 ± 0.82 | **27.83 ± 0.29** |
| BAT | ACC | 41.07 ± 2.32 | 42.14 ± 3.64 | 43.66 ± 1.47 | 45.04 ± 0.93 | 34.20 ± 1.37 | 50.84 ± 4.44 | 39.85 ± 4.33 | 38.47 ± 3.88 | **80.61 ± 1.02** |
| | F1 | 36.37 ± 2.81 | 39.40 ± 3.97 | 42.87 ± 1.85 | 40.22 ± 3.25 | 26.61 ± 1.92 | 50.05 ± 4.65 | 38.65 ± 4.41 | 34.46 ± 5.83 | **80.65 ± 0.97** |
| | NMI | 17.25 ± 1.86 | 12.14 ± 4.75 | 13.04 ± 2.05 | 23.83 ± 0.71 | 14.40 ± 2.33 | 24.95 ± 6.39 | 9.94 ± 3.49 | 9.77 ± 2.19 | **56.77 ± 1.52** |
| | ARI | 6.90 ± 1.63 | 7.99 ± 4.76 | 9.39 ± 2.05 | 17.70 ± 2.46 | 3.39 ± 0.89 | 19.81 ± 6.32 | 5.08 ± 2.13 | 4.31 ± 1.74 | **55.76 ± 2.13** |
| CoraFull | ACC | 36.82 ± 0.64 | 16.74 ± 6.54 | 37.28 ± 0.37 | 21.08 ± 1.55 | 34.72 ± 0.72 | 38.36 ± 0.72 | 37.47 ± 1.00 | 35.62 ± 1.61 | **42.42 ± 0.43** |
| | F1 | 31.45 ± 1.13 | 13.04 ± 6.23 | 30.70 ± 0.40 | 15.87 ± 1.38 | 26.05 ± 1.25 | 32.50 ± 0.85 | 32.78 ± 0.43 | 25.92 ± 2.01 | **33.62 ± 0.68** |
| | NMI | 48.99 ± 0.36 | 28.05 ± 12.23 | 53.39 ± 0.16 | 38.23 ± 1.38 | 49.90 ± 0.32 | 52.74 ± 0.28 | 52.34 ± 0.45 | 47.35 ± 0.43 | **54.48 ± 0.28** |
| | ARI | 13.17 ± 0.61 | 6.25 ± 3.50 | 25.66 ± 0.29 | 10.17 ± 1.07 | 20.26 ± 0.38 | 25.79 ± 0.97 | 22.97 ± 1.58 | 23.26 ± 1.02 | **29.47 ± 0.77** |
| Computers | ACC | 53.11 ± 0.72 | 41.03 ± 4.17 | 57.28 ± 1.60 | 38.55 ± 0.59 | 58.38 ± 5.54 | 31.56 ± 1.66 | 60.33 ± 1.16 | 58.23 ± 1.31 | **64.02 ± 3.93** |
| | F1 | 41.21 ± 0.35 | 13.87 ± 6.98 | 44.33 ± 4.32 | 22.29 ± 0.82 | 46.52 ± 7.38 | 27.83 ± 1.85 | **54.95 ± 2.59** | 50.09 ± 5.28 | 53.62 ± 2.75 |
| | NMI | 49.93 ± 0.75 | 14.49 ± 11.51 | 53.22 ± 0.73 | 30.08 ± 1.08 | 50.59 ± 2.16 | 20.89 ± 1.91 | 52.99 ± 0.83 | 53.48 ± 1.28 | **54.07 ± 1.80** |
| | ARI | 36.72 ± 1.08 | 11.28 ± 12.34 | 41.66 ± 0.70 | 18.80 ± 1.89 | 38.79 ± 4.36 | 6.83 ± 1.34 | 41.95 ± 0.64 | 40.82 ± 1.59 | **45.07 ± 6.16** |
| CS | ACC | 64.48 ± 1.71 | 58.38 ± 2.78 | 70.33 ± 3.10 | 59.21 ± 2.40 | 67.90 ± 2.53 | 64.85 ± 1.24 | 63.11 ± 0.85 | 70.74 ± 3.74 | **81.54 ± 3.27** |
| | F1 | 63.12 ± 2.61 | 50.23 ± 8.10 | 63.06 ± 4.52 | 55.50 ± 4.06 | 64.83 ± 4.21 | 59.53 ± 1.59 | 60.66 ± 2.06 | 66.32 ± 1.42 | **74.36 ± 4.26** |
| | NMI | 65.11 ± 0.73 | 57.67 ± 6.15 | 72.95 ± 0.83 | 61.44 ± 0.88 | 71.55 ± 0.44 | 68.75 ± 0.48 | 69.32 ± 0.67 | 72.77 ± 0.49 | **75.34 ± 0.72** |
| | ARI | 46.99 ± 1.60 | 46.41 ± 5.04 | 64.20 ± 2.09 | 44.84 ± 1.07 | 59.53 ± 2.68 | 55.84 ± 0.60 | 53.25 ± 0.68 | 62.04 ± 2.42 | **76.52 ± 1.78** |
| Physics | ACC | 72.88 ± 9.43 | 74.02 ± 10.04 | 83.50 ± 0.20 | 79.33 ± 1.12 | 88.78 ± 0.18 | 58.16 ± 2.79 | 83.57 ± 9.12 | 79.43 ± 10.48 | **92.31 ± 0.26** |
| | F1 | 70.81 ± 9.19 | 71.37 ± 8.55 | 77.38 ± 0.33 | 77.33 ± 0.82 | 83.80 ± 0.26 | 59.16 ± 3.96 | 75.25 ± 16.19 | 73.95 ± 10.93 | **89.37 ± 0.39** |
| | NMI | 58.37 ± 2.03 | 56.56 ± 2.25 | 64.61 ± 0.39 | 61.34 ± 0.69 | 71.81 ± 0.20 | 52.29 ± 2.17 | 68.57 ± 5.00 | 65.47 ± 5.92 | **76.06 ± 0.39** |
| | ARI | 54.08 ± 7.46 | 55.87 ± 8.27 | 72.72 ± 0.38 | 59.71 ± 2.63 | 81.41 ± 0.28 | 42.19 ± 4.40 | 78.06 ± 4.09 | 70.23 ± 14.02 | **85.32 ± 0.33** |
| Wiki | ACC | 38.43 ± 1.38 | 33.95 ± 6.02 | 42.46 ± 0.83 | 38.02 ± 2.80 | 41.17 ± 1.75 | 39.09 ± 1.77 | 42.79 ± 0.91 | 45.44 ± 1.46 | **52.68 ± 1.22** |
| | F1 | 35.62 ± 0.83 | 27.75 ± 7.72 | 35.83 ± 1.03 | 32.06 ± 3.11 | 35.97 ± 1.68 | 35.53 ± 1.78 | 36.01 ± 0.55 | 38.83 ± 1.18 | **42.97 ± 1.12** |
| | NMI | 36.69 ± 0.96 | 29.15 ± 8.17 | 38.34 ± 0.67 | 37.14 ± 1.27 | 39.16 ± 0.50 | 36.38 ± 1.57 | 37.56 ± 0.48 | 41.67 ± 1.17 | **47.22 ± 1.06** |
| | ARI | 15.16 ± 0.67 | 9.44 ± 4.17 | 23.11 ± 0.81 | 13.83 ± 1.48 | 12.76 ± 1.39 | 14.66 ± 1.50 | 23.51 ± 0.63 | 26.58 ± 0.54 | **31.11 ± 0.65** |
| UAT | ACC | 40.59 ± 0.56 | 39.06 ± 1.60 | 42.45 ± 0.70 | 42.37 ± 3.45 | 42.32 ± 1.47 | 46.59 ± 3.24 | 41.50 ± 1.32 | 40.30 ± 2.29 | **54.69 ± 1.99** |
| | F1 | 36.42 ± 0.89 | 35.75 ± 3.18 | 38.83 ± 0.81 | 40.47 ± 7.20 | 36.72 ± 1.82 | 44.27 ± 3.19 | 37.42 ± 1.71 | 36.51 ± 3.00 | **52.56 ± 5.60** |
| | NMI | 9.05 ± 1.04 | 8.15 ± 2.22 | 10.85 ± 0.37 | 17.23 ± 4.48 | 12.35 ± 0.87 | 17.75 ± 2.29 | 11.31 ± 1.71 | 8.52 ± 1.65 | **25.92 ± 2.40** |
| | ARI | 6.00 ± 0.69 | 5.38 ± 1.70 | 8.96 ± 0.72 | 8.59 ± 2.96 | 8.87 ± 1.24 | 14.73 ± 3.01 | 8.17 ± 1.01 | 5.08 ± 1.33 | **24.03 ± 1.69** |
| ACM | ACC | 73.55 ± 1.06 | 46.46 ± 7.05 | 70.94 ± 0.54 | 54.08 ± 1.09 | 40.56 ± 5.90 | 56.03 ± 2.75 | 80.26 ± 0.88 | 76.97 ± 8.09 | **82.84 ± 0.78** |
| | F1 | 73.70 ± 1.14 | 44.10 ± 7.36 | 71.06 ± 0.53 | 48.88 ± 0.53 | 37.18 ± 5.87 | 56.79 ± 3.02 | 80.46 ± 0.93 | 76.94 ± 8.02 | **82.69 ± 0.78** |
| | NMI | 41.86 ± 1.47 | 12.55 ± 10.35 | 36.55 ± 0.85 | 26.90 ± 1.60 | 4.77 ± 7.78 | 25.09 ± 2.12 | 48.17 ± 1.67 | 40.31 ± 10.05 | **50.84 ± 1.64** |
| | ARI | 34.22 ± 2.03 | 11.44 ± 8.80 | 29.78 ± 0.95 | 22.90 ± 3.20 | 5.02 ± 8.34 | 21.56 ± 1.49 | 48.73 ± 2.41 | 44.62 ± 13.47 | **55.32 ± 1.74** |
| TwitchGamers | ACC | 51.43 ± 0.99 | 52.99 ± 0.00 | 51.82 ± 1.48 | 51.46 ± 0.41 | 54.90 ± 0.06 | 50.62 ± 0.16 | 51.91 ± 0.09 | 52.66 ± 0.67 | **58.89 ± 0.23** |
| | F1 | 50.23 ± 0.71 | 34.64 ± 0.00 | 51.70 ± 1.42 | 46.74 ± 2.96 | 46.31 ± 0.13 | 49.73 ± 0.17 | 48.25 ± 0.13 | 52.28 ± 0.66 | **57.91 ± 0.52** |
| | NMI | 0.03 ± 0.05 | 0.00 ± 0.00 | 0.13 ± 0.12 | 0.06 ± 0.10 | 0.59 ± 0.02 | 0.00 ± 0.00 | 0.70 ± 0.05 | 0.17 ± 0.10 | **2.15 ± 0.11** |
| | ARI | 0.09 ± 0.12 | 0.00 ± 0.00 | 0.20 ± 0.20 | −0.01 ± 0.10 | 0.77 ± 0.03 | 0.00 ± 0.01 | 0.02 ± 0.01 | 0.29 ± 0.15 | **3.14 ± 0.15** |
| Arxiv | ACC | 36.57 ± 1.38 | 32.11 ± 1.23 | 32.97 ± 0.53 | 37.08 ± 0.95 | 14.48 ± 0.21 | 48.02 ± 2.84 | OOM | 35.37 ± 3.91 | **48.21 ± 0.43** |
| | F1 | 24.56 ± 0.67 | 19.50 ± 0.38 | 21.91 ± 0.25 | 23.39 ± 0.48 | 8.53 ± 0.19 | **27.44 ± 0.69** | | 21.71 ± 0.81 | 24.72 ± 0.62 |
| | NMI | 44.90 ± 0.44 | 37.86 ± 0.40 | 43.65 ± 0.13 | 41.99 ± 0.50 | 20.34 ± 0.31 | **45.72 ± 0.61** | | 39.73 ± 0.50 | 45.04 ± 0.21 |
| | ARI | 28.98 ± 1.54 | 23.44 ± 2.10 | 26.16 ± 0.98 | 32.73 ± 1.00 | 7.26 ± 0.25 | 38.59 ± 2.42 | | 26.07 ± 5.01 | **41.01 ± 0.77** |
| Reddit | ACC | **88.90 ± 0.47** | 73.60 ± 1.58 | 84.13 ± 2.33 | 28.62 ± 4.31 | 39.13 ± 1.06 | 34.58 ± 1.31 | FAIL | 79.98 ± 2.16 | 87.18 ± 0.55 |
| | F1 | **82.26 ± 0.61** | 64.35 ± 1.38 | 73.84 ± 1.96 | 24.92 ± 4.66 | 30.88 ± 0.98 | 22.55 ± 0.97 | FAIL | 64.59 ± 2.79 | 75.09 ± 2.57 |
| | NMI | 85.50 ± 0.21 | 76.58 ± 0.38 | 84.71 ± 0.58 | 38.31 ± 3.88 | 56.77 ± 0.50 | 40.66 ± 0.73 | FAIL | 79.10 ± 0.51 | **85.97 ± 0.10** |
| | ARI | **88.25 ± 1.39** | 69.25 ± 1.68 | 85.35 ± 3.56 | 19.06 ± 2.95 | 22.21 ± 1.34 | 14.29 ± 1.88 | FAIL | 79.11 ± 1.90 | 86.88 ± 1.74 |
| Products | ACC | 40.11 ± 1.41 | 27.31 ± 0.00 | 39.52 ± 0.92 | 36.54 ± 0.88 | 33.90 ± 2.00 | 26.56 ± 1.58 | FAIL | **50.06 ± 3.47** | 45.45 ± 0.84 |
| | F1 | 26.22 ± 1.57 | 0.91 ± 0.00 | 23.54 ± 0.78 | 23.40 ± 0.36 | 18.43 ± 0.61 | 10.53 ± 0.31 | FAIL | 22.85 ± 0.72 | **27.74 ± 0.37** |
| | NMI | **54.45 ± 1.10** | 0.00 ± 0.00 | 50.47 ± 0.33 | 50.50 ± 0.37 | 44.33 ± 0.56 | 22.34 ± 0.85 | FAIL | 50.96 ± 1.14 | 54.20 ± 0.54 |
| | ARI | 21.38 ± 0.75 | 0.00 ± 0.00 | 22.86 ± 0.93 | 18.97 ± 0.51 | 15.69 ± 2.09 | 3.47 ± 1.94 | FAIL | **50.83 ± 6.68** | 23.78 ± 1.30 |

Table 10: Comparison with scalable graph clustering methods.

| Dataset | Metric | SVGA | TDAR | MIGDiff | MATE | AMER | SAT | ITR | PCFI | VISTA |
|---|---|---|---|---|---|---|---|---|---|---|
| Cora | ACC | 63.46 ± 6.31 | 69.08 ± 1.23 | 69.33 ± 1.51 | 68.12 ± 2.02 | 55.97 ± 4.19 | 47.00 ± 6.27 | 50.52 ± 3.20 | 52.32 ± 1.51 | **72.70 ± 1.65** |
| | F1 | 62.46 ± 5.82 | 63.11 ± 1.19 | 67.40 ± 1.13 | 61.67 ± 2.12 | 53.56 ± 2.31 | 45.05 ± 6.07 | 49.36 ± 2.71 | 51.61 ± 5.67 | **70.23 ± 1.70** |
| | NMI | 49.24 ± 3.70 | 51.07 ± 1.17 | 50.61 ± 1.91 | 48.75 ± 1.50 | 39.58 ± 3.61 | 26.91 ± 3.76 | 33.24 ± 3.46 | 37.02 ± 2.69 | **54.97 ± 1.96** |
| | ARI | 40.86 ± 6.74 | 44.75 ± 1.51 | 46.65 ± 2.49 | 46.04 ± 1.52 | 31.51 ± 3.84 | 20.42 ± 4.24 | 23.60 ± 3.94 | 22.72 ± 2.00 | **50.98 ± 4.13** |
| CiteSeer | ACC | 49.08 ± 1.76 | 51.12 ± 0.64 | 55.93 ± 2.55 | 56.21 ± 2.15 | 38.33 ± 1.83 | 38.44 ± 2.76 | 49.93 ± 1.68 | 45.16 ± 2.07 | **65.37 ± 0.75** |
| | F1 | 48.27 ± 2.50 | 48.57 ± 0.84 | 53.03 ± 2.53 | 52.10 ± 2.54 | 37.43 ± 2.74 | 36.78 ± 2.76 | 50.79 ± 1.63 | 41.71 ± 3.21 | **60.22 ± 0.96** |
| | NMI | 27.84 ± 1.86 | 27.06 ± 0.31 | 31.64 ± 1.65 | 28.03 ± 2.11 | 17.26 ± 2.19 | 13.53 ± 2.26 | 26.26 ± 1.53 | 26.60 ± 1.82 | **37.67 ± 0.71** |
| | ARI | 17.40 ± 2.97 | 19.95 ± 0.61 | 28.49 ± 1.55 | 26.17 ± 1.45 | 9.01 ± 0.64 | 11.30 ± 2.04 | 20.26 ± 1.50 | 12.75 ± 1.22 | **39.69 ± 0.67** |
| DBLP | ACC | 63.81 ± 2.18 | 64.98 ± 2.60 | 56.56 ± 1.84 | 66.44 ± 1.65 | 50.57 ± 5.95 | 51.64 ± 3.71 | 49.68 ± 3.98 | 49.53 ± 1.67 | **78.26 ± 0.24** |
| | F1 | 41.85 ± 3.01 | 53.49 ± 4.25 | 52.11 ± 1.99 | 56.05 ± 5.09 | 39.23 ± 4.19 | 48.93 ± 3.70 | 46.39 ± 5.28 | 40.57 ± 1.98 | **73.95 ± 0.32** |
| | NMI | 29.26 ± 0.58 | 34.50 ± 2.99 | 26.59 ± 2.67 | 33.28 ± 4.11 | 19.09 ± 3.82 | 20.93 ± 2.18 | 21.83 ± 2.50 | 19.73 ± 0.75 | **47.03 ± 0.50** |
| | ARI | 35.38 ± 1.07 | 38.08 ± 1.89 | 26.62 ± 2.13 | 29.20 ± 5.37 | 17.81 ± 8.45 | 19.77 ± 1.50 | 18.39 ± 2.36 | 12.15 ± 1.82 | **52.06 ± 0.44** |
| PubMed | ACC | 56.27 ± 0.32 | 68.12 ± 0.44 | 61.21 ± 0.06$^{(2)}$ | 63.01 ± 3.43 | 54.49 ± 7.63 | 62.08 ± 1.99 | 52.12 ± 1.84 | 63.23 ± 0.32 | **70.70 ± 0.25** |
| | F1 | 49.53 ± 0.39 | 67.39 ± 0.43 | 61.56 ± 0.03$^{(2)}$ | 62.08 ± 3.59 | 48.60 ± 11.30 | 61.09 ± 1.70 | 47.37 ± 2.27 | 62.98 ± 0.39 | **69.86 ± 0.22** |
| | NMI | 13.22 ± 0.55 | 28.24 ± 0.95 | 20.00 ± 0.17$^{(2)}$ | 26.32 ± 2.37 | 14.32 ± 7.82 | 20.54 ± 1.92 | 11.55 ± 1.99 | 27.03 ± 1.14 | **32.29 ± 0.24** |
| | ARI | 12.28 ± 0.39 | 29.06 ± 0.79 | 18.84 ± 0.02$^{(2)}$ | 24.47 ± 3.01 | 12.21 ± 9.58 | 21.60 ± 2.46 | 9.36 ± 1.26 | 25.06 ± 0.81 | **33.10 ± 0.47** |
| Photo | ACC | 58.92 ± 4.54 | 60.09 ± 3.75 | 57.83 ± 6.38 | 59.35 ± 2.30 | 74.67 ± 2.17 | 61.20 ± 6.62 | 58.57 ± 2.47 | 30.81 ± 0.38 | **78.61 ± 0.95** |
| | F1 | 49.80 ± 5.42 | 52.25 ± 3.18 | 54.03 ± 5.35 | 56.06 ± 3.18 | 70.06 ± 3.09 | 52.07 ± 8.85 | 55.72 ± 4.31 | 22.75 ± 0.64 | **73.56 ± 1.19** |
| | NMI | 57.22 ± 1.75 | 58.05 ± 0.85 | 44.67 ± 4.89 | 55.49 ± 3.45 | 63.25 ± 1.53 | 51.49 ± 4.05 | 48.44 ± 2.13 | 13.98 ± 1.25 | **71.40 ± 0.98** |
| | ARI | 41.79 ± 3.07 | 43.76 ± 1.96 | 35.33 ± 6.52 | 37.24 ± 2.38 | 55.44 ± 1.44 | 43.23 ± 4.74 | 34.24 ± 1.51 | 6.57 ± 0.48 | **61.47 ± 1.68** |
| BlogCatalog | ACC | 45.68 ± 5.77 | 29.42 ± 4.98 | 44.74 ± 2.84 | 43.48 ± 1.14 | 28.62 ± 6.94 | 43.03 ± 6.72 | 30.79 ± 0.44 | 32.81 ± 1.86 | **62.49 ± 1.08** |
| | F1 | 41.43 ± 6.18 | 28.37 ± 7.10 | 43.99 ± 3.11 | 43.23 ± 1.13 | 27.18 ± 8.05 | 40.78 ± 6.26 | 26.91 ± 0.84 | 25.01 ± 2.14 | **60.10 ± 1.86** |
| | NMI | 27.27 ± 3.77 | 14.47 ± 5.18 | 26.24 ± 1.60 | 23.57 ± 1.36 | 12.30 ± 6.79 | 27.59 ± 5.63 | 17.43 ± 0.51 | 13.85 ± 1.81 | **38.02 ± 0.78** |
| | ARI | 15.35 ± 5.39 | 5.54 ± 0.54 | 17.43 ± 3.11 | 17.11 ± 0.99 | 7.45 ± 4.79 | 18.78 ± 5.69 | 7.82 ± 0.77 | 7.70 ± 1.39 | **33.19 ± 0.83** |
| USPS | ACC | 71.36 ± 0.46 | 70.33 ± 0.71 | 69.87 ± 0.68 | 73.67 ± 1.16 | 46.76 ± 4.70 | 68.64 ± 0.98 | 53.21 ± 1.43 | 48.62 ± 0.51 | **91.81 ± 0.06** |
| | F1 | 69.53 ± 0.49 | 68.54 ± 0.76 | 68.26 ± 0.56 | 71.65 ± 0.76 | 46.56 ± 5.04 | 66.94 ± 1.21 | 53.40 ± 1.23 | 46.71 ± 0.55 | **91.13 ± 0.09** |
| | NMI | 71.16 ± 0.55 | 68.88 ± 0.87 | 67.89 ± 0.79 | 72.24 ± 1.12 | 43.90 ± 5.27 | 63.84 ± 1.52 | 47.93 ± 0.52 | 49.46 ± 0.37 | **83.68 ± 0.11** |
| | ARI | 62.14 ± 0.78 | 60.39 ± 0.61 | 60.35 ± 0.89 | 64.35 ± 1.14 | 29.35 ± 5.06 | 56.85 ± 1.83 | 32.44 ± 0.52 | 36.17 ± 0.35 | **84.42 ± 0.10** |
| HHAR | ACC | 36.26 ± 1.91 | 71.51 ± 0.19 | 36.32 ± 1.80 | 67.20 ± 7.69 | 66.28 ± 6.59 | 36.70 ± 1.82 | 57.11 ± 0.42 | 45.24 ± 0.32 | **79.70 ± 1.61** |
| | F1 | 37.79 ± 3.39 | 66.54 ± 0.18 | 37.75 ± 3.33 | 67.59 ± 7.71 | 65.01 ± 7.33 | 38.59 ± 3.14 | 57.86 ± 0.49 | 45.24 ± 0.34 | **78.91 ± 3.11** |
| | NMI | 29.49 ± 0.74 | 72.66 ± 0.21 | 29.43 ± 0.73 | 61.63 ± 7.73 | 60.08 ± 4.99 | 29.61 ± 0.68 | 49.80 ± 0.37 | 49.63 ± 0.12 | **74.91 ± 1.68** |
| | ARI | 7.11 ± 0.19 | 64.17 ± 0.22 | 7.24 ± 0.17 | 49.09 ± 10.87 | 49.98 ± 5.81 | 7.12 ± 0.18 | 36.32 ± 0.64 | 28.85 ± 0.09 | **66.32 ± 1.37** |
| EAT | ACC | 42.71 ± 0.97 | 36.04 ± 3.14 | 36.19 ± 1.02 | 48.52 ± 4.03 | 47.77 ± 2.82 | 49.32 ± 1.07 | 33.33 ± 1.09 | 31.98 ± 1.64 | **58.25 ± 0.23** |
| | F1 | 40.40 ± 2.38 | 29.20 ± 1.09 | 33.54 ± 1.40 | 47.98 ± 5.75 | 47.85 ± 4.52 | 50.29 ± 1.02 | 32.77 ± 1.89 | 26.86 ± 1.83 | **58.42 ± 0.21** |
| | NMI | 20.44 ± 2.81 | 8.29 ± 2.90 | 7.17 ± 1.21 | 23.97 ± 4.11 | 22.71 ± 2.13 | 28.02 ± 2.11 | 4.84 ± 0.61 | 3.76 ± 0.96 | **34.38 ± 0.18** |
| | ARI | 14.79 ± 4.96 | 5.55 ± 3.01 | 5.42 ± 0.72 | 19.28 ± 2.47 | 16.18 ± 1.32 | 19.23 ± 1.22 | 2.27 ± 0.68 | 1.22 ± 0.49 | **27.83 ± 0.29** |
| BAT | ACC | 46.26 ± 1.50 | 36.79 ± 2.01 | 40.76 ± 1.04 | 53.74 ± 4.70 | 58.32 ± 5.50 | 59.85 ± 2.63 | 38.93 ± 1.45 | 35.57 ± 2.03 | **80.61 ± 1.02** |
| | F1 | 41.20 ± 4.93 | 33.04 ± 0.93 | 39.11 ± 1.21 | 50.32 ± 6.25 | 55.84 ± 6.07 | 57.20 ± 2.86 | 37.06 ± 2.76 | 32.00 ± 4.44 | **80.65 ± 0.97** |
| | NMI | 28.07 ± 4.63 | 10.92 ± 1.24 | 11.36 ± 3.36 | 33.06 ± 4.74 | 35.33 ± 5.89 | 41.08 ± 2.06 | 9.96 ± 1.06 | 9.79 ± 3.36 | **56.77 ± 1.52** |
| | ARI | 17.20 ± 5.36 | 3.43 ± 1.49 | 5.55 ± 1.33 | 27.31 ± 4.56 | 28.55 ± 5.88 | 32.98 ± 3.55 | 4.46 ± 1.18 | 2.07 ± 1.06 | **55.76 ± 2.13** |
| CoraFull | ACC | 36.51 ± 0.95 | 37.32 ± 0.54 | OOM | 40.12 ± 0.38 | 15.27 ± 5.21 | 20.72 ± 0.37 | 20.16 ± 0.50 | 25.31 ± 0.54 | **42.42 ± 0.43** |
| | F1 | 26.27 ± 0.92 | 29.12 ± 0.31 | | **34.71 ± 0.32** | 10.28 ± 5.26 | 16.64 ± 0.28 | 17.09 ± 1.10 | 16.00 ± 1.22 | 33.62 ± 0.68 |
| | NMI | 50.98 ± 0.32 | 52.63 ± 0.08 | | 53.81 ± 0.12 | 27.58 ± 7.32 | 37.08 ± 0.61 | 36.20 ± 1.00 | 36.98 ± 0.18 | **54.48 ± 0.28** |
| | ARI | 24.27 ± 0.93 | 25.26 ± 0.33 | | 26.81 ± 0.51 | 8.21 ± 3.31 | 11.78 ± 0.30 | 7.79 ± 1.39 | 10.78 ± 0.42 | **29.47 ± 0.77** |
| Computers | ACC | 46.86 ± 3.03 | 51.72 ± 0.88 | 36.49 ± 2.57 | 63.94 ± 1.80 | 49.80 ± 4.86 | 43.96 ± 3.37 | 43.13 ± 1.42 | 25.68 ± 0.76 | **64.02 ± 3.93** |
| | F1 | 35.03 ± 5.44 | 43.01 ± 0.86 | 29.53 ± 2.57 | 48.04 ± 0.94 | 41.47 ± 3.96 | 29.28 ± 3.97 | 30.99 ± 1.70 | 13.91 ± 1.06 | **53.62 ± 2.75** |
| | NMI | 38.66 ± 1.99 | 46.60 ± 0.42 | 35.66 ± 2.18 | 50.91 ± 2.02 | 45.04 ± 3.91 | 32.34 ± 4.59 | 37.50 ± 0.72 | 7.65 ± 3.74 | **54.07 ± 1.80** |
| | ARI | 27.58 ± 2.85 | 34.57 ± 0.52 | 21.49 ± 2.03 | 39.66 ± 4.01 | 31.60 ± 5.14 | 30.94 ± 3.14 | 24.29 ± 1.44 | 2.04 ± 0.73 | **45.07 ± 6.16** |
| CS | ACC | 67.01 ± 2.62 | 67.73 ± 1.39 | 69.76 ± 2.42 | 70.22 ± 2.02 | 62.21 ± 2.25 | 60.27 ± 0.64 | 54.97 ± 0.25 | 42.67 ± 2.10 | **81.54 ± 3.27** |
| | F1 | 65.65 ± 3.35 | 66.93 ± 3.07 | 66.18 ± 4.03 | 65.50 ± 2.74 | 57.36 ± 3.54 | 53.66 ± 1.93 | 49.83 ± 0.68 | 37.79 ± 1.47 | **74.36 ± 4.26** |
| | NMI | 74.54 ± 0.89 | 70.00 ± 0.38 | 72.30 ± 1.82 | 72.36 ± 0.76 | 66.81 ± 1.87 | 66.50 ± 0.85 | 58.04 ± 0.38 | 52.03 ± 0.82 | **75.34 ± 0.72** |
| | ARI | 61.44 ± 1.46 | 58.25 ± 0.36 | 60.85 ± 2.76 | 59.64 ± 2.50 | 52.39 ± 1.93 | 51.19 ± 1.17 | 41.12 ± 0.82 | 33.78 ± 2.71 | **76.52 ± 1.78** |
| Physics | ACC | 86.23 ± 0.46 | OOM | OOM | OOM | 55.57 ± 4.55 | 75.21 ± 0.65 | 78.56 ± 3.18 | 53.59 ± 1.06 | **92.31 ± 0.26** |
| | F1 | 82.19 ± 0.47 | | | | 55.13 ± 4.60 | 73.35 ± 1.08 | 73.44 ± 1.85 | 53.24 ± 1.16 | **89.37 ± 0.39** |
| | NMI | 68.75 ± 0.42 | | | | 54.49 ± 4.48 | 59.13 ± 0.50 | 54.96 ± 1.06 | 36.98 ± 0.27 | **76.06 ± 0.39** |
| | ARI | 74.64 ± 0.75 | | | | 33.72 ± 7.49 | 54.53 ± 1.19 | 61.00 ± 5.64 | 26.20 ± 0.67 | **85.32 ± 0.33** |
| Wiki | ACC | 25.86 ± 0.49 | 45.82 ± 0.98 | 26.47 ± 0.49 | 24.39 ± 1.46 | 27.67 ± 6.64 | 25.82 ± 1.59 | 33.22 ± 1.16 | 31.55 ± 1.93 | **52.68 ± 1.22** |
| | F1 | 19.92 ± 1.18 | 40.27 ± 0.74 | 20.58 ± 0.76 | 18.03 ± 2.11 | 19.64 ± 9.16 | 20.47 ± 2.35 | 23.90 ± 1.87 | 26.63 ± 1.98 | **42.97 ± 1.12** |
| | NMI | 21.62 ± 1.77 | 44.92 ± 0.39 | 21.47 ± 1.89 | 20.14 ± 2.31 | 22.34 ± 9.17 | 20.53 ± 1.87 | 28.47 ± 1.42 | 28.53 ± 1.80 | **47.22 ± 1.06** |
| | ARI | 1.48 ± 0.22 | 25.92 ± 0.83 | 2.67 ± 2.23 | 1.22 ± 0.15 | 9.55 ± 6.52 | 1.48 ± 0.22 | 6.26 ± 1.28 | 8.05 ± 0.95 | **31.11 ± 0.65** |
| UAT | ACC | 48.55 ± 1.00 | 36.50 ± 1.97 | 46.20 ± 2.02 | 48.97 ± 1.41 | 41.21 ± 1.97 | 47.23 ± 3.67 | 44.92 ± 1.53 | 40.00 ± 0.98 | **54.69 ± 1.99** |
| | F1 | 46.33 ± 3.10 | 33.09 ± 3.00 | 44.63 ± 1.60 | 47.13 ± 1.23 | 36.39 ± 5.01 | 44.79 ± 5.19 | 41.91 ± 1.78 | 36.38 ± 1.66 | **52.56 ± 5.60** |
| | NMI | 18.43 ± 1.10 | 7.20 ± 1.55 | 15.48 ± 0.71 | 19.28 ± 2.81 | 15.60 ± 5.87 | 18.17 ± 3.19 | 12.47 ± 1.15 | 10.07 ± 0.79 | **25.92 ± 2.40** |
| | ARI | 17.16 ± 1.98 | 3.90 ± 1.21 | 14.39 ± 1.01 | 19.01 ± 2.63 | 11.36 ± 3.55 | 13.70 ± 2.43 | 9.99 ± 1.10 | 5.43 ± 0.51 | **24.03 ± 1.69** |
| ACM | ACC | 52.32 ± 2.97 | 58.41 ± 0.46 | 77.98 ± 1.23 | 54.74 ± 0.93 | 59.17 ± 3.47 | 75.17 ± 3.46 | 76.32 ± 1.45 | 43.25 ± 0.67 | **82.84 ± 0.78** |
| | F1 | 53.62 ± 3.05 | 54.38 ± 0.15 | 78.01 ± 1.16 | 50.56 ± 1.34 | 59.08 ± 3.25 | 75.29 ± 3.32 | 76.62 ± 1.64 | 41.09 ± 1.22 | **82.69 ± 0.78** |
| | NMI | 24.41 ± 5.99 | 39.47 ± 1.06 | 39.74 ± 2.03 | 20.41 ± 4.72 | 20.38 ± 2.42 | 36.74 ± 3.35 | 43.20 ± 2.24 | 6.39 ± 1.28 | **50.84 ± 1.64** |
| | ARI | 17.28 ± 4.06 | 37.35 ± 0.79 | 44.98 ± 2.33 | 22.60 ± 4.51 | 16.54 ± 3.01 | 40.39 ± 5.76 | 40.99 ± 3.06 | 4.29 ± 1.16 | **55.32 ± 1.74** |

Table 11: Comparison with attribute completion methods.

## B Ablation Analysis

We assess the contribution of VISTA's view construction, sparse attribute recovery, and Laplacian smoothing. To make the variants easier to interpret, we denote the topology-conditioned second view by TV, bounded attribute recovery by BAR, and Laplacian smoothing by LS. VISTA is the complete BAR+LS+TV pipeline. The w/o variants remove TV, BAR, or LS, respectively. LS-only, BAR-only, and Raw-only retain the corresponding input construction and use the shared learner, while LS+KMeans directly clusters the fixed smoothed representation without the VISTA learner. Table 12 reports ACC, Macro-F1, NMI, and ARI for all variants in a single table. The table uses BAR+LS+TV as the complete model. Dataset-level entries are left unbolded; the macro-average summary and its best-value highlighting are reported in Table 4.

Table 12: Ablation results under a 60% attribute missing rate.

| Dataset | Metric | VISTA | w/o TV | w/o BAR | w/o LS | LS-only | BAR-only | Raw-only | LS+KMeans |
|---|---|---|---|---|---|---|---|---|---|
| Cora | ACC | 72.70±1.65 | 73.03±1.63 | 72.67±1.09 | 38.47±1.69 | 71.73±0.91 | 35.90±1.15 | 27.03±0.38 | 61.69±5.16 |
| | F1 | 70.23±1.70 | 69.59±3.98 | 70.19±0.99 | 33.87±3.29 | 69.12±1.30 | 27.59±2.78 | 14.55±1.44 | 58.75±5.45 |
| | NMI | 54.97±1.96 | 55.05±1.64 | 54.69±1.79 | 17.00±2.67 | 53.77±1.43 | 12.83±2.53 | 1.97±0.48 | 47.46±2.38 |
| | ARI | 50.98±4.13 | 51.73±2.78 | 51.74±2.00 | 10.19±1.11 | 50.88±1.77 | 6.96±2.84 | 0.21±0.35 | 41.01±4.46 |
| CiteSeer | ACC | 65.37±0.75 | 65.66±0.88 | 64.53±1.69 | 55.85±2.70 | 65.31±1.13 | 59.17±2.42 | 34.06±0.57 | 56.19±7.09 |
| | F1 | 60.22±0.96 | 60.52±0.98 | 59.52±1.69 | 51.88±3.65 | 60.16±1.28 | 55.49±2.30 | 31.29±0.70 | 50.87±6.17 |
| | NMI | 37.67±0.71 | 38.14±0.70 | 36.52±1.81 | 28.05±1.64 | 37.44±1.10 | 31.26±2.21 | 14.38±0.36 | 32.27±3.35 |
| | ARI | 39.69±0.67 | 40.08±1.01 | 38.51±2.22 | 28.07±1.79 | 39.68±1.32 | 31.35±2.83 | 3.84±0.14 | 30.65±4.33 |
| DBLP | ACC | 78.26±0.24 | 78.12±0.31 | 74.50±5.24 | 47.60±1.02 | 73.46±5.82 | 43.22±0.32 | 39.82±0.28 | 62.69±5.72 |
| | F1 | 73.95±0.32 | 73.80±0.33 | 69.46±5.56 | 37.15±4.91 | 69.37±5.76 | 30.68±2.46 | 26.05±0.73 | 55.86±6.63 |
| | NMI | 47.03±0.50 | 46.91±0.41 | 43.15±4.28 | 11.14±2.28 | 43.08±4.34 | 5.05±1.63 | 2.41±1.72 | 35.75±1.94 |
| | ARI | 52.06±0.44 | 51.67±0.59 | 48.36±5.17 | 8.98±2.96 | 47.04±5.38 | 5.62±1.13 | -0.02±0.19 | 36.60±7.38 |
| PubMed | ACC | 70.70±0.25 | 70.72±0.26 | 70.71±0.27 | 61.75±2.08 | 70.68±0.29 | 49.58±0.64 | 44.37±1.92 | 70.65±0.09 |
| | F1 | 69.86±0.22 | 69.88±0.23 | 69.89±0.23 | 62.00±2.35 | 69.86±0.27 | 49.31±1.11 | 42.02±4.57 | 69.85±0.08 |
| | NMI | 32.29±0.24 | 32.31±0.29 | 32.26±0.24 | 24.15±2.94 | 32.26±0.20 | 13.46±1.63 | 6.27±2.46 | 32.50±0.12 |
| | ARI | 33.10±0.47 | 33.16±0.45 | 33.12±0.43 | 22.44±3.95 | 33.04±0.49 | 13.55±1.55 | 2.82±1.25 | 33.17±0.14 |
| Photo | ACC | 78.61±0.95 | 78.80±0.79 | 78.06±0.86 | 64.27±3.10 | 77.21±2.70 | 66.35±0.44 | 31.54±1.89 | 76.70±0.77 |
| | F1 | 73.56±1.19 | 73.42±1.04 | 71.88±1.91 | 57.03±4.12 | 70.64±5.17 | 60.11±0.49 | 25.12±5.03 | 69.99±2.19 |
| | NMI | 71.40±0.98 | 71.43±0.92 | 70.53±1.59 | 52.76±1.05 | 70.56±1.78 | 52.72±0.88 | 15.70±3.34 | 67.69±0.99 |
| | ARI | 61.47±1.68 | 61.64±1.57 | 60.37±1.60 | 43.10±2.30 | 60.09±2.56 | 44.33±1.01 | 3.06±0.51 | 58.15±0.82 |
| BlogCatalog | ACC | 62.49±1.08 | 56.13±1.80 | 60.65±1.85 | 30.41±0.52 | 45.93±2.41 | 28.20±0.96 | 28.40±0.74 | 54.24±3.77 |
| | F1 | 60.10±1.86 | 55.31±1.87 | 58.91±1.77 | 31.91±0.96 | 46.92±2.08 | 29.16±1.12 | 29.07±1.17 | 52.48±3.71 |
| | NMI | 38.02±0.78 | 30.45±0.97 | 35.09±0.82 | 14.65±0.95 | 20.27±2.15 | 11.46±1.59 | 13.29±1.31 | 28.66±2.14 |
| | ARI | 33.19±0.83 | 27.06±0.62 | 32.83±0.69 | 4.87±2.05 | 15.57±1.93 | 2.90±0.17 | 2.58±0.26 | 26.59±2.78 |
| USPS | ACC | 91.81±0.06 | 91.80±0.06 | 91.78±0.12 | 62.02±2.83 | 91.79±0.12 | 63.06±1.83 | 31.30±0.69 | 70.87±3.74 |
| | F1 | 91.13±0.09 | 91.12±0.08 | 91.11±0.14 | 62.47±3.71 | 91.11±0.14 | 63.61±1.52 | 33.30±0.85 | 66.20±1.44 |
| | NMI | 83.68±0.11 | 83.68±0.11 | 83.67±0.19 | 52.45±1.12 | 83.67±0.19 | 52.62±0.68 | 27.85±0.90 | 78.04±0.49 |
| | ARI | 84.42±0.10 | 84.41±0.10 | 84.40±0.21 | 37.23±0.68 | 84.40±0.21 | 37.69±0.73 | 3.41±0.18 | 66.73±4.46 |
| HHAR | ACC | 79.70±1.61 | 79.70±1.62 | 79.37±0.68 | 66.01±0.99 | 78.81±1.03 | 66.02±1.14 | 33.14±2.52 | 57.66±7.53 |
| | F1 | 78.91±3.11 | 78.91±3.13 | 78.83±2.14 | 63.17±1.27 | 77.50±3.02 | 63.19±1.46 | 32.82±3.71 | 52.98±8.38 |
| | NMI | 74.91±1.68 | 74.92±1.68 | 74.60±2.15 | 62.17±0.55 | 75.52±2.29 | 62.19±0.63 | 26.34±3.60 | 66.12±1.97 |
| | ARI | 66.32±1.37 | 66.32±1.37 | 65.78±1.57 | 55.38±0.92 | 66.37±1.80 | 55.41±1.04 | 6.37±0.88 | 47.62±7.60 |
| EAT | ACC | 58.25±0.23 | 58.20±0.28 | 58.20±0.28 | 40.60±0.59 | 58.20±0.28 | 43.01±1.13 | 26.97±0.38 | 28.87±0.27 |
| | F1 | 58.42±0.21 | 58.35±0.29 | 58.35±0.28 | 36.33±3.32 | 58.34±0.28 | 38.72±3.39 | 13.78±0.84 | 18.82±0.30 |
| | NMI | 34.38±0.18 | 34.35±0.21 | 34.31±0.19 | 10.80±0.83 | 34.23±0.23 | 11.11±1.37 | 3.53±0.87 | 4.44±0.02 |
| | ARI | 27.83±0.29 | 27.84±0.29 | 27.81±0.27 | 9.08±1.30 | 27.75±0.31 | 10.39±1.27 | 0.09±0.09 | 0.53±0.06 |
| BAT | ACC | 80.61±1.02 | 80.31±1.00 | 79.23±1.25 | 48.55±2.20 | 79.39±1.43 | 51.30±2.72 | 30.99±0.68 | 42.59±1.47 |
| | F1 | 80.65±0.97 | 80.36±0.94 | 79.22±1.19 | 46.60±3.36 | 79.42±1.37 | 46.94±2.01 | 20.28±2.22 | 36.44±2.06 |
| | NMI | 56.77±1.52 | 56.33±1.46 | 54.83±1.44 | 15.94±1.68 | 55.10±1.80 | 19.84±2.09 | 8.47±1.15 | 13.14±1.43 |
| | ARI | 55.76±2.13 | 55.14±2.06 | 53.34±2.26 | 12.96±2.26 | 53.51±2.65 | 18.22±2.44 | 0.40±0.13 | 10.12±1.06 |
| CoraFull | ACC | 42.42±0.43 | 42.31±0.36 | 42.24±0.22 | 35.58±0.66 | 42.28±0.38 | 33.70±0.42 | 14.02±0.44 | 40.36±1.22 |
| | F1 | 33.62±0.68 | 33.39±0.58 | 33.49±0.67 | 29.98±0.53 | 33.53±0.35 | 27.99±0.69 | 12.08±0.51 | 32.06±1.11 |
| | NMI | 54.48±0.28 | 54.58±0.08 | 54.39±0.24 | 46.37±0.19 | 54.56±0.13 | 43.77±0.40 | 20.49±0.54 | 54.10±0.52 |
| | ARI | 29.47±0.77 | 29.51±0.43 | 29.31±0.53 | 19.63±0.49 | 29.58±0.72 | 17.19±0.73 | 0.28±0.05 | 28.50±1.12 |
| Computers | ACC | 64.02±3.93 | 63.78±4.30 | 65.31±3.04 | 39.45±0.33 | 65.33±3.01 | 39.35±0.63 | 29.55±0.82 | 53.61±4.33 |
| | F1 | 53.62±2.75 | 52.26±5.03 | 51.07±2.74 | 25.33±1.26 | 51.08±2.74 | 24.23±2.66 | 9.75±1.61 | 37.48±10.13 |
| | NMI | 54.07±1.80 | 53.57±1.25 | 55.50±1.44 | 27.19±1.31 | 55.50±1.44 | 26.19±2.58 | 2.55±2.57 | 47.61±2.85 |
| | ARI | 45.07±6.16 | 44.93±5.99 | 48.63±5.48 | 16.87±0.68 | 48.65±5.45 | 16.35±1.29 | 0.73±0.61 | 33.75±2.62 |
| CS | ACC | 81.54±3.27 | 80.53±3.15 | 80.31±2.58 | 65.46±2.04 | 80.89±2.60 | 54.72±2.68 | 37.91±0.75 | 71.11±3.33 |
| | F1 | 74.36±4.26 | 74.87±4.49 | 71.84±3.42 | 60.41±3.67 | 73.51±3.94 | 55.40±2.67 | 35.62±3.86 | 64.74±4.22 |
| | NMI | 75.34±0.72 | 75.28±0.79 | 74.59±0.39 | 61.86±1.15 | 74.58±0.56 | 53.69±1.24 | 34.37±0.56 | 72.74±1.28 |
| | ARI | 76.52±1.78 | 74.46±3.76 | 75.68±1.06 | 50.87±2.10 | 72.63±5.89 | 31.80±3.77 | 4.84±0.87 | 63.13±2.07 |
| Physics | ACC | 92.31±0.26 | 90.97±1.29 | 92.23±0.22 | 65.30±2.68 | 92.01±0.13 | 56.47±3.55 | 43.54±0.81 | 78.16±6.12 |
| | F1 | 89.37±0.39 | 87.03±2.27 | 89.25±0.37 | 65.73±1.88 | 88.84±0.29 | 56.97±2.46 | 32.89±2.11 | 69.56±6.63 |
| | NMI | 76.06±0.39 | 73.78±1.90 | 75.83±0.44 | 49.33±3.00 | 75.40±0.30 | 38.43±2.53 | 20.18±0.67 | 65.95±3.82 |
| | ARI | 85.32±0.33 | 83.78±1.13 | 85.19±0.23 | 38.29±4.47 | 84.70±0.23 | 27.89±4.80 | 5.14±0.97 | 69.33±10.03 |
| Wiki | ACC | 52.68±1.22 | 52.68±1.22 | 53.06±1.76 | 49.23±2.70 | 53.05±1.78 | 49.56±2.49 | 28.32±1.83 | 46.70±3.97 |
| | F1 | 42.97±1.12 | 42.96±1.12 | 43.86±1.18 | 39.91±1.80 | 43.84±1.21 | 40.90±1.66 | 21.03±1.18 | 37.19±3.77 |
| | NMI | 47.22±1.06 | 47.20±1.06 | 46.68±0.71 | 41.99±1.26 | 46.65±0.75 | 42.28±1.11 | 24.29±1.01 | 43.42±1.15 |
| | ARI | 31.11±0.65 | 31.00±0.69 | 33.22±1.45 | 28.37±1.49 | 33.19±1.51 | 28.07±1.43 | 2.32±0.34 | 26.07±3.34 |
| UAT | ACC | 54.69±1.99 | 54.76±1.71 | 54.74±1.09 | 48.12±1.48 | 54.55±1.36 | 47.16±1.40 | 32.94±1.31 | 38.03±2.49 |
| | F1 | 52.56±5.60 | 52.16±5.92 | 55.75±1.09 | 45.54±3.23 | 55.53±1.40 | 43.55±1.80 | 22.47±2.29 | 29.42±4.03 |
| | NMI | 25.92±2.40 | 25.85±2.18 | 26.47±0.56 | 16.61±2.72 | 26.26±0.88 | 14.21±1.98 | 7.28±1.48 | 9.46±1.45 |
| | ARI | 24.03±1.69 | 24.11±1.30 | 22.78±1.13 | 14.66±1.71 | 22.68±1.39 | 13.16±1.49 | 2.09±0.48 | 6.23±0.92 |
| ACM | ACC | 82.84±0.78 | 82.83±0.81 | 82.24±0.81 | 81.81±0.73 | 82.21±0.97 | 81.59±0.54 | 53.96±1.51 | 74.69±12.90 |
| | F1 | 82.69±0.78 | 82.68±0.82 | 82.07±0.82 | 81.67±0.73 | 82.05±1.00 | 81.44±0.54 | 51.10±1.79 | 74.76±13.05 |
| | NMI | 50.84±1.64 | 50.89±1.54 | 49.71±1.75 | 48.50±1.70 | 49.74±1.83 | 48.13±1.01 | 17.87±2.43 | 43.36±10.50 |
| | ARI | 55.32±1.74 | 55.31±1.79 | 53.99±1.75 | 52.91±1.63 | 53.91±2.11 | 52.42±1.26 | 8.33±0.96 | 44.06±12.88 |

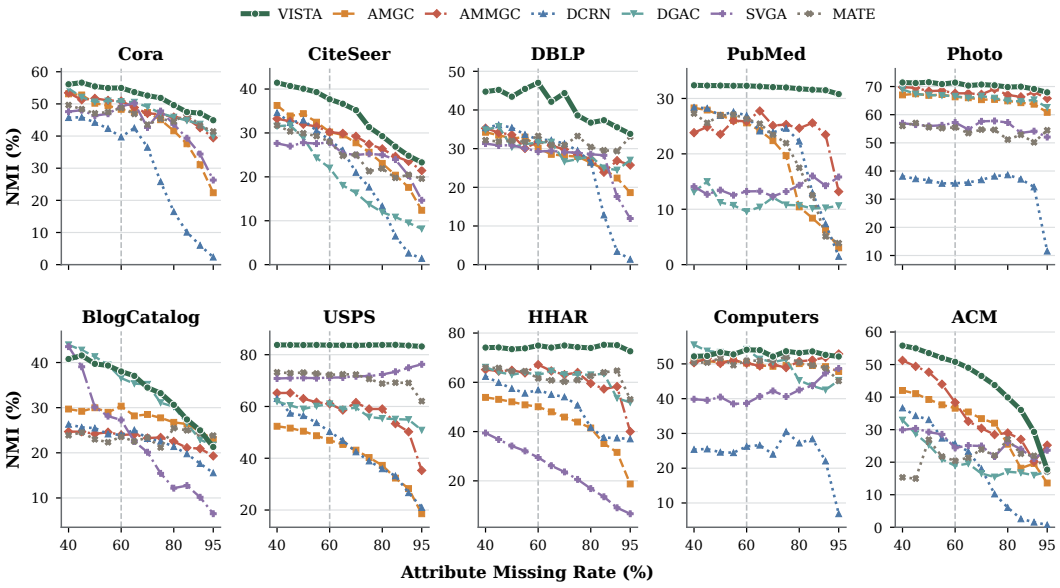


Figure 6: NMI across different attribute missing rates.

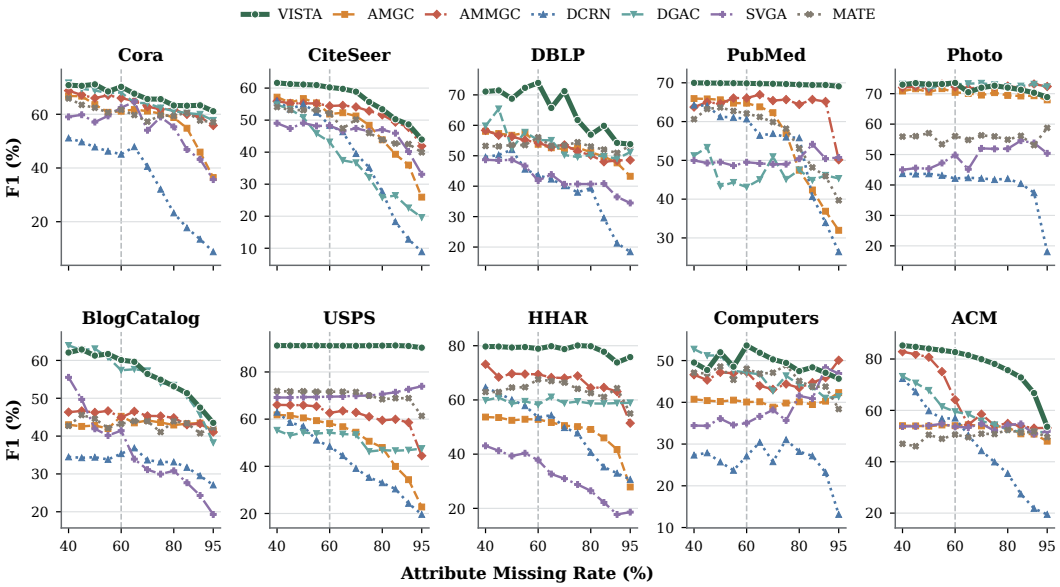


Figure 7: Macro-F1 across different attribute missing rates.

Table 12 presents detailed ablation results for VISTA under different component combinations. Overall, the complete BAR+LS+TV framework provides the most stable performance across the evaluated datasets and metrics, suggesting that the three components are complementary. Within the scope of this ablation study, LS is the main source of the performance gain, while BAR and TV provide additional information on top of the smoothed representation.

Removing LS causes the clearest degradation. The w/o LS variant retains BAR and TV but no longer applies Laplacian smoothing, and its performance drops substantially on many datasets. This result shows that attribute recovery and view construction alone do not directly produce representations that are well suited to clustering. LS propagates information along the graph and further integrates neighborhood semantics, allowing the recovered attributes to form more discriminative clustering

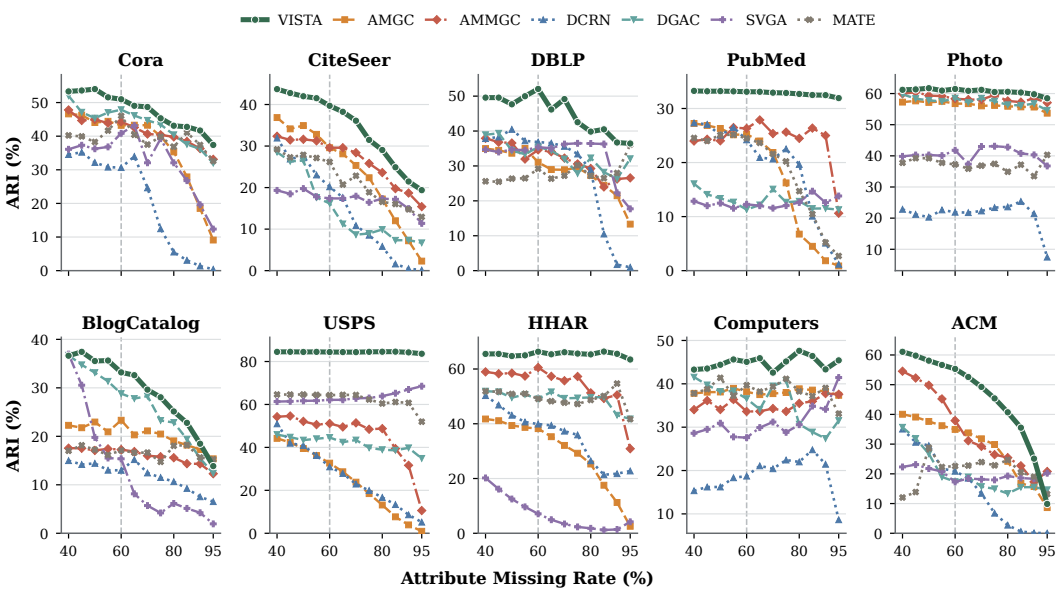


Figure 8: ARI across different attribute missing rates.

representations. In this framework, LS therefore provides the central connection between missing semantic information and graph topology.

By contrast, removing BAR or TV causes relatively limited changes. The w/o BAR variant retains LS and TV, allowing the model to exploit topology-aware propagation and the topology-conditioned view. The w/o TV variant retains BAR and LS, allowing the recovered attributes to be fully exploited through structural smoothing. Thus, when either BAR or TV is removed individually, the remaining components can partly compensate for the missing information. However, LS-only still falls clearly below the complete model, showing that LS alone is insufficient when both BAR and TV are absent. BAR and TV do not individually determine the final performance, but they complement LS and together improve the quality of the learned representation.

The LS-only, BAR-only, and Raw-only variants further clarify the role of the input-construction modules. LS-only substantially outperforms BAR-only, indicating that recovering missing attributes alone is insufficient to obtain a strong clustering structure. BAR provides initial semantic evidence for missing nodes, whereas LS subsequently propagates this information through the graph and makes the representation more suitable for clustering. The inferior Raw-only results show that the VISTA learner cannot by itself recover effective structural information from a severely incomplete attribute matrix, which confirms the importance of front-end information construction.

Finally, comparing LS-only with LS+KMeans highlights the contribution of the VISTA learner. Although the fixed smoothed representation already contains useful topological information, directly applying KMeans to it performs worse than optimizing the representation with the shared learner. This indicates that VISTA's advantage does not come solely from topology smoothing; the cross-view prototype-learning objective further shapes the representation space for clustering.

Overall, the ablation results reveal a hierarchical design. BAR provides initial semantic recovery, LS establishes the topology-aware representation, and TV with cross-view prototype learning further refines the clustering space. These lightweight components are complementary rather than merely stacked, jointly improving clustering on attribute-missing graphs.

## C Robustness to Non-Random Missingness

Tables 13 and 14 extend Section 5.4 with results on ten datasets under high-degree and high-norm node-wise missingness, respectively. Both settings retain a 60% attribute missing rate and use seeds 41–45. Results are percentages reported as mean±standard deviation. The highest and second-

highest means in each row are boldfaced and underlined, respectively; OOM denotes out-of-memory runs. Unlike the missing-rate sweep, this experiment changes which nodes are more likely to lose their attributes rather than the overall amount of missing data. High-degree missingness preferentially selects highly connected nodes, whereas high-norm missingness favors nodes with larger attribute norms in the shared standardized feature space. Selection is biased rather than restricted deterministically to the highest-scoring nodes. The graph itself is retained in both settings. Thus, the two mechanisms probe robustness to structure-dependent and attribute-dependent changes in the available semantic evidence.

The full results show that the advantage extends beyond the three datasets highlighted in the main text. VISTA achieves the highest mean ACC in all 20 dataset–mechanism comparisons. Its advantage also extends to Macro-F1 and ARI throughout these comparisons, indicating that the improvement is not restricted to overall label-matching accuracy: it is also reflected in class-balanced performance and agreement between the predicted and reference partitions. NMI provides a similar picture. On Physics under high-degree missingness, THESAURUS has a slightly higher NMI, while VISTA leads on the other three metrics; under high-norm missingness, VISTA leads on all four. The overall consistency across metrics is more informative than relying on a single clustering score.

Comparing the two tables also reveals that the strongest competing method can change with the missingness mechanism. On ACM, AMMGC is the strongest baseline on all four metrics under high-degree missingness, whereas THESAURUS takes that position under high-norm missingness. VISTA remains ahead in both cases. On USPS, SVGA is the strongest baseline under both mechanisms, yet VISTA maintains higher scores on all four metrics, with small standard deviations across the five runs. These examples distinguish robustness across missingness mechanisms from superiority over a particular baseline: VISTA remains competitive even when the distribution of missing attributes changes which alternative method performs best.

This behavior is consistent with the complementary roles of recovery and representation learning in VISTA. Although the location of missing attributes changes, BAR can still draw on available neighborhood evidence, and LS propagates and integrates the recovered information over the retained graph. The topology-conditioned view and prototype-learning objective then use these inputs to learn clustering-oriented representations. The two mechanisms need not affect every dataset in the same direction: for example, VISTA's ACC is lower under high-norm than high-degree missingness on ACM and USPS, but slightly higher on Physics. Robustness therefore concerns the ability to maintain effective clustering under different observation patterns, rather than identical scores across mechanisms. Together, the results support the effectiveness of VISTA when attribute availability depends on either graph structure or node attributes.

## D Comparison of Attribute Recovery Strategies

Some existing attribute-missing graph clustering methods focus primarily on recovering missing attributes or constructing structural views, while their outputs still need to be processed by a downstream clustering procedure. Therefore, comparing front-ends alone does not fully explain differences in final clustering performance, nor does it reveal whether the recovered or constructed information is effectively used. We consequently use several representative recovery and view-construction methods as front-ends and combine them with either direct KMeans or the same VISTA learner to examine their behavior under different downstream clustering procedures. All configurations use the same missing masks and preprocessing to ensure a consistent comparison.

Specifically, we consider FP, CMV-ND, and DTRGC. FP uses graph-based feature propagation to transfer attributes from observed nodes to missing nodes while keeping the observed attributes unchanged during propagation, producing recovered features without an additional learnable imputer. CMV-ND focuses on organizing recovered information: based on the recovered features, it further separates neighborhood information at different hop distances and constructs complementary multi-hop structural views, allowing node-level semantics and topological information at different scales to be used separately. In contrast, DTRGC adopts a clustering-driven recovery strategy that uses temporary cluster assignments to adjust information transfer during propagation, together with hierarchical neighborhood interpolation and multi-hop representation enhancement, thereby coupling attribute recovery more closely with the clustering process.

| Dataset | Metric | SDCN | DCRN | DGAC | THESAURUS | AMGC | AMMGC | HCN-PAI | SVGA | VISTA |
|---|---|---|---|---|---|---|---|---|---|---|
| Cora | ACC | 33.23 ± 1.98 | 30.59 ± 2.52 | 65.60 ± 2.24 | 57.87 ± 5.49 | 63.78 ± 2.82 | 70.54 ± 0.99 | 56.03 ± 2.46 | 53.04 ± 1.83 | **73.02 ± 1.18** |
| | F1 | 17.28 ± 2.97 | 19.52 ± 3.96 | 64.27 ± 2.82 | 52.59 ± 5.93 | 57.78 ± 3.22 | 69.00 ± 1.81 | 53.90 ± 2.48 | 46.90 ± 1.96 | **69.81 ± 2.17** |
| | NMI | 9.70 ± 3.16 | 11.96 ± 3.53 | 46.15 ± 3.17 | 39.09 ± 4.16 | 45.51 ± 1.43 | 52.47 ± 0.98 | 41.14 ± 1.12 | 38.28 ± 1.01 | **53.90 ± 2.32** |
| | ARI | 3.87 ± 2.31 | 4.67 ± 4.35 | 39.98 ± 2.40 | 32.45 ± 6.70 | 38.92 ± 2.51 | 47.58 ± 0.58 | 33.96 ± 2.24 | 24.73 ± 1.63 | **50.84 ± 3.11** |
| CiteSeer | ACC | 31.10 ± 2.44 | 33.13 ± 1.25 | 40.42 ± 0.95 | 43.80 ± 1.85 | 56.50 ± 2.13 | 59.09 ± 2.02 | 46.58 ± 2.01 | 46.91 ± 2.95 | **66.85 ± 1.40** |
| | F1 | 24.95 ± 2.36 | 26.99 ± 0.94 | 37.25 ± 1.03 | 41.20 ± 2.08 | 52.96 ± 2.17 | 55.02 ± 1.84 | 44.32 ± 1.62 | 43.13 ± 4.29 | **59.46 ± 1.53** |
| | NMI | 8.10 ± 1.73 | 11.37 ± 1.04 | 16.98 ± 1.04 | 19.86 ± 1.61 | 29.23 ± 1.47 | 31.51 ± 1.63 | 20.37 ± 1.14 | 25.03 ± 3.82 | **38.45 ± 1.60** |
| | ARI | 3.93 ± 2.23 | 3.16 ± 0.61 | 6.11 ± 1.26 | 16.31 ± 1.63 | 28.35 ± 2.23 | 30.79 ± 2.59 | 19.14 ± 1.21 | 15.23 ± 2.58 | **40.68 ± 1.80** |
| DBLP | ACC | 53.99 ± 2.29 | 53.17 ± 1.22 | 61.23 ± 2.06 | 64.82 ± 0.96 | 59.93 ± 3.04 | 60.36 ± 4.40 | 52.02 ± 1.59 | 60.23 ± 0.25 | **73.09 ± 5.41** |
| | F1 | 29.96 ± 1.02 | 35.69 ± 2.07 | 54.02 ± 5.34 | 58.63 ± 1.73 | 53.77 ± 4.30 | 55.18 ± 3.70 | 46.99 ± 1.58 | 47.83 ± 0.29 | **68.99 ± 5.82** |
| | NMI | 9.91 ± 1.57 | 14.41 ± 1.82 | 24.61 ± 3.40 | 30.39 ± 2.32 | 29.59 ± 2.63 | 32.41 ± 3.09 | 29.02 ± 1.46 | 30.95 ± 0.18 | **42.32 ± 3.09** |
| | ARI | 12.52 ± 2.38 | 8.62 ± 1.37 | 26.26 ± 2.09 | 37.42 ± 1.48 | 32.90 ± 3.10 | 32.98 ± 6.33 | 26.56 ± 1.10 | 35.50 ± 0.75 | **48.26 ± 2.92** |
| PubMed | ACC | 43.88 ± 2.30 | 68.98 ± 1.04 | 56.02 ± 1.56 | 40.35 ± 0.26 | 63.85 ± 1.83 | 65.63 ± 2.43 | 62.31 ± 0.81 | 55.94 ± 0.54 | **71.00 ± 0.25** |
| | F1 | 34.50 ± 9.51 | 67.97 ± 0.79 | 44.15 ± 5.35 | 30.67 ± 3.96 | 63.53 ± 1.82 | 65.12 ± 2.48 | 62.10 ± 0.80 | 49.38 ± 0.52 | **70.25 ± 0.25** |
| | NMI | 4.79 ± 3.79 | 27.97 ± 2.10 | 9.70 ± 1.61 | 0.45 ± 0.34 | 23.32 ± 1.77 | 24.50 ± 3.55 | 18.82 ± 1.12 | 12.31 ± 1.40 | **32.33 ± 0.31** |
| | ARI | 2.57 ± 1.93 | 29.24 ± 1.84 | 11.57 ± 2.14 | 0.24 ± 0.33 | 23.06 ± 2.53 | 25.37 ± 3.86 | 19.15 ± 1.07 | 11.87 ± 0.85 | **33.44 ± 0.32** |
| ACM | ACC | 46.70 ± 1.40 | 43.36 ± 2.46 | 52.75 ± 1.90 | 53.17 ± 1.66 | 43.54 ± 8.30 | 68.40 ± 10.28 | 57.26 ± 4.89 | 53.32 ± 0.97 | **85.45 ± 0.49** |
| | F1 | 46.73 ± 1.17 | 40.02 ± 3.52 | 52.96 ± 1.67 | 54.18 ± 1.74 | 38.57 ± 7.17 | 68.38 ± 10.40 | 56.27 ± 4.48 | 54.60 ± 0.96 | **85.44 ± 0.48** |
| | NMI | 11.11 ± 0.81 | 7.73 ± 2.48 | 16.99 ± 2.04 | 20.08 ± 2.20 | 9.74 ± 15.69 | 37.62 ± 6.96 | 29.24 ± 3.23 | 26.49 ± 0.94 | **55.06 ± 1.35** |
| | ARI | 6.42 ± 1.38 | 2.54 ± 1.01 | 14.70 ± 3.15 | 15.33 ± 1.60 | 9.62 ± 15.02 | 38.22 ± 10.45 | 24.34 ± 6.20 | 18.43 ± 1.95 | **61.25 ± 1.24** |
| CS | ACC | 42.35 ± 3.20 | 46.29 ± 1.41 | 68.55 ± 1.56 | 68.16 ± 0.78 | 75.42 ± 0.73 | 76.27 ± 1.34 | 61.58 ± 1.07 | 67.03 ± 1.74 | **81.10 ± 1.27** |
| | F1 | 20.19 ± 3.08 | 28.46 ± 1.06 | 63.31 ± 1.85 | 59.54 ± 1.66 | 71.73 ± 1.24 | 70.14 ± 1.53 | 50.93 ± 2.15 | 66.71 ± 1.82 | **76.30 ± 3.50** |
| | NMI | 37.21 ± 4.82 | 54.03 ± 2.10 | 72.41 ± 0.45 | 72.70 ± 1.00 | 76.40 ± 0.47 | 73.95 ± 0.88 | 61.08 ± 1.56 | 75.02 ± 1.00 | **77.06 ± 0.57** |
| | ARI | 26.62 ± 3.69 | 32.50 ± 4.34 | 60.74 ± 2.12 | 62.15 ± 1.27 | 67.47 ± 0.46 | 68.01 ± 1.09 | 51.91 ± 2.14 | 59.99 ± 3.08 | **75.90 ± 3.59** |
| USPS | ACC | 36.42 ± 2.59 | 45.78 ± 1.31 | 55.91 ± 2.12 | 56.59 ± 1.77 | 61.17 ± 2.58 | 61.41 ± 1.61 | 69.36 ± 0.37 | 70.56 ± 0.60 | **91.96 ± 0.14** |
| | F1 | 39.22 ± 1.27 | 43.93 ± 1.63 | 53.45 ± 2.32 | 54.77 ± 1.61 | 59.99 ± 3.10 | 60.64 ± 1.78 | 67.50 ± 0.43 | 68.74 ± 0.59 | **91.28 ± 0.15** |
| | NMI | 35.26 ± 0.99 | 43.83 ± 1.79 | 58.79 ± 2.45 | 48.89 ± 1.19 | 51.52 ± 1.06 | 56.32 ± 1.39 | 66.24 ± 0.56 | 69.91 ± 0.48 | **83.98 ± 0.20** |
| | ARI | 6.59 ± 1.17 | 26.57 ± 3.29 | 42.88 ± 2.94 | 40.27 ± 1.60 | 43.16 ± 1.39 | 46.32 ± 1.04 | 58.63 ± 0.74 | 60.59 ± 0.77 | **84.75 ± 0.27** |
| HHAR | ACC | 35.87 ± 3.26 | 36.29 ± 1.25 | 61.12 ± 2.81 | 47.12 ± 0.69 | 56.30 ± 0.79 | 68.16 ± 5.75 | 50.52 ± 2.23 | 34.64 ± 0.19 | **79.25 ± 1.69** |
| | F1 | 35.26 ± 6.60 | 35.45 ± 2.02 | 57.51 ± 2.45 | 46.43 ± 1.76 | 53.44 ± 0.58 | 65.86 ± 7.29 | 48.15 ± 3.87 | 34.99 ± 0.32 | **79.14 ± 1.52** |
| | NMI | 27.66 ± 6.05 | 38.06 ± 1.38 | 61.69 ± 2.94 | 40.94 ± 1.70 | 53.78 ± 0.82 | 65.04 ± 3.43 | 46.84 ± 0.77 | 28.33 ± 0.14 | **73.46 ± 0.94** |
| | ARI | 7.47 ± 2.60 | 20.87 ± 0.61 | 47.22 ± 4.65 | 26.44 ± 2.26 | 40.98 ± 1.55 | 57.80 ± 4.83 | 31.84 ± 1.12 | 6.76 ± 0.05 | **65.14 ± 1.47** |
| BAT | ACC | 36.03 ± 2.01 | 57.56 ± 3.37 | 63.51 ± 2.13 | 71.45 ± 3.43 | 41.07 ± 2.34 | 66.11 ± 2.03 | 50.53 ± 1.22 | 48.24 ± 3.84 | **78.62 ± 0.97** |
| | F1 | 28.12 ± 2.74 | 55.73 ± 4.65 | 63.42 ± 2.44 | 70.90 ± 4.29 | 36.52 ± 3.04 | 62.88 ± 3.29 | 47.44 ± 1.53 | 43.07 ± 4.12 | **78.65 ± 0.94** |
| | NMI | 19.41 ± 2.97 | 39.30 ± 1.99 | 42.18 ± 2.81 | 46.04 ± 4.61 | 20.16 ± 2.61 | 45.98 ± 1.32 | 27.20 ± 7.92 | 29.48 ± 5.49 | **54.08 ± 1.26** |
| | ARI | 5.25 ± 1.07 | 27.86 ± 2.03 | 33.17 ± 3.90 | 41.56 ± 5.04 | 11.79 ± 4.16 | 41.41 ± 1.36 | 21.02 ± 5.68 | 19.52 ± 6.87 | **52.20 ± 1.79** |
| Physics | ACC | 72.76 ± 6.78 | OOM | 80.40 ± 2.18 | 90.83 ± 1.68 | 67.60 ± 10.22 | 71.96 ± 2.21 | 78.82 ± 4.21 | 88.99 ± 0.29 | **91.82 ± 0.16** |
| | F1 | 56.32 ± 8.85 | | 74.23 ± 4.58 | 86.99 ± 2.57 | 65.88 ± 8.85 | 64.57 ± 6.41 | 64.88 ± 5.44 | 84.66 ± 0.50 | **88.84 ± 0.25** |
| | NMI | 46.97 ± 10.49 | | 60.02 ± 3.57 | **75.70 ± 2.73** | 62.27 ± 2.04 | 55.78 ± 2.22 | 60.68 ± 4.24 | 72.39 ± 0.29 | 74.99 ± 0.29 |
| | ARI | 45.76 ± 12.50 | | 64.90 ± 2.38 | 83.84 ± 2.55 | 54.72 ± 6.60 | 53.60 ± 7.76 | 70.74 ± 4.78 | 80.82 ± 0.20 | **84.18 ± 0.21** |

Table 13: Clustering results under high-degree missingness.

Based on these front-ends, we construct two groups of variants. The first group directly applies KMeans to the resulting representations, including FP-KMeans, FP-CMV-KMeans, and DTRGC-KMeans. The second group uses the shared VISTA learner, including FP-VISTA, FP-CMV-VISTA, DTRGC-VISTA, and BAR-CMV-VISTA. Specifically, these variants replace the recovery operator or view organization while keeping other components unchanged: FP uses propagation-based recovery, CMV-ND provides multi-hop view construction, DTRGC uses clustering-driven recovery, and BAR replaces FP in BAR-CMV-VISTA. These combinations allow us to isolate the effects of recovery, view organization, and downstream representation learning.

Tables 15 and 16 report the complete dataset-level results for the variants above, with Table 15 reporting ACC and Macro-F1 and Table 16 reporting NMI and ARI. The dataset-level results show that the effects of different front-end designs depend on both the graph and the way the components are combined. For example, multi-hop views provide useful complementary information on DBLP and Photo, but do not produce the same benefit on ACM and Computers. Similarly, DTRGC performs relatively strongly in some fixed-representation configurations, but this advantage is not consistently retained when the representations are passed to the shared learner. Meanwhile, when the CMV-ND view organization and VISTA learner are fixed, replacing the recovery operator does not produce a consistent change in performance. These observations show that the recovery operator, view organization, and downstream representation learning are not independent; their effects also depend on the graph and the compatibility among components. In other words, strengthening recovery alone or adding structural views does not guarantee better clustering. More importantly, recovered information must be organized appropriately for the graph and effectively used by the downstream learner.

### D.1 Transferability of the Recovery Module

To evaluate the transferability of BAR+LS, we apply it to five representative clustering methods: CoCo, Dink-Net, SDCN, SAGSC, and GGD. These methods are not designed for attribute-missing

| Dataset | Metric | SDCN | DCRN | DGAC | THESAURUS | AMGC | AMMGC | HCN-PAI | SVGA | VISTA |
|---|---|---|---|---|---|---|---|---|---|---|
| Cora | ACC | 36.21 ± 3.05 | 54.18 ± 1.44 | 68.53 ± 1.75 | 67.61 ± 2.67 | 66.95 ± 1.35 | 67.97 ± 0.94 | 57.78 ± 5.26 | 59.71 ± 5.46 | **73.16 ± 0.66** |
| | F1 | 22.64 ± 5.09 | 48.62 ± 3.90 | 65.20 ± 1.64 | 65.75 ± 2.90 | 63.23 ± 0.96 | 66.91 ± 1.55 | 55.74 ± 5.07 | 55.23 ± 7.97 | **70.82 ± 0.40** |
| | NMI | 10.90 ± 3.03 | 38.65 ± 2.38 | 49.05 ± 1.25 | 48.38 ± 1.32 | 49.19 ± 1.18 | 50.54 ± 0.85 | 40.64 ± 2.73 | 46.55 ± 3.13 | **55.11 ± 0.82** |
| | ARI | 8.33 ± 6.17 | 26.22 ± 1.58 | 44.17 ± 3.72 | 42.44 ± 4.94 | 42.41 ± 1.97 | 43.32 ± 0.18 | 33.36 ± 3.52 | 38.22 ± 3.73 | **51.71 ± 1.46** |
| CiteSeer | ACC | 33.53 ± 2.39 | 50.67 ± 0.84 | 48.30 ± 2.75 | 52.67 ± 4.16 | 58.54 ± 1.99 | 58.26 ± 2.32 | 44.09 ± 1.22 | 47.84 ± 2.34 | **64.75 ± 0.57** |
| | F1 | 24.85 ± 4.58 | 45.73 ± 1.19 | 42.19 ± 2.64 | 50.38 ± 4.35 | 55.25 ± 1.85 | 55.15 ± 2.15 | 42.49 ± 1.13 | 46.74 ± 3.01 | **59.98 ± 0.67** |
| | NMI | 11.09 ± 2.20 | 26.33 ± 0.57 | 21.01 ± 1.80 | 26.83 ± 2.48 | 31.41 ± 1.68 | 30.63 ± 2.43 | 19.63 ± 0.76 | 25.41 ± 2.66 | **37.46 ± 1.00** |
| | ARI | 6.29 ± 1.49 | 16.32 ± 1.84 | 14.72 ± 3.13 | 25.28 ± 2.76 | 31.00 ± 2.39 | 30.11 ± 2.90 | 17.50 ± 1.48 | 19.33 ± 1.42 | **38.94 ± 0.74** |
| DBLP | ACC | 47.96 ± 4.91 | 64.18 ± 1.04 | 64.20 ± 1.85 | 66.53 ± 4.70 | 58.38 ± 2.28 | 62.31 ± 2.12 | 56.73 ± 0.95 | 64.20 ± 0.84 | **72.90 ± 3.91** |
| | F1 | 26.06 ± 8.56 | 48.49 ± 1.33 | 49.25 ± 3.71 | 60.26 ± 5.75 | 53.48 ± 1.92 | 55.48 ± 3.84 | 50.52 ± 0.85 | 39.91 ± 0.57 | **63.35 ± 9.54** |
| | NMI | 5.43 ± 6.71 | 33.58 ± 0.83 | 27.51 ± 1.70 | 33.90 ± 3.21 | 28.92 ± 0.58 | 29.84 ± 2.32 | 30.17 ± 0.83 | 28.31 ± 0.82 | **42.56 ± 2.98** |
| | ARI | 6.39 ± 8.99 | 34.81 ± 1.79 | 29.37 ± 4.98 | 38.47 ± 3.86 | 29.03 ± 2.44 | 33.29 ± 3.85 | 32.14 ± 1.35 | 34.70 ± 1.71 | **45.72 ± 4.72** |
| PubMed | ACC | 46.90 ± 1.69 | 66.00 ± 1.66 | 57.91 ± 2.47 | 41.40 ± 2.17 | 64.15 ± 1.20 | 65.20 ± 0.87 | 61.41 ± 0.42 | 56.46 ± 0.18 | **70.46 ± 0.10** |
| | F1 | 34.89 ± 0.84 | 65.13 ± 1.75 | 48.29 ± 7.57 | 33.66 ± 5.73 | 63.68 ± 1.27 | 65.01 ± 0.62 | 61.30 ± 0.32 | 49.65 ± 0.32 | **69.50 ± 0.10** |
| | NMI | 2.86 ± 0.69 | 28.40 ± 1.22 | 11.77 ± 2.36 | 2.32 ± 3.79 | 24.47 ± 1.49 | 24.85 ± 2.06 | 17.85 ± 0.50 | 14.51 ± 0.06 | **31.91 ± 0.57** |
| | ARI | 1.86 ± 0.84 | 27.05 ± 1.87 | 13.83 ± 3.68 | 1.84 ± 3.57 | 23.65 ± 1.90 | 24.30 ± 1.73 | 17.89 ± 0.53 | 12.77 ± 0.20 | **32.71 ± 0.44** |
| ACM | ACC | 48.20 ± 2.29 | 52.22 ± 2.15 | 57.85 ± 1.55 | 77.57 ± 1.52 | 58.21 ± 1.32 | 63.21 ± 8.51 | 59.03 ± 6.33 | 53.30 ± 0.76 | **82.86 ± 0.26** |
| | F1 | 42.83 ± 2.07 | 47.08 ± 2.19 | 57.91 ± 2.52 | 77.71 ± 1.45 | 55.72 ± 1.45 | 62.19 ± 9.10 | 58.08 ± 6.47 | 54.68 ± 0.74 | **82.97 ± 0.37** |
| | NMI | 9.81 ± 4.58 | 18.36 ± 4.60 | 19.52 ± 2.34 | 42.94 ± 2.77 | 35.35 ± 1.03 | 36.01 ± 5.28 | 21.83 ± 3.66 | 28.07 ± 1.08 | **50.96 ± 0.70** |
| | ARI | 8.39 ± 6.22 | 13.98 ± 4.35 | 17.18 ± 4.04 | 43.11 ± 2.84 | 34.85 ± 0.85 | 35.17 ± 6.60 | 21.56 ± 3.87 | 20.33 ± 1.35 | **54.75 ± 0.33** |
| CS | ACC | 41.22 ± 5.33 | 52.65 ± 2.86 | 67.47 ± 1.79 | 66.69 ± 1.43 | 72.22 ± 0.89 | 72.41 ± 1.76 | 62.24 ± 0.76 | 69.27 ± 4.86 | **80.23 ± 2.06** |
| | F1 | 17.39 ± 2.97 | 40.23 ± 2.47 | 61.62 ± 2.69 | 56.20 ± 3.35 | 66.21 ± 1.56 | 65.41 ± 4.47 | 50.52 ± 1.63 | 67.61 ± 5.36 | **73.51 ± 2.43** |
| | NMI | 37.58 ± 7.50 | 60.18 ± 1.49 | 71.20 ± 0.94 | 68.89 ± 1.05 | 73.48 ± 0.19 | 71.85 ± 1.35 | 60.36 ± 2.05 | 74.10 ± 1.04 | **74.97 ± 0.50** |
| | ARI | 28.10 ± 9.32 | 39.02 ± 3.58 | 60.08 ± 1.24 | 59.02 ± 1.30 | 64.80 ± 0.50 | 65.42 ± 0.98 | 52.19 ± 1.37 | 61.78 ± 4.61 | **75.92 ± 0.72** |
| USPS | ACC | 45.62 ± 1.97 | 44.88 ± 1.70 | 54.01 ± 1.62 | 41.80 ± 3.37 | 51.14 ± 0.73 | 64.88 ± 1.94 | 63.96 ± 3.41 | 72.96 ± 0.90 | **90.61 ± 0.21** |
| | F1 | 44.85 ± 2.89 | 46.19 ± 1.65 | 49.68 ± 2.28 | 41.87 ± 3.57 | 53.42 ± 0.86 | 63.24 ± 2.57 | 62.22 ± 3.88 | 71.10 ± 0.74 | **89.70 ± 0.23** |
| | NMI | 44.24 ± 1.06 | 44.32 ± 1.50 | 59.18 ± 1.09 | 36.77 ± 2.31 | 44.84 ± 0.53 | 59.69 ± 2.53 | 58.92 ± 1.88 | 73.23 ± 0.60 | **81.91 ± 0.26** |
| | ARI | 15.00 ± 0.83 | 22.25 ± 0.83 | 42.39 ± 1.86 | 19.92 ± 2.19 | 26.13 ± 0.36 | 50.01 ± 2.47 | 49.93 ± 2.65 | 64.39 ± 0.92 | **82.52 ± 0.34** |
| HHAR | ACC | 39.23 ± 2.91 | 47.73 ± 0.22 | 64.28 ± 4.40 | 41.98 ± 0.83 | 54.68 ± 0.92 | 70.36 ± 3.28 | 48.76 ± 1.50 | 38.70 ± 0.32 | **76.94 ± 2.42** |
| | F1 | 34.03 ± 8.07 | 46.92 ± 0.24 | 61.44 ± 4.58 | 41.16 ± 0.79 | 54.90 ± 0.82 | 67.73 ± 3.39 | 47.07 ± 2.33 | 41.13 ± 0.38 | **75.69 ± 3.02** |
| | NMI | 29.32 ± 5.67 | 42.37 ± 0.63 | 60.26 ± 4.40 | 32.71 ± 0.85 | 46.54 ± 0.84 | 64.27 ± 2.84 | 46.05 ± 0.76 | 30.28 ± 0.28 | **74.10 ± 2.10** |
| | ARI | 12.05 ± 2.54 | 26.75 ± 0.53 | 47.39 ± 5.33 | 17.58 ± 0.82 | 31.72 ± 1.17 | 56.18 ± 3.05 | 30.94 ± 1.04 | 7.08 ± 0.11 | **63.70 ± 2.55** |
| BAT | ACC | 37.71 ± 1.24 | 58.17 ± 4.46 | 63.21 ± 2.79 | 74.81 ± 3.48 | 43.05 ± 2.30 | 67.48 ± 2.30 | 51.60 ± 1.14 | 49.47 ± 2.01 | **79.39 ± 1.28** |
| | F1 | 28.85 ± 1.84 | 55.93 ± 5.28 | 62.56 ± 2.92 | 74.56 ± 4.28 | 39.33 ± 3.82 | 64.34 ± 3.48 | 48.40 ± 1.93 | 44.81 ± 1.38 | **79.42 ± 1.16** |
| | NMI | 15.34 ± 2.99 | 38.55 ± 4.08 | 42.31 ± 3.23 | 51.07 ± 2.30 | 21.22 ± 4.14 | 46.69 ± 1.05 | 28.94 ± 8.82 | 28.21 ± 6.03 | **55.17 ± 1.73** |
| | ARI | 5.09 ± 1.48 | 27.96 ± 5.43 | 33.65 ± 4.91 | 47.33 ± 2.64 | 13.44 ± 5.12 | 42.46 ± 1.15 | 22.90 ± 6.83 | 20.54 ± 4.83 | **53.53 ± 2.68** |
| Physics | ACC | 59.28 ± 4.24 | OOM | 70.62 ± 2.84 | 89.53 ± 2.48 | 55.26 ± 0.39 | 76.86 ± 4.31 | 83.76 ± 3.08 | 84.71 ± 1.33 | **92.27 ± 0.19** |
| | F1 | 29.85 ± 4.00 | | 59.73 ± 8.16 | 85.86 ± 2.69 | 54.01 ± 0.33 | 74.34 ± 3.16 | 73.74 ± 7.55 | 81.31 ± 0.94 | **89.25 ± 0.29** |
| | NMI | 30.33 ± 12.81 | | 51.67 ± 2.28 | 71.92 ± 4.26 | 56.54 ± 1.26 | 58.97 ± 2.86 | 61.26 ± 3.07 | 66.73 ± 1.20 | **75.86 ± 0.25** |
| | ARI | 33.16 ± 14.59 | | 52.56 ± 7.82 | 80.29 ± 5.31 | 44.39 ± 1.58 | 55.47 ± 8.54 | 73.37 ± 1.57 | 70.53 ± 2.98 | **85.23 ± 0.32** |

Table 14: Clustering results under high-norm missingness.

settings, making them suitable for testing whether BAR+LS can benefit existing clustering learners beyond VISTA. The experiment covers 16 datasets. For each method, we prepend one BAR step and one LS step while keeping the original preprocessing, training configuration, clustering head, and checkpoint selection unchanged. This front-end introduces no additional learnable parameters and does not modify the clustering objective. Raw results from directly applying the original methods to masked attributes are reported in Appendix A.

Tables 17 and 18 report the dataset-level results for ACC, Macro-F1, NMI, and ARI, respectively. Here, $\Delta$ denotes the change after adding BAR+LS relative to the corresponding Raw result, measured in percentage points. The Mean row uses an equal weight for the 16 datasets and summarizes the overall gain for each method, while Gains $> 0$ counts the datasets with a positive gain and reflects the consistency of the improvement across datasets. Results use a 60% node-wise attribute missing rate and seeds 41–45; only complete five-seed results are included in the tables.

Overall, BAR+LS yields positive improvements on most datasets and evaluation metrics across the five downstream methods, and increases the average performance of every method on all four metrics. SDCN shows the most pronounced improvement: its average gains in ACC, Macro-F1, NMI, and ARI are 14.89, 15.89, 17.68, and 19.37 percentage points, respectively, and all four metrics improve on all 16 datasets. GGD also exhibits consistent gains, with average improvements of 11.40, 12.08, 10.96, and 13.78 percentage points; ACC and Macro-F1 improve on all 16 datasets, while NMI and ARI improve on 15. These results show that recovered attribute information can be effectively exploited by different graph representation learners, and that the benefits of BAR+LS are not limited to VISTA's own learning process.

From a mechanistic perspective, BAR first provides missing nodes with usable semantic evidence, after which LS propagates and integrates this information along the graph to produce a more reliable input representation for the downstream clustering learner. A small number of dataset–metric pairs still show negative gains, but the decreases are generally limited in magnitude; positive gains are more common and the average improvements remain positive for every method. Together with the

| | | Fixed representations + KMeans | | | Shared VISTA learner | | | | Reference |
|---|---|---|---|---|---|---|---|---|---|
| Dataset | Metric | FP-KMeans | FP-CMV-KMeans | DTRGC-KMeans | FP-VISTA | FP-CMV-VISTA | DTRGC-VISTA | BAR-CMV-VISTA | VISTA (Ours) |
| Cora | ACC | 32.50±4.73 | 46.03±3.30 | 27.45±2.39 | 56.89±9.38 | 55.48±2.88 | 31.34±1.00 | 59.01±5.43 | **72.70±1.65** |
| | F1 | 14.58±5.37 | 29.80±2.27 | 10.21±2.54 | 52.68±8.19 | 51.51±4.70 | 15.45±5.21 | 55.35±4.23 | **70.23±1.70** |
| CiteSeer | ACC | 39.80±4.91 | 38.44±3.36 | 22.06±1.69 | 54.66±6.90 | 49.04±0.64 | 43.82±3.83 | 49.26±0.56 | **65.37±0.75** |
| | F1 | 30.86±7.74 | 26.58±6.11 | 7.69±2.33 | 47.39±9.40 | 46.00±2.49 | 38.32±3.98 | 45.21±2.97 | **60.22±0.96** |
| DBLP | ACC | 41.76±3.55 | 63.70±5.52 | 44.77±0.02 | 60.91±7.58 | 63.37±7.96 | 45.33±0.19 | 61.71±9.51 | **78.26±0.24** |
| | F1 | 23.56±2.89 | 49.46±2.52 | 15.64±0.06 | 55.18±8.64 | 48.36±14.74 | 17.55±0.65 | 51.60±13.45 | **73.95±0.32** |
| PubMed | ACC | 49.83±7.11 | 60.37±12.26 | 39.95±0.02 | 70.69±0.26 | 64.74±10.59 | 48.10±7.27 | 68.12±1.22 | **70.70±0.25** |
| | F1 | 47.65±10.03 | 56.13±17.41 | 19.09±0.02 | 69.83±0.23 | 62.35±14.75 | 42.84±10.53 | 67.70±0.96 | **69.86±0.22** |
| Photo | ACC | 34.05±4.33 | 47.36±3.52 | 29.60±3.46 | 37.28±1.11 | 47.99±3.15 | 29.33±6.29 | 41.47±6.66 | **78.61±0.95** |
| | F1 | 28.05±6.34 | 40.96±7.55 | 12.33±3.73 | 31.10±1.48 | 43.72±2.05 | 23.80±7.99 | 36.16±3.51 | **73.56±1.19** |
| BlogCatalog | ACC | 27.06±0.74 | 25.14±1.79 | 29.07±3.11 | 46.56±2.83 | 37.81±3.52 | 38.51±5.20 | 27.49±1.68 | **62.49±1.08** |
| | F1 | 26.33±1.07 | 20.52±3.40 | 27.84±4.22 | 43.25±3.46 | 34.24±4.05 | 37.61±7.99 | 26.56±1.30 | **60.10±1.86** |
| USPS | ACC | 58.21±5.78 | 63.02±7.56 | 17.10±0.14 | 76.31±4.75 | 76.57±5.05 | 68.61±7.00 | 76.46±5.68 | **91.81±0.06** |
| | F1 | 54.13±5.96 | 58.72±8.30 | 3.74±0.28 | 70.00±5.76 | 75.44±5.81 | 65.07±8.45 | 75.37±6.50 | **91.13±0.09** |
| HHAR | ACC | 53.71±5.16 | 51.62±8.04 | 19.01±0.16 | 52.15±7.52 | 56.00±8.75 | 59.52±7.95 | 51.78±4.73 | **79.70±1.61** |
| | F1 | 50.19±8.19 | 45.02±9.46 | 5.82±0.35 | 46.86±8.01 | 51.54±11.54 | 55.77±10.30 | 48.10±7.35 | **78.91±3.11** |
| EAT | ACC | 39.90±2.59 | 36.79±4.79 | 47.72±3.07 | 54.44±2.76 | 34.29±1.85 | 40.90±3.78 | 34.59±1.41 | **58.25±0.23** |
| | F1 | 31.22±1.98 | 29.52±5.24 | 41.92±3.92 | 53.99±3.67 | 31.22±1.75 | 32.84±4.38 | 30.92±2.19 | **58.42±0.21** |
| BAT | ACC | 40.00±3.64 | 41.37±6.28 | 60.31±10.89 | 77.56±2.89 | 36.49±1.82 | 49.77±8.52 | 36.49±2.44 | **80.61±1.02** |
| | F1 | 36.42±3.95 | 36.79±7.79 | 56.47±13.18 | 77.47±2.96 | 33.86±1.46 | 45.10±8.35 | 35.01±3.08 | **80.65±0.97** |
| CoraFull | ACC | 24.63±2.22 | 35.09±2.21 | 5.40±0.46 | 38.03±1.43 | 38.33±0.44 | 8.04±1.23 | 37.88±0.88 | **42.42±0.43** |
| | F1 | 15.97±1.21 | 21.99±2.50 | 3.73±0.49 | 32.00±0.56 | 32.03±0.33 | 5.09±1.23 | 31.72±1.32 | **33.62±0.68** |
| Computers | ACC | 22.73±1.32 | 25.98±1.96 | 37.06±1.55 | 54.21±1.71 | 39.24±3.18 | 36.07±4.63 | 36.59±2.95 | **64.02±3.93** |
| | F1 | 15.24±2.04 | 17.83±1.68 | 9.79±3.12 | 38.33±3.94 | 26.97±1.67 | 24.42±6.09 | 24.56±3.37 | **53.62±2.75** |
| CS | ACC | 57.13±1.72 | 62.48±5.20 | 19.62±2.18 | 64.95±5.92 | 65.01±3.06 | 22.91±3.53 | 62.74±2.08 | **81.54±3.27** |
| | F1 | 49.57±3.89 | 52.35±8.41 | 9.39±0.83 | 57.66±6.12 | 59.00±2.64 | 8.27±1.23 | 55.87±3.75 | **74.36±4.26** |
| Physics | ACC | 57.60±4.37 | 61.38±10.01 | 49.69±1.79 | 83.56±11.48 | 66.52±9.96 | 50.60±1.16 | 67.84±11.91 | **92.31±0.26** |
| | F1 | 50.98±2.31 | 58.76±11.00 | 18.25±4.30 | 79.40±12.80 | 64.28±9.05 | 16.17±1.64 | 63.44±12.83 | **89.37±0.39** |
| Wiki | ACC | 35.95±3.58 | 31.19±3.11 | 19.48±2.74 | 43.97±3.92 | 40.05±4.94 | 24.86±6.53 | 36.41±4.99 | **52.68±1.22** |
| | F1 | 27.37±4.02 | 26.42±3.18 | 8.85±2.10 | 36.90±2.64 | 33.86±4.10 | 21.47±6.38 | 31.14±3.37 | **42.97±1.12** |
| UAT | ACC | 36.86±6.30 | 35.58±1.77 | 41.19±5.79 | 54.45±1.46 | 38.94±2.33 | 48.40±7.06 | 38.79±2.61 | **54.69±1.99** |
| | F1 | 28.92±9.26 | 25.20±2.08 | 34.11±8.31 | 51.31±4.88 | 36.38±1.91 | 42.79±8.51 | 34.71±2.92 | **52.56±5.60** |
| ACM | ACC | 59.11±5.81 | 45.51±14.98 | 35.15±0.22 | 73.65±9.50 | 52.65±1.16 | 49.90±4.36 | 55.99±9.23 | **82.84±0.78** |
| | F1 | 51.83±10.24 | 33.17±22.82 | 17.65±0.31 | 72.56±11.72 | 53.18±0.80 | 49.45±5.13 | 56.51±8.72 | **82.69±0.78** |

Table 15: Front-end comparison on ACC and Macro-F1.

Mean and Gains $> 0$ results, this pattern indicates that BAR+LS provides a stable and transferable front-end across the evaluated clustering frameworks. The experiment nevertheless evaluates the combined module and does not isolate the individual contributions of BAR and LS.

## E EMBEDDING VISUALIZATION

Figure 9 shows the node representations obtained by different methods with seed 42 at 60% node-wise attribute missingness. Raw denotes the original node features with missing nodes' feature vectors set to zero. The other panels show the representations used for clustering, except that SDCN is visualized through its autoencoder latent representation. For consistent comparisons within each dataset, we uniformly sample at most 3,000 nodes without replacement and use the same nodes across all methods. Each representation is independently reduced to at most 50 dimensions by PCA and then projected into two dimensions using t-SNE with perplexity 30, 1,000 iterations, and random seed 42. Ground-truth labels are used only for coloring, consistently within each row. These projections support qualitative inspection of within-class compactness and between-class separation rather than replacing quantitative clustering metrics; absolute distances across independently projected panels are not directly comparable.

The Raw representations show limited class structure under substantial attribute missingness. In particular, on DBLP, Photo, and ACM, many missing nodes share identical zero vectors and appear mixed across classes in the projections; these projection shapes should not themselves be interpreted as meaningful class structure. Graph clustering methods reorganize the representation space

| | | Fixed representations + KMeans | | | Shared VISTA learner | | | | Reference |
|---|---|---|---|---|---|---|---|---|---|
| Dataset | Metric | FP-KMeans | FP-CMV-KMeans | DTRGC-KMeans | FP-VISTA | FP-CMV-VISTA | DTRGC-VISTA | BAR-CMV-VISTA | VISTA (Ours) |
| Cora | NMI | 11.35±7.84 | 33.34±1.08 | 2.79±1.06 | 43.66±3.62 | 42.57±1.56 | 13.08±7.29 | 43.26±1.23 | **54.97±1.96** |
| | ARI | 2.83±4.58 | 16.79±5.74 | 0.47±1.07 | 30.70±8.12 | 32.48±2.83 | 2.36±2.30 | 33.62±4.59 | **50.98±4.13** |
| CiteSeer | NMI | 19.24±3.74 | 18.13±2.71 | 1.96±1.96 | 31.97±4.40 | 26.46±1.79 | 19.31±3.16 | 26.25±1.88 | **37.67±0.71** |
| | ARI | 11.19±2.90 | 13.68±2.69 | 0.03±0.09 | 31.04±5.88 | 20.10±0.80 | 14.69±3.52 | 19.85±1.17 | **39.69±0.67** |
| DBLP | NMI | 5.01±1.82 | 36.08±1.94 | 0.23±0.03 | 34.35±3.00 | 35.43±4.04 | 1.95±0.59 | 32.57±5.78 | **47.03±0.50** |
| | ARI | 0.05±1.74 | 38.24±5.87 | 0.03±0.03 | 35.15±7.74 | 37.34±7.02 | 0.46±0.33 | 33.79±10.75 | **52.06±0.44** |
| PubMed | NMI | 12.73±4.42 | 25.23±8.92 | 0.06±0.04 | 32.22±0.44 | 26.99±8.34 | 7.86±7.29 | 28.79±1.95 | **32.29±0.24** |
| | ARI | 6.98±4.32 | 23.40±11.87 | 0.00±0.01 | **33.14±0.48** | 26.24±11.57 | 7.89±8.36 | 29.33±1.99 | 33.10±0.47 |
| Photo | NMI | 23.09±5.40 | 37.82±4.04 | 8.22±3.48 | 31.31±1.98 | 41.11±4.77 | 13.45±7.86 | 29.58±4.96 | **71.40±0.98** |
| | ARI | 15.04±4.24 | 23.96±5.20 | 3.53±2.67 | 18.60±1.82 | 27.44±4.86 | 6.51±4.15 | 18.86±6.48 | **61.47±1.68** |
| BlogCatalog | NMI | 8.81±0.69 | 6.29±3.23 | 12.39±3.16 | 30.23±1.63 | 13.47±2.66 | 20.02±4.46 | 7.78±0.72 | **38.02±0.78** |
| | ARI | 2.77±0.23 | 2.13±0.76 | 4.05±1.71 | 21.75±1.87 | 10.14±1.76 | 8.77±1.52 | 3.19±0.58 | **33.19±0.83** |
| USPS | NMI | 58.70±3.15 | 68.19±3.53 | 1.17±0.24 | 78.25±1.77 | 72.50±0.94 | 64.15±4.11 | 72.08±2.03 | **83.68±0.11** |
| | ARI | 45.53±6.81 | 54.13±7.82 | 0.03±0.02 | 71.79±5.45 | 64.77±2.94 | 55.33±6.36 | 64.50±4.20 | **84.42±0.10** |
| HHAR | NMI | 57.31±2.07 | 63.37±1.20 | 0.74±0.29 | 64.12±1.79 | 63.62±2.83 | 62.32±2.85 | 57.12±1.18 | **74.91±1.68** |
| | ARI | 40.87±1.33 | 43.35±5.88 | 0.05±0.05 | 44.27±7.64 | 44.55±6.43 | 48.16±6.34 | 40.68±2.64 | **66.32±1.37** |
| EAT | NMI | 15.40±4.84 | 9.63±5.05 | 27.45±3.81 | 31.62±1.87 | 4.02±1.19 | 17.95±5.48 | 6.22±1.31 | **34.38±0.18** |
| | ARI | 10.09±4.12 | 6.13±4.46 | 21.14±2.43 | 25.59±0.99 | 2.11±0.97 | 14.07±7.35 | 3.87±2.14 | **27.83±0.29** |
| BAT | NMI | 16.69±3.97 | 17.76±6.29 | 40.61±11.24 | 53.68±2.63 | 8.48±3.00 | 28.89±7.92 | 8.30±2.30 | **56.77±1.52** |
| | ARI | 7.22±4.66 | 9.86±7.34 | 33.53±10.46 | 51.16±4.19 | 3.39±2.08 | 21.81±9.83 | 3.18±2.04 | **55.76±2.13** |
| CoraFull | NMI | 36.05±1.25 | 49.12±0.75 | 6.99±2.56 | 52.25±0.54 | 51.51±0.22 | 11.29±3.40 | 51.15±0.23 | **54.48±0.28** |
| | ARI | 4.29±0.51 | 20.21±0.94 | 0.73±0.54 | 20.99±2.09 | 24.12±0.31 | 0.27±0.26 | 23.76±0.67 | **29.47±0.77** |
| Computers | NMI | 9.06±3.73 | 11.35±2.57 | 3.79±1.92 | 47.91±0.35 | 26.90±4.86 | 22.89±6.95 | 22.20±3.20 | **54.07±1.80** |
| | ARI | 4.91±1.45 | 6.28±2.14 | 4.02±4.55 | 35.58±0.37 | 17.39±4.00 | 12.25±7.32 | 13.20±3.10 | **45.07±6.16** |
| CS | NMI | 63.69±1.45 | 68.99±2.58 | 5.47±1.48 | 70.83±1.73 | 69.56±0.95 | 7.25±2.33 | 67.70±1.33 | **75.34±0.72** |
| | ARI | 42.57±2.35 | 52.71±5.94 | 2.84±1.37 | 56.90±5.64 | 54.60±2.78 | 0.66±2.06 | 51.65±1.93 | **76.52±1.78** |
| Physics | NMI | 45.18±3.88 | 57.29±4.16 | 4.70±4.41 | 71.28±5.50 | 56.26±2.65 | 2.99±1.59 | 54.82±4.94 | **76.06±0.39** |
| | ARI | 29.22±8.39 | 46.91±8.42 | 7.88±8.05 | 74.11±14.78 | 49.25±8.76 | 1.08±1.62 | 50.61±11.77 | **85.32±0.33** |
| Wiki | NMI | 35.19±2.22 | 28.06±4.82 | 8.44±2.77 | 42.19±2.02 | 35.67±4.89 | 18.14±6.92 | 32.82±4.22 | **47.22±1.06** |
| | ARI | 7.39±1.95 | 8.87±1.83 | 1.54±0.93 | 20.75±2.51 | 16.52±3.49 | 5.99±3.11 | 12.84±4.89 | **31.11±0.65** |
| UAT | NMI | 14.88±8.04 | 8.10±1.58 | 18.46±6.09 | 24.53±1.67 | 8.56±1.18 | 17.32±5.37 | 8.09±2.03 | **25.92±2.40** |
| | ARI | 5.50±3.76 | 4.78±1.43 | 7.23±3.29 | 23.93±0.84 | 6.70±1.87 | 16.71±6.84 | 6.35±2.78 | **24.03±1.69** |
| ACM | NMI | 33.39±4.26 | 12.41±16.41 | 0.52±0.16 | 41.54±7.95 | 22.63±4.14 | 12.51±6.83 | 27.55±5.38 | **50.84±1.64** |
| | ARI | 24.13±3.60 | 9.23±12.69 | 0.00±0.02 | 41.81±8.74 | 19.40±2.71 | 11.94±6.95 | 23.85±5.64 | **55.32±1.74** |

Table 16: Front-end comparison on NMI and ARI.

to varying degrees, producing different class distributions. SDCN forms locally compact regions on some datasets, but these regions still contain nodes from different classes. THESAURUS, SSGC, and PMAGC also exhibit class-related structure with varying degrees of overlap. VISTA shows relatively clear class groupings, particularly on USPS, where different classes occupy largely distinct regions. On ACM, the three classes also exhibit discernible distribution patterns. Class-related groupings are visible on DBLP as well, while some overlap remains on Cora and Photo. Overall, these qualitative observations complement the preceding clustering comparisons, suggesting that VISTA learns node representations with useful class discrimination despite severe attribute missingness.

## F Prototype Assignment Diagnostics

Figure 10 reports prototype-assignment diagnostics for eight datasets under 60% node-wise attribute missingness. Each dataset is shown by a pair of plots over 400 training epochs and five random seeds. The left plot shows the maximum mean soft probability $\max_k \bar{q}_k$; the dashed line marks the uniform reference $1/K$. Values close to one would indicate concentration on a single prototype, whereas values close to $1/K$ indicate that the marginal prototype probabilities are nearly uniform. The right plot shows the mean node entropy and marginal entropy, each normalized by $\log K$. High mean node entropy indicates diffuse predictions for individual nodes, whereas high marginal entropy indicates balanced average probability across prototypes; the latter alone does not imply uncertain

| Dataset | Metric | CoCo | | Dink-Net | | SDCN | | SAGSC | | GGD | |
|---|---|---|---|---|---|---|---|---|---|---|---|
| | | BAR+LS | Δ | BAR+LS | Δ | BAR+LS | Δ | BAR+LS | Δ | BAR+LS | Δ |
| Cora | ACC | 64.69 ± 1.30 | +2.37 | 66.18 ± 3.36 | +22.10 | 51.38 ± 4.44 | +14.97 | 63.51 ± 2.80 | +8.81 | 72.87 ± 2.43 | +26.06 |
| | F1 | 59.12 ± 1.39 | +2.66 | 61.74 ± 3.01 | +17.84 | 38.56 ± 4.68 | +17.06 | 60.75 ± 3.20 | +6.92 | 68.76 ± 3.65 | +24.67 |
| CiteSeer | ACC | 49.24 ± 2.09 | +4.39 | 48.85 ± 3.36 | +20.00 | 58.78 ± 4.09 | +27.42 | 57.59 ± 1.06 | +7.75 | 59.20 ± 1.06 | +24.59 |
| | F1 | 46.67 ± 3.86 | +6.03 | 46.99 ± 3.00 | +21.29 | 51.31 ± 6.78 | +27.37 | 54.90 ± 1.02 | +5.62 | 57.12 ± 1.03 | +23.49 |
| DBLP | ACC | 68.16 ± 3.10 | +11.44 | 60.32 ± 3.06 | +3.99 | 66.46 ± 3.60 | +17.11 | 50.38 ± 2.41 | +4.37 | 58.73 ± 6.67 | +13.38 |
| | F1 | 55.63 ± 7.25 | +6.73 | 50.34 ± 1.97 | +1.66 | 48.99 ± 9.17 | +18.14 | 46.61 ± 3.59 | +3.08 | 54.79 ± 8.31 | +13.98 |
| PubMed | ACC | 61.76 ± 2.74 | +7.00 | 66.43 ± 1.52 | +17.09 | 63.20 ± 3.88 | +16.41 | 70.55 ± 0.08 | +2.10 | 68.12 ± 0.47 | +7.98 |
| | F1 | 60.35 ± 3.98 | +7.71 | 66.07 ± 1.35 | +16.82 | 62.72 ± 3.75 | +25.75 | 69.31 ± 0.07 | +2.00 | 67.51 ± 0.49 | +9.00 |
| Photo | ACC | 66.19 ± 1.51 | +12.79 | 71.51 ± 4.75 | +12.19 | 57.08 ± 5.74 | +20.69 | 66.14 ± 4.11 | −2.09 | 51.87 ± 1.41 | +15.39 |
| | F1 | 60.70 ± 1.84 | +9.85 | 66.30 ± 6.52 | +12.79 | 39.00 ± 8.87 | +18.36 | 66.73 ± 4.50 | −2.44 | 47.11 ± 3.24 | +18.82 |
| USPS | ACC | 65.41 ± 1.76 | +1.18 | 55.48 ± 3.32 | +13.66 | 65.64 ± 5.86 | +31.00 | 60.04 ± 3.59 | +14.96 | 66.22 ± 0.83 | +23.07 |
| | F1 | 65.91 ± 2.18 | +0.78 | 53.22 ± 3.58 | +10.09 | 61.27 ± 4.94 | +24.08 | 57.61 ± 4.66 | +9.58 | 64.91 ± 0.82 | +19.67 |
| HHAR | ACC | 52.20 ± 1.47 | +4.69 | 45.12 ± 6.80 | +6.41 | 48.74 ± 2.56 | +12.23 | 69.67 ± 7.98 | +13.81 | 48.00 ± 2.54 | +8.90 |
| | F1 | 51.73 ± 1.49 | +3.51 | 40.70 ± 13.71 | +6.90 | 36.83 ± 4.66 | +0.49 | 69.47 ± 8.56 | +12.02 | 48.42 ± 2.44 | +9.54 |
| EAT | ACC | 58.50 ± 1.01 | +2.51 | 42.06 ± 2.67 | −0.65 | 43.11 ± 5.31 | +11.68 | 44.51 ± 0.38 | −0.75 | 44.41 ± 1.10 | +0.75 |
| | F1 | 59.07 ± 1.03 | +3.73 | 37.85 ± 4.70 | −2.23 | 36.75 ± 8.70 | +15.07 | 38.93 ± 0.67 | −1.31 | 40.36 ± 1.84 | +4.73 |
| BAT | ACC | 79.39 ± 0.54 | +5.34 | 45.80 ± 3.28 | +3.66 | 43.36 ± 2.72 | +9.47 | 55.73 ± 2.35 | +4.89 | 49.47 ± 3.34 | +4.43 |
| | F1 | 79.13 ± 0.64 | +5.94 | 41.15 ± 4.52 | +1.74 | 32.87 ± 4.77 | +7.50 | 55.97 ± 2.14 | +5.92 | 46.19 ± 4.56 | +5.97 |
| CoraFull | ACC | 41.40 ± 0.71 | +4.56 | 28.45 ± 8.55 | +11.70 | 26.83 ± 0.30 | +14.70 | 38.10 ± 0.82 | −0.26 | 28.82 ± 1.37 | +7.74 |
| | F1 | 32.26 ± 1.57 | +3.40 | 22.56 ± 9.47 | +9.52 | 21.78 ± 0.69 | +16.44 | 32.46 ± 0.25 | −0.03 | 22.20 ± 1.59 | +6.33 |
| Computers | ACC | 48.45 ± 1.13 | +8.30 | 43.67 ± 6.23 | +2.64 | 53.85 ± 4.10 | +13.44 | 33.50 ± 0.60 | +1.93 | 39.70 ± 0.47 | +1.15 |
| | F1 | 52.50 ± 2.64 | +8.71 | 13.28 ± 4.23 | −0.59 | 27.80 ± 8.47 | +15.19 | 32.51 ± 2.52 | +4.68 | 26.39 ± 0.58 | +4.11 |
| CS | ACC | 82.94 ± 1.95 | +5.94 | 57.85 ± 10.63 | −0.53 | 59.29 ± 3.73 | +9.32 | 64.81 ± 3.53 | −0.04 | 70.12 ± 1.99 | +10.91 |
| | F1 | 73.69 ± 4.14 | +4.03 | 46.54 ± 17.23 | −3.69 | 33.30 ± 5.64 | +9.98 | 60.34 ± 4.91 | +0.81 | 66.82 ± 3.89 | +11.32 |
| Physics | ACC | 88.47 ± 2.10 | −3.03 | 69.22 ± 12.06 | −4.80 | 83.09 ± 1.21 | +19.68 | 59.80 ± 1.25 | +1.65 | 84.24 ± 1.85 | +4.91 |
| | F1 | 85.28 ± 3.14 | −3.91 | 67.68 ± 11.45 | −3.69 | 77.48 ± 2.12 | +41.94 | 61.28 ± 1.33 | +2.12 | 81.14 ± 1.44 | +3.81 |
| Wiki | ACC | 49.50 ± 1.22 | +2.49 | 40.37 ± 4.57 | +6.41 | 38.27 ± 4.18 | +4.14 | 44.18 ± 1.91 | +5.09 | 40.91 ± 2.53 | +2.89 |
| | F1 | 38.89 ± 1.23 | −1.05 | 33.17 ± 6.08 | +5.42 | 24.80 ± 3.50 | +3.28 | 38.60 ± 1.39 | +3.07 | 35.61 ± 2.56 | +3.54 |
| UAT | ACC | 56.47 ± 0.52 | +3.41 | 48.54 ± 1.12 | +9.48 | 42.32 ± 2.78 | +7.41 | 51.11 ± 1.00 | +4.52 | 46.99 ± 0.72 | +4.62 |
| | F1 | 53.48 ± 2.06 | +5.86 | 46.35 ± 0.83 | +10.60 | 35.28 ± 5.33 | +8.88 | 48.81 ± 1.52 | +4.53 | 43.67 ± 2.28 | +3.20 |
| ACM | ACC | 50.20 ± 0.41 | +8.42 | 58.47 ± 6.38 | +12.01 | 59.03 ± 2.10 | +8.56 | 79.29 ± 3.33 | +23.25 | 79.73 ± 0.92 | +25.65 |
| | F1 | 47.42 ± 0.57 | +8.66 | 56.28 ± 7.58 | +12.18 | 53.31 ± 5.61 | +4.70 | 79.28 ± 2.97 | +22.49 | 80.06 ± 0.85 | +31.18 |
| Mean | ACC | 61.43 | +5.11 | 53.02 | +8.46 | 53.78 | +14.89 | 56.81 | +5.62 | 56.84 | +11.40 |
| | F1 | 57.61 | +4.54 | 46.89 | +7.29 | 42.63 | +15.89 | 54.60 | +4.94 | 53.19 | +12.08 |
| Gains $> 0$ | ACC | 15/16 | | 13/16 | | 16/16 | | 12/16 | | 16/16 | |
| | F1 | 14/16 | | 12/16 | | 16/16 | | 13/16 | | 16/16 | |

Table 17: ACC and F1 gains from one-step BAR+LS.

node-level predictions. Lines in the right plot show five-seed means, and shaded regions show the min–max range. These quantities characterize the prototype-prediction head and do not by themselves establish whether the final clustering embeddings have collapsed.

## G Computational Complexity Analysis

Let $N$ be the number of nodes, $E$ the number of stored sparse edges after adding self-loops, $d$ the input attribute dimension, $h$ the encoder width, $K$ the number of clusters, $S$ the maximum number of bounded recovery steps, and $L$ the number of smoothing steps. Let $T$ denote the number of training epochs and $I$ the number of Lloyd iterations in KMeans. All graph operations use sparse–dense multiplication with $\mathrm{nnz}(\hat{\mathbf{A}}) = E$.

The normalized adjacency construction costs $\mathcal{O}(N + E)$ time and memory. Each recovery step costs $\mathcal{O}(Ed + Nd)$, giving $\mathcal{O}\big(S(Ed + Nd)\big)$ over at most $S$ steps. The $L$ smoothing steps and one additional topology propagation cost $\mathcal{O}\big((L + 1)(Ed + Nd)\big)$. Hence, the complete fixed preprocessing stage has complexity

$$\mathcal{O}\big((S + L + 1)(Ed + Nd) + N + E\big).$$

For each training epoch, view construction costs $\mathcal{O}(Nd)$, the shared encoder costs $\mathcal{O}(Ndh)$, and prototype prediction costs $\mathcal{O}(NKh)$. Thus, one epoch costs $\mathcal{O}(Ndh + NKh)$ and the full training stage costs $\mathcal{O}\big(TN(dh + Kh)\big)$. The prediction loss uses $K$ prototype scores per node and therefore does not require an $N \times N$ node-pair matrix. Fusing the two views costs $\mathcal{O}(Nh)$, while KMeans with $I$ iterations costs $\mathcal{O}(INKh)$. Ignoring optimizer-state constants, the total working memory is

$$\mathcal{O}(E + Nd + Nh + Kh + NK).$$

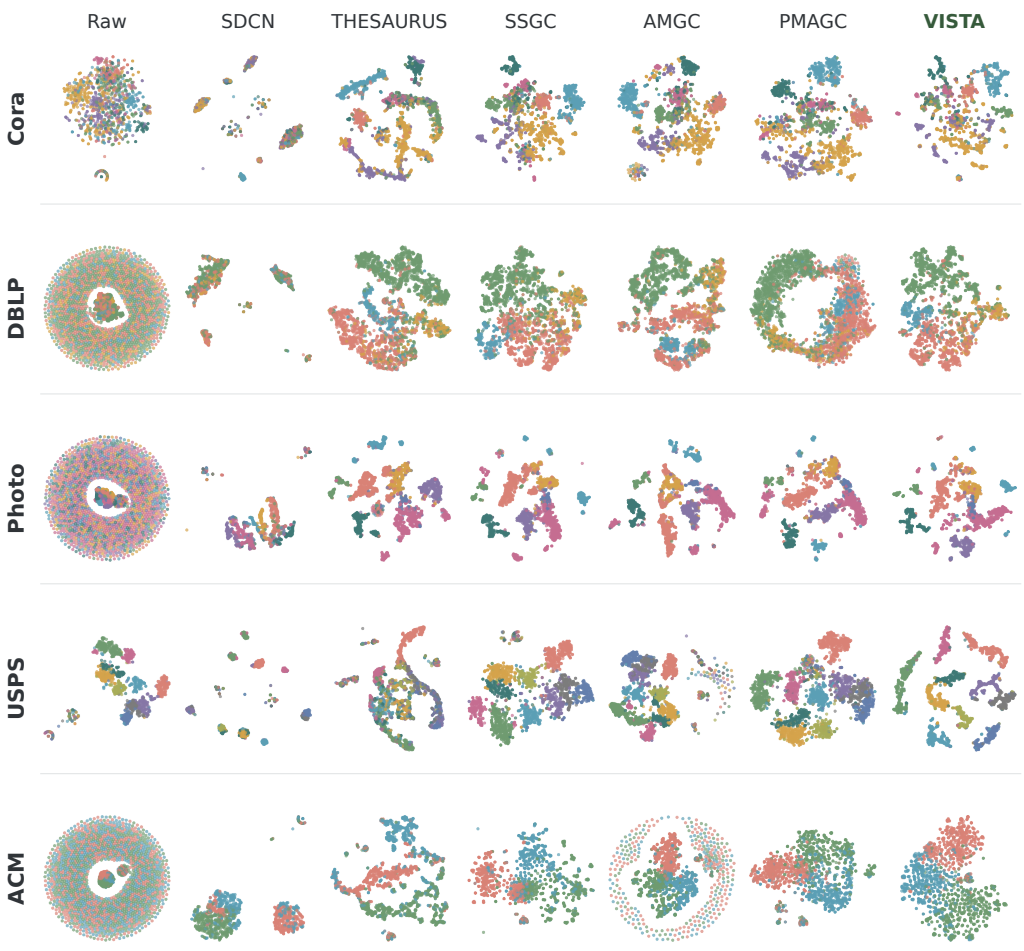


Figure 9: Visualization of node representations.

For fixed $d$, $h$, $K$, $S$, and $L$, preprocessing is linear in the stored sparse edges and nodes, and each training epoch is linear in $N$; thus VISTA retains a scalable computation profile as graph size grows.

## H Empirical Efficiency Analysis

We further evaluate the practical computational efficiency of VISTA. Using a fixed random seed of 42, we measure the wall-clock time and peak GPU memory of different methods on 15 benchmark datasets. EAT with 399 nodes and BAT with 131 nodes are excluded from this efficiency comparison because their extremely small graph sizes lead to generally low computational costs and provide limited information for distinguishing how different methods scale with graph size. Table 19 reports the wall-clock time and peak GPU memory for each dataset and method combination.

Table 19 shows that VISTA maintains low computational costs across datasets of different scales. Its running time remains relatively low, while its peak GPU memory usage is also stable. In contrast, as the dataset size increases, the running time of several baseline methods grows substantially and reaches hundreds or even thousands of seconds. Some methods also require considerably more GPU memory and even encounter OOM. These efficiency differences become particularly evident on larger datasets such as CoraFull and Physics. Overall, VISTA maintains low running time while avoiding high memory overhead, demonstrating favorable practical computational efficiency.

To further examine how the efficiency of different methods changes with graph scale, Figure 11 reorganizes the above measurements according to the joint graph scale $S_{\text{graph}} = N + E$. It presents wall-clock time and peak

| Dataset | Metric | CoCo | | Dink-Net | | SDCN | | SAGSC | | GGD | |
|---|---|---|---|---|---|---|---|---|---|---|---|
| | | BAR+LS | Δ | BAR+LS | Δ | BAR+LS | Δ | BAR+LS | Δ | BAR+LS | Δ |
| Cora | NMI | 45.17 ± 1.83 | +5.65 | 48.15 ± 2.77 | +22.50 | 31.20 ± 3.55 | +17.74 | 48.42 ± 2.68 | +10.33 | 55.86 ± 1.64 | +22.77 |
| | ARI | 38.39 ± 2.25 | +7.37 | 42.90 ± 3.95 | +24.91 | 25.31 ± 4.84 | +17.12 | 40.86 ± 3.43 | +10.20 | 52.72 ± 2.01 | +36.53 |
| CiteSeer | NMI | 25.05 ± 2.79 | +2.00 | 25.51 ± 1.73 | +19.68 | 31.17 ± 2.93 | +20.66 | 30.12 ± 1.10 | +4.86 | 33.54 ± 0.92 | +19.99 |
| | ARI | 18.42 ± 2.07 | +5.75 | 19.13 ± 2.18 | +16.12 | 30.52 ± 3.86 | +26.51 | 29.73 ± 1.32 | +8.02 | 31.62 ± 1.08 | +24.30 |
| DBLP | NMI | 34.33 ± 2.69 | +12.63 | 31.77 ± 1.76 | +6.51 | 31.95 ± 3.51 | +25.45 | 20.86 ± 3.59 | +5.19 | 36.92 ± 5.29 | +14.60 |
| | ARI | 38.77 ± 1.38 | +16.36 | 32.44 ± 2.83 | +7.10 | 38.26 ± 5.47 | +31.03 | 17.98 ± 3.29 | +4.48 | 33.64 ± 5.55 | +18.56 |
| PubMed | NMI | 21.13 ± 4.83 | +9.57 | 26.85 ± 2.48 | +15.29 | 22.21 ± 5.87 | +18.39 | 30.04 ± 0.13 | +2.21 | 30.97 ± 0.15 | +9.58 |
| | ARI | 19.77 ± 4.44 | +7.66 | 26.43 ± 2.71 | +17.37 | 22.08 ± 5.68 | +18.53 | 32.83 ± 0.14 | +2.88 | 29.84 ± 0.57 | +11.21 |
| Photo | NMI | 50.72 ± 1.82 | +10.34 | 62.95 ± 2.58 | +12.07 | 48.18 ± 7.44 | +28.18 | 59.16 ± 1.47 | +1.08 | 47.39 ± 0.49 | +17.63 |
| | ARI | 40.77 ± 2.34 | +12.38 | 52.25 ± 4.19 | +11.56 | 37.73 ± 7.43 | +25.59 | 44.19 ± 2.42 | −0.21 | 29.64 ± 0.74 | +14.46 |
| USPS | NMI | 57.01 ± 1.54 | −0.17 | 50.56 ± 3.89 | +13.59 | 63.38 ± 2.25 | +28.95 | 56.33 ± 1.58 | +18.44 | 63.29 ± 0.69 | +20.23 |
| | ARI | 46.27 ± 2.16 | +0.60 | 39.85 ± 5.03 | +21.09 | 54.38 ± 6.63 | +48.98 | 47.70 ± 1.69 | +29.49 | 52.43 ± 1.18 | +34.95 |
| HHAR | NMI | 50.36 ± 1.58 | +6.50 | 43.85 ± 7.62 | +7.92 | 53.40 ± 5.32 | +23.06 | 65.04 ± 6.11 | +19.72 | 46.46 ± 3.39 | +6.37 |
| | ARI | 35.96 ± 1.40 | +8.66 | 27.14 ± 5.94 | +3.77 | 37.12 ± 3.88 | +28.83 | 56.85 ± 8.68 | +23.62 | 28.52 ± 3.24 | +6.33 |
| EAT | NMI | 33.59 ± 0.78 | +1.68 | 17.19 ± 3.79 | +1.94 | 12.55 ± 4.67 | +5.92 | 23.93 ± 0.73 | −0.73 | 20.95 ± 1.87 | −1.28 |
| | ARI | 26.10 ± 0.83 | +0.69 | 13.15 ± 4.49 | +0.35 | 10.39 ± 5.44 | +9.03 | 22.05 ± 0.82 | −0.05 | 16.36 ± 3.03 | −1.23 |
| BAT | NMI | 55.80 ± 0.63 | +5.31 | 22.54 ± 4.43 | +10.40 | 18.11 ± 4.50 | +8.01 | 25.37 ± 3.55 | +0.42 | 29.85 ± 1.95 | +6.02 |
| | ARI | 54.55 ± 0.74 | +7.43 | 17.31 ± 3.33 | +9.32 | 12.04 ± 3.83 | +10.44 | 21.23 ± 3.21 | +1.42 | 21.32 ± 2.61 | +3.62 |
| CoraFull | NMI | 51.08 ± 0.74 | +3.80 | 44.68 ± 8.91 | +16.63 | 41.30 ± 0.47 | +23.22 | 52.85 ± 0.25 | +0.11 | 47.35 ± 1.38 | +9.12 |
| | ARI | 25.37 ± 0.87 | +5.71 | 17.92 ± 6.80 | +11.67 | 11.57 ± 0.42 | +8.45 | 24.68 ± 1.03 | −1.11 | 18.18 ± 1.16 | +8.01 |
| Computers | NMI | 42.66 ± 1.37 | +10.32 | 16.38 ± 12.82 | +1.89 | 33.82 ± 8.35 | +21.80 | 27.61 ± 0.38 | +6.72 | 37.34 ± 1.44 | +7.26 |
| | ARI | 27.18 ± 1.47 | +10.55 | 14.39 ± 13.36 | +3.11 | 29.15 ± 7.61 | +19.07 | 11.03 ± 0.22 | +4.20 | 24.74 ± 1.37 | +5.94 |
| CS | NMI | 74.28 ± 1.13 | +2.39 | 60.14 ± 10.01 | +2.46 | 59.26 ± 2.47 | +14.02 | 70.40 ± 0.68 | +1.65 | 70.81 ± 0.68 | +9.37 |
| | ARI | 76.43 ± 2.52 | +7.39 | 49.52 ± 9.35 | +3.11 | 49.45 ± 9.02 | +11.68 | 56.04 ± 2.85 | +0.20 | 58.90 ± 0.95 | +14.05 |
| Physics | NMI | 71.05 ± 2.68 | −4.00 | 60.32 ± 3.84 | +3.76 | 63.36 ± 1.28 | +23.52 | 56.49 ± 0.15 | +4.21 | 67.34 ± 1.46 | +5.99 |
| | ARI | 77.12 ± 2.68 | −5.09 | 52.74 ± 9.24 | −3.13 | 71.27 ± 4.13 | +27.05 | 45.98 ± 0.49 | +3.79 | 70.20 ± 3.89 | +10.49 |
| Wiki | NMI | 41.47 ± 1.12 | +0.08 | 35.85 ± 6.40 | +6.70 | 30.42 ± 3.96 | +4.35 | 39.02 ± 0.88 | +2.64 | 40.24 ± 2.13 | +3.10 |
| | ARI | 25.03 ± 1.52 | +1.98 | 17.56 ± 5.40 | +8.12 | 14.31 ± 5.23 | +3.29 | 24.40 ± 1.18 | +9.74 | 19.53 ± 2.57 | +5.70 |
| UAT | NMI | 26.44 ± 0.96 | +3.43 | 21.64 ± 0.84 | +13.49 | 12.29 ± 2.88 | +5.59 | 21.46 ± 0.27 | +3.71 | 20.44 ± 1.75 | +3.22 |
| | ARI | 23.54 ± 1.68 | +1.95 | 19.59 ± 1.63 | +14.21 | 11.33 ± 2.48 | +8.17 | 18.97 ± 0.23 | +4.23 | 10.90 ± 1.10 | +2.31 |
| ACM | NMI | 19.88 ± 2.49 | +15.10 | 29.66 ± 7.86 | +17.11 | 29.32 ± 3.34 | +13.98 | 45.90 ± 4.48 | +20.80 | 48.30 ± 1.11 | +21.40 |
| | ARI | 16.24 ± 1.92 | +12.01 | 27.55 ± 7.96 | +16.11 | 28.71 ± 4.13 | +16.23 | 48.07 ± 5.94 | +26.50 | 48.09 ± 2.07 | +25.19 |
| Mean | NMI | 43.75 | +5.29 | 37.38 | +10.75 | 36.37 | +17.68 | 42.06 | +6.33 | 43.57 | +10.96 |
| | ARI | 36.87 | +6.34 | 29.37 | +10.30 | 30.23 | +19.37 | 33.91 | +7.96 | 34.16 | +13.78 |
| Gains $> 0$ | NMI | 14/16 | | 16/16 | | 16/16 | | 15/16 | | 15/16 | |
| | ARI | 15/16 | | 15/16 | | 16/16 | | 13/16 | | 15/16 | |

Table 18: NMI and ARI gains from one-step BAR+LS.

GPU memory on log–log axes. On smaller graphs, the computational costs of different methods are relatively comparable. As graph scale increases, however, the running time and memory requirements of most baselines grow substantially, whereas VISTA exhibits a much flatter growth trend. This observation is consistent with the preceding complexity analysis.

VISTA mainly relies on sparse graph propagation and a lightweight shared encoder, while avoiding dense node-pair construction during representation learning. Therefore, VISTA not only achieves low practical computational costs but also exhibits favorable scalability.

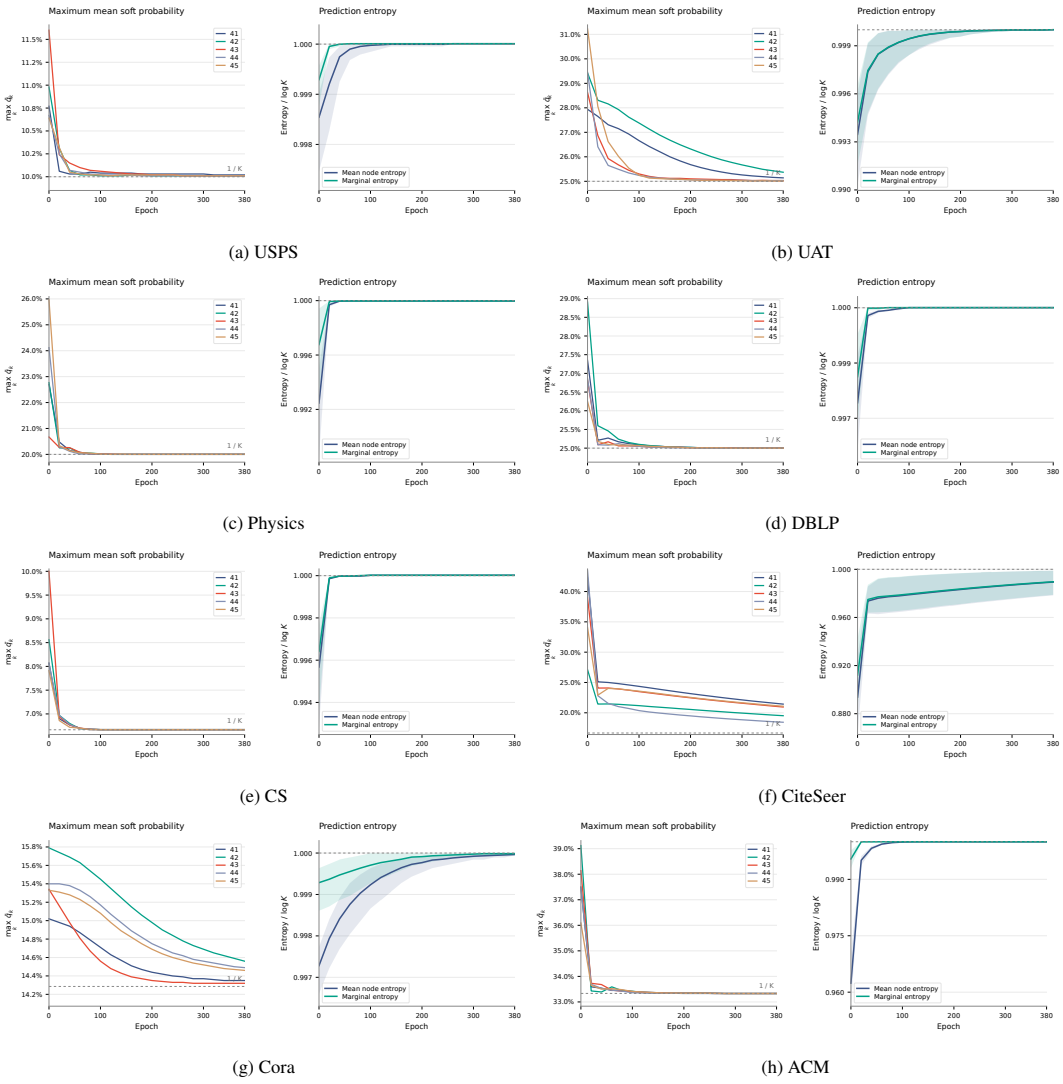


(a) USPS (b) UAT

(c) Physics (d) DBLP

(e) CS (f) CiteSeer

(g) Cora (h) ACM

Figure 10: Prototype assignment diagnostics.

Across most datasets, the maximum mean soft probability remains close to $1/K$, while both normalized entropy measures remain close to one. This indicates that the prototype-prediction head does not exhibit confident collapse onto a single prototype, but instead tends to produce relatively balanced soft assignments. This behavior is consistent with the role of prototype prediction in VISTA: it serves as an auxiliary cross-view consistency constraint for shaping the representation space, rather than directly determining the final clustering partition. Final clustering is performed by applying KMeans to the fused node embeddings. Thus, even when prototype assignments are not highly discriminative, the embedding space can still preserve useful clustering structure.

| Dataset | Metric | VISTA | AMGC | MVCG | AMMGC | PMAGC | CGIR | CSAGC | HyperAE | HCN-PAI |
|---|---|---|---|---|---|---|---|---|---|---|
| UAT | Time | **8.5** | 313.7 | 21.6 | 35.1 | 26.7 | 12.8 | 16.2 | 11.6 | 9.2 |
| | GPU | 1.38 | 1.42 | 4.16 | 1.41 | 1.54 | 1.59 | 1.42 | 2.70 | **0.86** |
| Wiki | Time | 20.9 | 807.5 | 35.2 | 83.8 | 85.0 | 45.2 | 48.9 | **11.9** | 14.6 |
| | GPU | 2.96 | 1.50 | 4.00 | 1.74 | 1.83 | 2.08 | 2.51 | 2.54 | **1.14** |
| Cora | Time | 11.6 | 881.1 | 23.7 | 63.6 | 38.5 | 47.9 | 31.8 | **11.1** | 12.8 |
| | GPU | 1.51 | 1.37 | 3.32 | 1.60 | 1.56 | 2.00 | 2.05 | 2.09 | **1.08** |
| ACM | Time | **9.5** | 809.8 | 19.6 | 25.5 | 20.6 | 51.6 | 24.7 | 13.3 | 10.8 |
| | GPU | 1.78 | 1.48 | 4.29 | 1.70 | 1.71 | 2.01 | 2.35 | 3.03 | **0.40** |
| CiteSeer | Time | 14.7 | 1001.9 | 24.6 | 86.4 | 35.7 | 74.1 | 43.9 | **13.2** | 14.7 |
| | GPU | 2.61 | 1.42 | 3.66 | 1.75 | 1.80 | 2.18 | 2.98 | 2.46 | **1.28** |
| BlogCatalog | Time | **14.8** | 2122.3 | 85.5 | 140.8 | 119.3 | 125.2 | 70.1 | 75.0 | 26.2 |
| | GPU | **1.44** | 3.90 | 23.28 | 2.79 | 4.84 | 3.22 | 6.61 | 21.94 | 2.27 |
| Photo | Time | **9.6** | 3089.6 | 54.5 | 111.8 | 90.9 | 297.9 | 90.8 | 50.5 | 22.0 |
| | GPU | **1.68** | 3.37 | 21.58 | 2.64 | 3.70 | 3.81 | 6.79 | 16.55 | 2.51 |
| USPS | Time | **13.6** | 2981.2 | 46.8 | 134.8 | 105.2 | 463.1 | 100.3 | 20.7 | 32.2 |
| | GPU | 1.87 | **1.54** | 5.88 | 3.42 | 1.92 | 4.73 | 7.98 | 3.84 | 3.47 |
| HHAR | Time | **9.5** | 3289.1 | 41.3 | 125.8 | 66.0 | 515.3 | 97.5 | 21.0 | 26.1 |
| | GPU | 1.78 | **1.69** | 6.93 | 3.94 | 2.03 | 5.05 | 9.59 | 3.80 | 4.14 |
| Computers | Time | **15.9** | 4961.4 | 492.9 | 213.9 | 170.5 | 1032.7 | 178.8 | 368.1 | 41.8 |
| | GPU | **3.04** | 4.91 | 23.24 | 5.26 | 5.48 | 8.69 | 17.42 | 23.43 | 6.10 |
| DBLP | Time | **14.8** | 7045.8 | 71.7 | 120.9 | 66.0 | 1552.5 | 272.8 | 42.4 | 43.6 |
| | GPU | **2.52** | 2.67 | 15.37 | 8.20 | 3.06 | 11.43 | 23.34 | 9.16 | 8.98 |
| CS | Time | **22.2** | 7172.0 | 124.0 | 273.7 | 219.0 | 1780.6 | 961.3 | 60.6 | 72.9 |
| | GPU | **1.58** | 3.43 | 22.21 | 11.82 | 6.49 | 13.52 | 23.42 | 16.83 | 12.85 |
| PubMed | Time | **8.5** | 2801.2 | 74.0 | 88.8 | 50.8 | 2196.9 | 535.0 | 37.8 | 49.2 |
| | GPU | **2.03** | 2.71 | 13.60 | 10.45 | 2.67 | 13.58 | 23.35 | 9.11 | 11.95 |
| CoraFull | Time | **51.9** | 7883.1 | 364.2 | 1665.1 | 1268.3 | 2285.6 | 2152.1 | 119.8 | 184.3 |
| | GPU | **2.89** | 6.46 | 23.26 | 14.45 | 7.62 | 20.04 | 23.41 | 16.25 | 15.52 |
| Physics | Time | **28.5** | 11067.9 | 9039.6 | 933.1 | 119.8 | 9243.4 | | 5211.4 | 1571.6 |
| | GPU | **2.70** | 9.04 | 23.36 | 23.18 | 12.65 | 23.22 | OOM | 23.43 | 23.38 |

Table 19: Wall-clock time and peak GPU memory on 15 benchmark datasets.

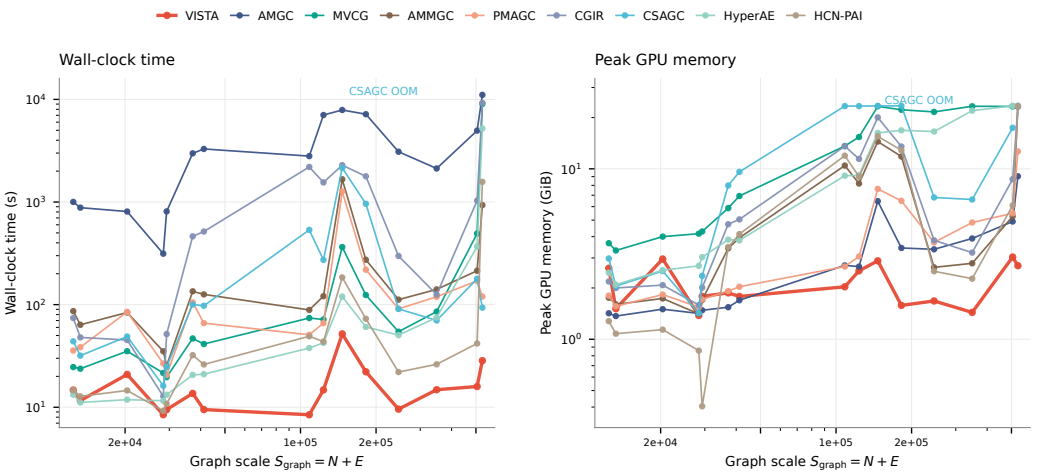


Figure 11: Runtime and memory scaling with graph size.